The role of serotonin and gap junctions in left-right development of *Xenopus laevis*

Dissertation zur Erlangung des Doktorgrades
der Naturwissenschaften (Dr. rer. nat.)

Fakultät Naturwissenschaften
Universität Hohenheim

Institut für Zoologie

vorgelegt von

Tina Beyer
aus Dresden

2011

Dekan:	Prof. Dr. Heinz Breer
1. berichtende Person:	Prof. Dr. Martin Blum
2. berichtende Person:	Prof. Dr. Heinz Breer
Eingereicht am:	01.06.2011
Mündliche Prüfung am:	02.08.2011

Die vorliegende Arbeit wurde am 18.07.2011 von der Fakultät Naturwissenschaften der Universität Hohenheim als „Dissertation zur Erlangung des Doktorgrades der Naturwissenschaften“ angenommen.

Danksagung

Bei Herrn Prof. Dr. Martin Blum bedanke ich mich herzlich für die Unterstützung während der letzten Jahre, das Überlassen interessanter Themen und sein Vertrauen in meine Fähigkeiten. Seine Begeisterung für die Wissenschaft, sein Optimismus und seine Fähigkeit, zu motivieren haben mir sehr geholfen.

Ich danke Prof. Dr. Heinz Breer für sein Interesse an dieser Arbeit und der Bereitschaft, diese zu begutachten.

Ich möchte mich herzlich bei Dr. Axel Schweickert für alles bedanken, was er mir von meiner Zeit als Laborhelfer an beigebracht hat, dass er immer ein offenes Ohr für Probleme hatte und bei kniffligen Fragen geholfen hat. Sein Wissen und seine Ideen für Experimente waren immer motivierend und haben die Arbeit in der Form überhaupt möglich gemacht.

Bei Thomas Thumberger bedanke ich mich ganz besonders für seine unendliche Geduld, mir beim Auswerten von Daten, beim Erklären von Bildbearbeitungs-möglichkeiten und beim Mikroskopieren immer wieder zu helfen. Aber vor allem wäre es ohne ihn als Kollege und Computerplatz-Nachbar nicht annähernd eine so tolle und lustige Zeit gewesen.

Bei Philipp Vick bedanke ich mich für die vielen Diskussionen und seine motivierende Art, an Experimente und Fragestellungen heranzugehen. Außerdem bin ich ihm sehr dankbar für das Leben, das er in das Labor gebracht hatte und das ich im letzten Jahr sehr vermisst habe.

Bei allen anderen Kollegen der Embryologie möchte ich mich für die angenehme Arbeitsatmosphäre, die vielen Gespräche und die konstruktive Zusammenarbeit. Besonderer Dank geht dabei an die "gute Seele" des Labors, Susanne Bogusch, die mir immer geholfen hat, wenn ich mal wieder mit Fragen zu ihr gekommen bin.

Natürlich möchte ich mich bei meinem Freund bedanken der mich immer unterstützt hat obwohl ihn meine Arbeit viele Nerven gekostet hat und ihm immer wieder Verständnis für manchmal wenig gemeinsame Zeit abverlangt wurde.

Der letzte aber nicht geringste Dank geht an meine Eltern, die immer hinter mir standen, viel mit mir diskutiert haben und einfach immer für mich da waren. Damit haben sie mir überhaupt all das ermöglicht.

Abstract

In vertebrates, the correct determination of the left-right (LR) axis is essential for accurate placement of the inner organs, such that the heart points to the left, lung lobation differs between left and right side, spleen and stomach are located on the left, liver on the right body side and the gut coils asymmetrically. Disturbance of this organization can lead to severe impairments of organ function. In the African clawed frog *Xenopus laevis,* already in four-day old tadpoles asymmetric organ arrangement is visible. This coordinated organ development strictly requires prior Nodal cascade activity in the left lateral plate mesoderm (LPM) in all model organisms examined so far. The initial symmetry breaking event necessary for unilateral induction of Nodal signaling is still under debate. In *X. laevis,* two models, namely 'ion-flux' and 'cilia-driven leftward fluid flow', were discussed in this context. Leftward flow was first described in the mouse model and later on in fish and rabbit, whereas the 'ion-flux' hypothesis is supported by data derived from chick development. In the present work it was intended to enlighten this putative discrepancy by re-investigating the function of two 'ion-flux' components in context of leftward flow in the model organism *X. laevis*.

First, a link between cell-cell communication via gap junctional communication (GJC) and LR axis establishment was analyzed by using heptanol for general inhibition of channel conductance on the one hand, and single knock-down (KD) of specific subunits on the other hand. Both treatments resulted in absence of the left-sided Nodal cascade. The KD led to shorter GRP cilia when compared to wildtype embryos and loss of bilateral *Nodal* expression at the GRP margin, respectively. Furthermore, heptanol treatments of stages in which the GRP already has been fully developed also resulted in laterality defects, thus implying a second function of GJC most likely for the signal transfer to the left side. These results indicated a role of GJC in leftward flow establishment and/or post-flow in neurula stages rather than a function in early cleavage stages for LR determination.

Second, the early signaling function of the neurotransmitter serotonin (5-HT) was inhibited by over-expression of either a frog or a human receptor ligand binding domain (*LBD*). In addition, specific KD of a receptor class 3 subunit was performed. Both applications resulted in impaired left-sided marker gene expression and disturbed GRP morphogenesis. Remarkably, marker gene expression of the superficial mesoderm

(SM) which gives rise to the GRP during development, was reduced in 5-HT signaling-impaired embryos. Very importantly, receptor 3 specific 5-HT signaling was shown to represent a necessary competence factor required for Wnt-dependent axis development in the frog double axis induction assay. Besides the new function of 5-HT during early development, it was further shown that the expression of the SM marker *Foxj1* (a master regulator of motile cilia) depended on maternal factors.

Based on the work presented here, the following model is proposed: (1) *Foxj1* expression is induced maternally, followed by (2) zygotic refinement in post-MBT stages, i.e. inhibition on the ventral and maintenance on the dorsal side. In the organizer region, an interplay of Wnt and 5-HT signaling is required for dorsal development. (3) Cilia driven leftward flow initiate an unknown downstream signal which is transferred to the left LPM. Both events, leftward flow and transfer, require active GJC (4) A to date unknown signal gets transferred towards the left LPM in a GJC-dependent process and induces the Nodal cascade activity, a prerequisite for proper organ arrangement. Taken together, the data presented in this study indicate that the directed fluid flow in neurula embryos represent the decisive step for symmetry breakage with the 'ion-flux' components being involved in correct flow function.

Zusammenfassung

Die Festlegung der links-rechts (LR) Achse ist essentiell für die korrekte Positionierung der inneren Organe. Beispielsweise ist das Herz zur linken Seite hin ausgerichtet und die Anzahl der Lungenloben unterscheidet sich auf der linken und rechten Seite. Die Milz und der Magen befinden sich auf der linken, die Leber auf der rechten Körperseite und der Darm weist eine asymmetrische Windung auf. Eine Beeinträchtigung dieser Ordnung kann zu schweren Funktionsstörungen dieser Organe führen. Die asymmetrische Anordnung des Herzens, der Gallenblase und des Darms ist bereits in fünf Tage alten Embryonen des afrikanischen Krallenfrosches *Xenopus laevis* sichtbar. In allen bisher untersuchten Modellorganismen hängt die asymmetrische Positionierung der inneren Organe von der vorangegangenen Aktivität der Nodal-Kaskade im linken Seitenplattenmesoderm ab. Der initiale Mechanismus für den Symmetriebruch des zuerst bilateral organisierten Embryos ist jedoch bisher noch nicht vollständig geklärt.

Die zwei Modelle, das "Ionenfluss"-Modell und die Hypothese des linksgerichteten Flüssigkeitsstromes, welche in dieser Dissertation diskutiert werden, sind beide in *X. laevis* beschrieben. Der durch Cilien getriebene, nach links gerichtete Flüssigkeitsstrom wurde erstmals für Maus und später auch für Fisch und Kaninchen experimentell nachgewiesen. Das Modell des "Ionenflusses" wird durch Daten gestützt, die im Huhn gewonnen wurden. Um diese vermeintlich kontroverse Datenlage zu klären wurden zwei Faktoren, welche dem "Ionenfluss" zugeordnet sind, hier neu aufgegriffen und auf einen möglichen Zusammenhang mit dem linksgerichteten Flüssigkeitsstromes über der cilierten Struktur der Dachplatte des Gastrocoels (gastrocoel roof plate, GRP) in *X. laevis* hin analysiert.

Als erstes wurde eine mögliche Funktion der durch Gap junctions (GJ) vermittelten Kommunikation der Zellen für die Entwicklung der LR-Achse untersucht. Dafür wurde zum Einen der Kanal der GJ mittels Heptanol blockiert, zum Anderen wurde die Translation einzelner Untereinheiten (Connexine, Cx) inhibiert. Beide Behandlungen verhinderten eine Induktion der Nodal-Kaskade auf der linken Seite. Die Inhibition der Translation einer bestimmten Untereinheit, dem Cx26, führte zu, verglichen mit der wildtypischen Situation, kürzeren GRP-Cilien und zusätzlich zu einem Verlust der bilateralen Nodaldomäne in der Randzone der GRP. Durch die Blockierung der GJ-Kanäle mittels Heptanol konnten jedoch auch Effekte beobachtet werden, wenn die Behandlung in älteren Stadien durchgeführt wurde, in welchen die GRP und die bilateral Nodal-Expression voll ausgebildet waren. Diese Ergebnisse lassen vermuten, dass die Zell-Zell Kommunikation über GJ neben der Rolle für die Morphogenese der GRP eine zweite Funktion für den Transfer eines Signals zur linken Seite haben könnte, welche möglicherweise dem Flüssigkeitsstrom nachgeschaltet ist.

Als zweites wurde der Signalweg des Neurotransmitters Serotonin (5-HT) inhibiert, indem die Liganden-Bindedomäne einer Untereinheit des Rezeptors 3 überexprimiert wurde. Die Annahme war, dass dadurch 5-HT abgefangen wird, was zu einem Funktionsverlust des 5-HT Signalweges führen würde. Zum Vergleich wurde ein Funktionsverlust eben dieser Untereinheit mittels Inhibition der Translation durchgeführt. Beide experimentellen Ansätze führten zu einem Verlust der linksseitigen Expression von Markergenen und zu einer gestörten Entwicklung der GRP. Interessanterweise war auch die Markergen-Expression des Epithels (superficial mesoderm, SM) in Gastrula-Stadien gestört, welches die Struktur der GRP im Neurula-Stadien bildet. Zudem konnte gezeigt werden, dass der 5-HT-Signalweg für die

Entwicklung der dorsalen Achse im Doppelachsen-Experiment notwendig war. Neben dieser neu beschriebenen Funktionen von 5-HT wurde weiterhin gezeigt, dass die Expression des Markers *Foxj1* (ein Hauptregulator für die Entwicklung motiler Cilien) von maternalen Faktoren abhängt.

Basierend auf den Daten, die in dieser Arbeit beschrieben wurden, wird das folgende Model vorgeschlagen: (1) Maternale Faktoren induzieren die Expression von *Foxj1* im gesamten Mesoderm. (2) In Blastula-Stadien, in denen nun auch zygotische Gene aktiv sind, wird die *Foxj1*-Expressionsdomäne durch ihre Inhibition auf der ventralen und Aufrechterhaltung auf der dorsalen Seite weiter spezifiziert. In der Region des Organisators sind der 5-HT und der Wnt-Signalweg notwendig für die *Foxj1*-Domäne in Gastrula-Stadien. (3) In Neurula-Stadien sind die Cilien der GRP posterior lokalisiert und bewegen sich im Uhrzeigersinn wodurch ein nach links gerichteter Flüssigkeitsstrom generiert wird. An diesem Prozess sind GJ entscheidend beteiligt. (4) Ein bisher unbekanntes Signal wird, in Abhängigkeit von GJ, zur linken Seite transportiert wodurch die linksseitige Nodal-Kaskade induziert wird. Diese ist für die asymmetrische Position der Organe notwendig. Zusammengenommen zeigen diese Daten, dass die durch Cilien generierte extrazelluläre Flüssigkeitsbewegung den eigentlichen Symmetriebruch darstellt und die Faktoren des "Ionenflusses" für die Entwicklung und Funktion eben dieser cilierten Struktur notwendig sind.

Table of contents

Introduction

I. Early development of the vertebrate embryo

During embryogenesis the three main body axes have to be determined: the dorso-ventral (DV), the anterio-posterior (AP) and the left-right (LR) axis. After fertilization, the cells cleave, the germ layers get specified and positioned during gastrulation and the nervous system is set up during neurulation. In the course of these early developmental stages, the three axes are established but timing and molecular mechanisms are still not quite clear in all model organisms or differ between them. Therefore, comparative analysis of one of these important processes, the LR axis, in vertebrate model organisms will enlighten decisive steps. The introduction section will shortly address basic developmental features but will focus on the development of the African clawed frog *Xenopus laevis*, the model organism used for the presented dissertation.

I.1 Fertilization

The fertilization process is started by docking of a sperm to the oocyte in almost all sexually reproducing animals. The fusion of the gametes is catalyzed by enzymes which are stored in so-called acrosomal vesicles and released by the sperm, i.e. acrosomal reaction. To prevent polyspermy immediately after fusion of the first sperm, Na^+ channels localized in the egg membrane open and the membrane potential depolarizes upon Na^+ influx. The depolarization induces Ca^{2+} release out of the endoplasmatic reticulum which results in the fusion of cortical granules with the plasma membrane. This process is called the slow block of polyspermy and represents a stable protection against entry of more than one sperm about one minute after fertilization by secretion of mucopolysaccharides during the cortical granule reaction. These phases of fertilization are best described in sea urchin embryos but are not fully understood in other deuterostomian animals and can therefore vary in other species (Gardner et al.

2006; Gilbert 2000). After the sperm has entered the cytoskeleton, the fertilized egg or zygote gets re-organized. Microtubules arrange in a star-like pattern, called sperm aster, with the center at the sperm entry point. The re-arrangement of the cytoskeleton is probably a prerequisite for the first cleavage whereas cleavage patterns differ between the species depending on the yolk content of the egg. Cells containing a high yolk mass undergo meroblastic or partial cleavage. Holoblastic or complete cleavage occurs in cells with less yolk, e.g. in amphibian or mammalian embryos as well as in non-vertebrates, e.g. echinoderms. By fast cleavage without a G-phase the so-called blastula (e.g. amphibians) or morula (e.g. mouse) stage is formed (Gilbert 2000). During early development, the genome of the zygote is not yet used and the embryo depends more on mRNA/proteins provided by the mother. The stage in which transcription of genomic DNA is initiated is called midblastula transition (MBT). The timing of MBT onset differs between the species whereas it seems to depend on the ratio of the cytoplasm to the DNA. For example the large eggs of *X. laevis* exhibit a high yolk content with the MBT occurring after the 13th cell division, whereas in mouse transcription of the genome takes place already in the 2-cell stage embryo (Bolton et al. 1984; Street et al. 1998).

I.2 Gastrulation: the three germ layers

During gastrulation the cells of the morula/blastula stage change their adhesion properties and start to migrate which results in re-arrangement of the whole embryo. This process and the underlying mechanisms are very well described in *X. laevis* (see below, II.4). In amphibians the gastrulation movements are initiated at a structure called the Spemann's organizer which was discovered by Hans Spemann and Hilde Mangold in 1924 (Spemann et al. 1924). In this region the cells start to involute and ingress into the embryo to end up as endodermal lining of the archenteron or mesodermal tissue between the endoderm and the ectoderm. The ectoderm does not involute into the embryo but starts the process of epiboly during which ectodermal cells intercalate into the outer epithelium which spreads and, at the end, covers the whole embryo. During further development, endodermal cells form the gastrointestinal tract and its derivatives

like the gallbladder, liver and the pancreas. The respiratory tract is also derived from the digestive tube. Axial mesodermal cells form the notochord which is the common structure in the embryos of all chordata. Paraxial mesoderm develops into the somites, which can be subdivided into dermamyotome and sclerotome, and the intermediate mesoderm which will give rise to the primitive kidney, the pronephros. The lateral and ventral mesoderm (lateral plate mesoderm, LPM) is subdivided into the somatic layer which underlies the ectoderm, and the splanchnic layer which will form for example the heart (Gilbert 2000).

I.3 Neurulation

After gastrulation, the ectoderm overspreads the whole embryo. On the dorsal side, elongated along the AP axis, the neuroectoderm forms the neural plate. Non-neural, more ventrally localized tissue of the ectodermal layer will become epidermis. The formation of the neural tube starts with patterning of the neural plate which includes signals from the underlying notochord to induce floor plate specification along the midline of the neural plate. At the lateral-most edges of the neural plate, the tissue thickens to form the neural folds. At three hinge points, the neural tube starts to fold up. During this process the neural tissue also lengthens along the AP axis via convergence extension movements (see below, II.5.2) of the neural plate cells towards the midline. After the fusion of the neural folds epidermal cells cover the whole embryo (Gilbert 2000; Colas et al. 2001). At the dorsal-most edge of the neural tube, the neural crest cells become differentiated and start to migrate ventrally. These cells will end up in different tissues for example as melanocytes, smooth muscle cells, glia and craniofacial bone and cartilage structures (Gilbert 2000).

II. Development of *Xenopus laevis*

II.1 The model organism *Xenopus laevis*: history and methods

Amphibians have been used for research in developmental biology since the 19th century. Advantages are easy access to a high number of eggs, large embryos for manipulation and transplantation experiments and very good regeneration after surgery. A disadvantage of most amphibians has been the seasonal breeding only two times a year. The African clawed frog *Xenopus laevis* was used for pregnancy tests already in the 1950s. The females respond to the human hormone chorion gonadotropin with spontaneous spawning, thus representing an ideal model organism for research. *X. laevis* individuals can live for 15 up to 20 years and can be used up to four times a year for hormone-induced egg production. After *in vitro* fertilization the jelly-coat can be removed to isolate single eggs for manipulation. Depending on the researchers question, *X. laevis* is used for quite different experimental procedures during early development. Embryos serve as model organisms to test toxicity of substances by adding the toxic component to the medium the embryos develop in. Specific tissues of interest can be explanted and kept in culture or be stained and transplanted to an unstained embryo, e.g. for observation of cell migration movements. For manipulation on the molecular level either gain of function experiments can be performed by injection of mRNA or DNA encoding single genes, or loss of function experiments by injection of dominant-negative constructs or of so-called morpholino oligonucleotides (MOs). MOs are synthetic RNA-like molecules consisting of about 25 bases and can be designed complementary to the target of interest. After transfer into the cell, e.g. by microinjection, the chosen antisense MO binds to the target mRNA thus inhibiting splicing of the pre-mRNA or translation of the protein. Targeting specific tissues on only one side of the embryo is possible with a few limitations, e.g. independent targeting of anterior and posterior structures cannot be obtained (Sive et al. 2000).

But there are also some basic information/procedures still missing or just hard to be performed in *X. laevis*. The pseudo-tetraploid genome is not sequenced completely making cloning and analysis of homologous genes difficult. In addition, due to

tetraploidy it is hard to establish transgenic lines which carry a deletion of the gene of interest. Therefore a related species, *Xenopus tropicalis*, can be used which has a diploid genome. However, the embryos of *X. tropicalis* are smaller and the adults need warmed up water (26-28°C). Because of the easy handling of *X. laevis* adults and embryos and the availability of a variety of experimental procedures, this model organism was used for the present study.

II.2 Fertilization: Cortical rotation and first cleavage stages

So far, *X. laevis* represents the only vertebrate model system for which mechanisms and signaling pathways of primary axis specification are well understood. In the unfertilized egg, the oozyte, the first body axis is already determined by mRNAs/proteins provided maternally. The animal pole, which corresponds roughly to the future anterior side is pigmented whereas the vegetal pole, which has a high yolk content, is not. After sperm entry and release of mucopolysaccharides (see above, I.1) into the extracellular space between plasma and vitelline membrane, the zygote gets re-orientated according to gravity with the heavy yolk-rich part pointing down and the pigmented animal pole up. Sperm entry also initiates determination of the DV axis by inducing rotation of the cortex. For this, centriolar microtubules (MT) are re-arranged which triggers the rotation of the cortex and causes a shift of the animally localized pigment towards the sperm entry point. At the vegetal pole components of the Wnt signaling pathway (Dsh and Wnt11, see below, II.5.1) can be found which get translocated towards the opposite side of the sperm entry point. Thereby, the future dorsal side of the embryo is specified which is clearly visible by formation of the so-called gray crescent in some amphibians. Experimentally, MT polymerization and subsequent induction of the DV axis can be prevented by UV irradiation applied directly after fertilization, giving rise to ventralized embryos (Gerhart et al. 1989; Gurdon 1960; Cha et al. 1999). Interestingly, this effect can be rescued by rotation of the UV-treated zygote in an angle of 90° along the animal-vegetal axis (Scharf 1980). During the last years accumulating data showed that motor proteins, like kinesins and dyneins, contribute to this process in different ways. Dyneins are needed for cortical localization

of MT, kinesins for transport of dorsalizing factors from the vegetal pole towards the future dorsal side (Weaver et al. 2004).
The first cleavage occurs about 90 min post-fertilization and begins animally, splitting the zygote in left and right half. The next cleavages arise in an interval of about 20 min depending on the temperature. During the first cleavage stages the embryo stays at about the same size and no cell migration occurs. Animally, a fluid-filled cavity is formed which is called the blastocoel (Gilbert 2000).

II.3 Nieuwkoop's center and Spemann's organizer

In the oocyte maternal mRNAs and proteins define prospective endoderm and ectoderm. In the marginal zone of the early zygote, where endo- and ectoderm are in juxtaposition to each other, mesodermal cell fate is induced by signals coming from the vegetal pole. Consequently, the blastocoel is necessary for the separation of the animal pole from the vegetal pole to allow development of ectodermal cell fate in absence of mesoderm-inducing signals. Together with vegetally localized signaling components shifted during the cortical rotation, the so called Nieuwkoop's center is defined at the dorsal-most vegetal region, which is sufficient for dorsal axis induction and development. This early dorsal axis determining center was first analyzed in 1969 (Nieuwkoop 1969). Pieter Nieuwkoop performed transplantation experiments to examine inducing properties of the germ layers. He showed that endodermal tissue is capable of inducing the whole range of mesodermal cell fates in neighboring cells (Nieuwkoop sandwich experiment). This finding was confirmed by more specific transplantation experiments performed already at the 16-64-cell stage embryo (Gimlich et al. 1984; Dale et al. 1987; Gerhart et al. 1989). Gimlich and Gerhart combined single vegetal blastomeres with labeled animal cells. They showed that mesodermal tissue induction occurs in a dorsal to ventral gradation (Dale et al. 1987). When transplanted into the ventral side of a recipient embryo, the dorsal-most transplanted cell/tissue was capable of specifying the organizer of dorsal development in adjacent and/or overlapping tissue, thereby inducing a secondary axis/siamese twin. Already in 1924 Hans Spemann and Hilde Mangold succeeded in induction of a secondary axis after

transplantation of the dorsal-most tissue of an early gastrula to the ventral side of a second embryo (Spemann et al. 1924). They used differently pigmented embryos to distinguish between host and recipient cells. Adjacent to the transplanted tissue dorsal structures like notochord and somites were induced. What is known about the mechanisms on the molecular level is resumed below (chapter II.5). Taken together, these experiments demonstrated that the dorsal-most vegetal cell of early cleavage stages (Nieuwkoop's center) and mesodermal tissue of gastrula stages (Spemann's organizer) pattern dorsal embryonic structures.

II.4 Convergent extension: gastrulation and neurulation

During gastrulation cell properties change to enable cell migration, shape changes and re-arrangements which results in thickening, lengthening and spreading of tissues, which result in re-organization of the whole embryo (see also I.2). These orientated cell and tissue behaviors are described as convergence (towards one axis) and extension (along one axis). For directed movement each migrating cell must be polarized in relation to the surrounding tissue. In this chapter, such convergence and extension movements will be described in the context of gastrulation and neurulation in *Xenopus* development. Gastrulation starts at the dorsal side of the embryo with formation of the so-called bottle cells after zygotic gene transcription is initiated (see also I.1). Bottle cells develop via apical accumulation of actin, which is organized in a ring-like pattern, followed by constriction of the apical cell pole and membrane internalization. Thus a small indentation is formed which pulls surrounding tissue inside the embryo. Additionally, ectoderm of the animal cap expands via intercalation of deep cells into the superficial layer, pushing endodermal and mesodermal involution. After gastrulation is finished, the three germ layers are at their final position, i.e. endoderm lining the archenteron, ectoderm covering the whole embryo and mesoderm in between. Axial dorsal tissues like the neural plate and notochord undergo extension along the AP axis. This elongation is driven by medio-lateral intercalation which depends on polarization of the cytoskeleton of the migrating cells. The polarized cells develop protrusions, which are necessary for such orientated movement. Even so, there are differences between

neural and mesodermal cell behavior. Mesodermal cell protrusions occur randomly and cell intercalation is a result of 'boundary capture' along the midline where cells become anchored. Contrary to this, neural tissue aligns by directed medial cell migration (Wallingford et al. 2000). The mechanisms which control these developmental processes have been studied intensively during the last decades, mostly focusing on non-canonical Wnt signaling (see below, II.5.2).

II.5 Wnt signaling

The Wnt signaling pathway, first described in *Drosophila* in the 1980s, is necessary to trigger a variety of mechanisms during embryogenesis. The effect on the cell or tissue depends on the interaction of different ligands, receptors or co-factors (van Amerongen et al. 2009; Wallingford et al. 2011; Simons et al. 2008; Rao et al. 2010). Wnt-dependent signaling is known to use three distinct pathways: (1) The canonical or β-catenin pathway signals via the core component β-catenin (β-cat) leading to transcriptional regulation of target genes. This pathway is necessary to specify tissue identity and cell proliferation rate. (2,3) Two non-canonical pathways are independent of β-cat function and rearrange the cytoskeleton as a prerequisite for cell migration and positioning along a defined plane and, in some tissues, for cilia polarization.
Irrespective of the pathway, receptors of the Frizzled (Fz) family and the cytoplasmic protein Dishevelled (Dsh) are essential core proteins. Dsh has three main domains, namely the DIX, the PDZ and the DEP domain. The abbreviations result from proteins for which these domains have been described initially, i.e. DIX (Dsh/axin), PDZ (PSD-95/Dlg/ZO-1/2) and DEP (Dsh/egl-10/pleckstrin). The DIX domain is thought to be involved only in canonical, the DEP domain in the non-canonical and the PDZ domain in both Wnt signaling pathways (Sheldahl et al. 2003a; Sokol 1996; Wallingford et al. 2000; Park et al. 2005). Fz proteins are seven transmembrane-spanning G-protein coupled receptors and contain a cysteine-rich extracellular domain which has been implicated in ligand binding. About ten Fz proteins have been described in human, mouse and *Xenopus*. The Wnt ligand family includes up to 19 proteins in mouse and human. Wnts are named after the *wingless* phenotype in *Drosophila* and the cancer-

promoting gene *Int-1* in mouse. Some ligands and receptors are more associated with the canonical Wnt pathway, e.g. Wnt8, Wnt3, Wnt2 and Fz8 in *Xenopus.* These components have been characterized by their ability to induce the transcription of typical canonical Wnt target genes like *Xenopus nodal-related 3* (*Xnr-3*), or a secondary organizer region and thus a second axis (Landesman et al. 1997; Cui et al. 1995; Wolda et al. 1993; Deardorff et al. 1998). The non-canonical Wnt pathway involves Wnt5a, Wnt11 and Fz7 which are not capable of secondary axes induction but misexpression can lead to dysfunction of convergent extension like gastrulation or neural tube closure defects (NTDs; Winklbauer et al. 2001; Sheldahl et al. 2003b; Tada et al. 2000, 2009).

For several years it was believed that some ligands and receptors exclusively contribute either to the non-canonical or to the canonical pathway. However, during the last years this strict classification has been more and more disproven by new findings that some proteins can, dependent on the ligand-receptor combination, act in both Wnt signaling pathways (Rao et al. 2010; Cha et al. 2008; Tada et al. 2000; Wallingford et al. 2001).

II.5.1 Canonical Wnt signaling

In the absence of a Wnt ligand the so-called APC-complex (adenomatous polyposis coli), which consists mainly of the four core proteins axin, glykogen synthase kinase 3 (GSK-3), casein kinase 1 (Ck1) and APC, promotes β-cat degradation by phosphorylation at the amino terminal region. In the presence of the ligand the cytoplasmic protein Dsh gets activated and inhibits the function of the APC-complex by binding and relocation to the membrane. After the inhibition of the APC-complex, β-cat can enter the nucleus, bind to the co-factors TCF/Lef and initiate target gene transcription, e.g *goosecoid* (*gsc*) and *siamois* (*Sia*). In absence of β-cat, TCF/Lef repress target gene induction. Two proteins, the low density lipoprotein receptor-related proteins 5 and 6 (Lrp5 and 6) are canonical Wnt-specific co-receptors (Mosimann et al. 2009; Amerongen et al. 2009; Rao et al. 2010; Niehrs et al. 2010). During the last few years, a new feature of this very signaling pathway has emerged. Wnt/Lrp6/Fz/Dsh accumulate in vesicle-like structures called signalosomes. Thereby, Lrp6

phosphorylation at multiple sites is induced which is a prerequisite for downstream signaling (Cruciat et al. 2010; Niehrs and Boutros 2010; Niehrs and Shen 2010).
Some of these proteins, although designated canonical Wnt components, have other functions in the cell as well, e.g. β-cat as factor involved in cell adhesion by interaction with cadherins (Heuberger et al. 2010).

II.5.2 Non-canonical Wnt signaling

The non-canonical Wnt signaling pathway is independent of the APC-complex and the following transcriptional regulation of target genes by β-cat. Additionally in *Drosophila*, an involvement of the Wnt ligand has not been proven. Non-canonical Wnt signaling is subdivided into the Wnt/Jun N-terminal kinase (JNK) or PCP and the Wnt/Ca^{2+} pathway (Simons et al. 2008b; Rao et al. 2010). In vertebrates, both pathways signal via core proteins, i.e. specific Wnt ligands and transmembrane proteins like Fz receptors and the receptor type protein tyrosine kinases PTK7 and Ror2. In the case of Wnt/JNK, recruitment of Dsh leads to activation of effector proteins of the small GTPase protein class (e.g. rhoA, rac, cdc42) which modulate the cytoskeleton. This can be seen by apical enrichment of actin which is the basis for apical constriction (bottle cell formation, see above, II.4), asymmetrical protein localization, ciliogenesis and cilia polarization. Dysfunction of this pathway can lead to gastrulation defects, NTDs and failure of neural crest migration (Tada et al. 2009; Wallingford et al. 2011; Kim et al. 2005; Simons et al. 2008a). Activation of the Wnt/Ca^{2+} pathway results in an intracellular increase of Ca^{2+} and therewith regulation of Ca^{2+}-dependent proteins like the calmodulin kinase 2 (CAMKII) and the protein kinase C (PKC) (Choi et al. 2002; Sheldahl et al. 2003a; Slusarski et al. 1997). A downstream effector of this pathway via calcineurin is the nuclear factor of activated T-cells (NFAT) which is a transcriptional regulator (Saneyoshi et al. 2002). Dysfunction of this pathway affects DV patterning, regulation of the canonical Wnt pathway and heart development (Simons et al. 2008a; Park et al. 2005).
A general feature of Wnt pathways lies in their mutually exclusive activation and inhibitory relationship, e.g. CAMKII activates a kinase (NLK) which antagonizes canonical Wnt signaling by inhibition of β-cat (Ishitani et al. 2003). On the other hand,

the canonical Wnt signaling influences/inhibits the non-canonical pathways, e.g. via Lrp6 (Bryja et al. 2009).
Besides the role of Wnt pathways for DV and AP axis specification and orientation, also the third body axis, the LR axis, probably relies on Wnt-dependent cell/tissue polarization. The establishment of the LR axis is introduced in detail in the next section.

III. Left-right axis determination

Theoretically, the definition of two body axes (AP, DV) results automatically in the determination of a third, the LR axis. In vertebrates, asymmetrically oriented development along this very axis is often not readily seen from the outside but the majority of the viscera are asymmetrically positioned and/or patterned. In human, liver and gall bladder are localized on the right, spleen and stomach on the left body side and the gut is coiled asymmetrically. The lung consists of five lobes in total with three lobes situated on the right and two on the left side. The apex of the heart points to the left and, in addition, displays an intrinsic asymmetry, i.e. the ventricles differ in muscle thickness as a result of the asymmetric organization of the pulmonary and systemic circulatory system. This normal organ arrangement is called *situs solitus* (Cooke 2004). With a prevalence of 1:10,000, a complete mirror-image of all organs can be found (*situs inversus totalis*) which does not give rise to any symptoms. In contrast, single organ inversion (*heterotaxia)* or development of either left or right side isomerism (left-sided identity on the right side and vice versa) inevitably cause severe health problems (Storm van's Gravesande et al. 2005).
The establishment of the LR axis can be subdivided into four steps:
(1) Symmetry breakage of the bilateral symmetrical embryo (III.2 and III.3).
(2) Transfer of an asymmetric signal to the left lateral plate mesoderm (LPM).
(3) Nodal cascade induction on the left side in the LPM (III.1).
(4) Asymmetric organ morphogenesis.

III.1 Left-sided Nodal cascade

Nodal signaling is involved in a variety of developmental processes. In particular, the Nodal pathway is pivotal for the patterning of the endo- and mesoderm and for the specification of the body axes. Here, the function of Nodal as a morphogen, the key components of the Nodal signaling pathway and its role in LR axis determination are introduced.

III.1.1 The Nodal signaling pathway

Nodal is a member of the transforming growth factor beta (TGFβ) family and is produced and secreted as proprotein. Each proprotein consists of a signal peptide necessary for secretion, a pro- and a mature domain. Nodal can form either homo- or heterodimers, e.g. with its inhibitors of the Cerberus/DAN family which prevents ligand-receptor binding (Schweickert et al. 2010; Hashimoto et al. 2004; Vonica et al. 2007). For activation of downstream signaling, the subtilisin-like proprotein convertase family members Furin and PACE4 (SPC1 and SPC4) cleave the proprotein in the extracellular space separating the mature domain (Beck et al. 2002; Toyoizumi et al. 2006). Following cleavage, Nodal binds to the receptor complex which consists of type 1 serine-threonine kinases (ALK4) and type 2 receptors (ActRII or ActRIIB). Unlike other TGFβ family members Nodal signaling depends also on the presence of co-receptors of the EGF-CFC (Epidermal Growth Factor-like Cripto/FRL1/Cryptic) family. By ligand-receptor binding cytoplasmic Smad2/3 gets phosphorylated and dimerizes with Smad4. The Smad-complex translocates into the nucleus where it mediates target gene transcription dependent on other DNA-binding co-factors, e.g. FoxH1 (Fig. 1A).
Nodal is able to induce target gene transcription at a distance to the protein source, specifying it as classical morphogen. The morphogen concept was first proposed by Lewis Wolpert and is known as the 'French Flag Model' (Wolpert 1969). The idea was that secreted molecules can distribute extracellularly and induce downstream events in a concentration/threshold-dependent manner (Fig. 1B; Williams et al. 2004; Smith et al. 2008; Schier 2009; Kurth et al. 2000). Long-range signaling in the extracellular space of

the Nodal protein is supposed to depend on glycosaminoglycans (GAGs) (Oki et al. 2007; Yost 1990). Additionally, Nodal can form heterodimers with proteins of the growth differentiation factor family (GDF) thereby getting stabilized resulting in enhancement of long-range signaling (Shen 2007).

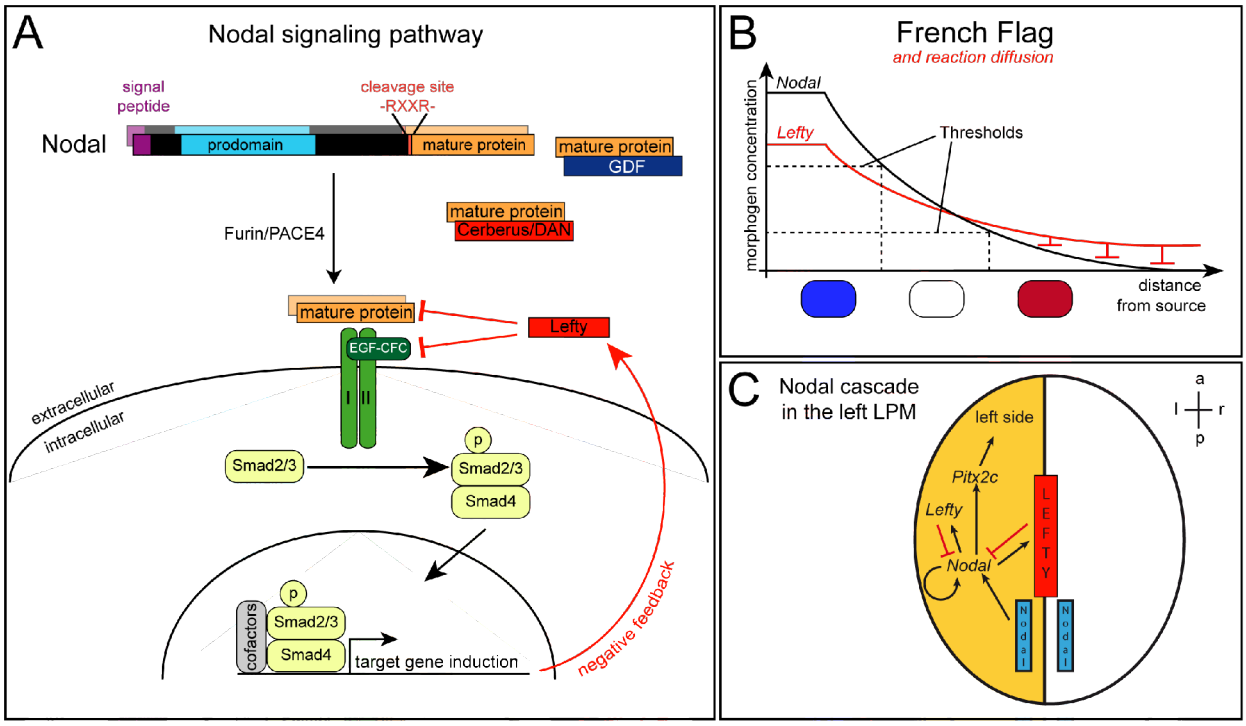

Figure 1: Nodal signaling

(A) Scheme of the Nodal pathway (modified after Shen 2007). Nodal proprotein is cleaved by subtilisin-like convertase activity in the extracellular space. By binding of Nodal to the ALK4/ActRII/ActRIIB receptor-complex, Smad2/3 gets phosphorylated. Translocation of the Smad2/3/4-complex into the nucleus is followed by co-factor-dependent induction of Nodal signaling target gene expression. Lefty represents a target gene and represses Nodal signaling in a negative feedback loop by binding to the co-receptor EGF-CFC and Nodal.

(B) Nodal signaling models (modified after Schier 2010 and Brink 2007). Nodal and Lefty are both classified as morphogens which induce downstream signaling (here indicated by blue, white or red color) in a concentration-dependent manner (thresholds) at a distance to the protein source. Lefty displays a longer signaling range and distributes faster what results in spatial and temporal restriction of Nodal activity.

(C) Scheme of left-sided Nodal signaling. Asymmetric signaling depends on bilateral *Nodal* expression (blue) in the posterior midline. In the left LPM (orange), Nodal induces its own expression, transcription of its inhibitor *Lefty* and of the transcription factor *Pitx2c*. *Pitx2c* is required for asymmetric organogenesis.
a, anterior; l, left;.LPM, lateral plate mesoderm; p, posterior; r, right;

III.1.2 Nodal signaling in the left LPM

In 1995, Levin and colleagues showed expression of three genes which are involved in LR patterning including the chick n*odal-related gene cNR-1* (Levin et al. 1995). In all vertebrates examined so far a LR-asymmetric *Nodal* expression was described. Nodal synthesized in the left LPM induces its own transcription (positive feedback loop) and the transcription of the target genes *Lefty* and *Pitx2c*. Lefty inhibits the Nodal pathway by binding to Nodal and the co-receptor EGF-CFC (negative feedback loop). Like Nodal, Lefty is classified as a morphogen whereas its extracellular distribution occurs faster and the range is longer than it is described for Nodal. By this, Lefty restricts Nodal activity expansion and duration in the left LPM ('Reaction-Diffusion-Model'; Bisgrove et al. 1999; Schier 2009; Chen et al. 2002, 2004). The second target gene *Pitx2c* is a homeobox transcription factor which is necessary for establishment of organ laterality and represents a common marker for LR development (Fig. 1C; Schweickert et al. 2000; Simard et al. 2009).

Interestingly, a bilateral *Nodal* expression domain located in the posterior midline is a prerequisite for left-asymmetric Nodal cascade induction in the mouse which has not been confirmed in other model organisms so far (Fig. 1C; Saijoh 2003; Brennan et al. 2002). This bilateral pattern is highly conserved among the vertebrates implying a similar function as shown for mouse (Levin et al. 1995; Blum et al. 2007; Vonica et al. 2007). In this domain *Nodal* is co-expressed with its inhibitor of the Cerberus/DAN-family, i.e. *Coco* (*Xenopus*) / *Charon* (zebrafish) / *Caronte* (chick) / *Cerl-2* (mouse), and Nodal signaling promoting factors, i.e. *derrière* (*Xenopus*) / *Gdf-1/2* (mouse) (Vonica et al. 2007; Schweickert et al. 2010; Rankin et al. 2000; Tanaka et al. 2007; Hashimoto et al. 2004; Hanafusa et al. 2000). The overlapping expression of Nodal-regulating factors and Nodal itself indicates that there must be a mechanism which specifies whether the Nodal cascade is active or not. Additionally, symmetry breakage and left-sided *Nodal* induction is proposed to occur in the structure marked by this bilateral domain (Blum et al. 2007, 2009; Schweickert et al. 2007).

III.2 Symmetry breakage: Cilia-driven fluid flow in mouse, rabbit and fish

Cilia are protrusions of the cell surface which can occur either as so-called primary or single cilium found on most vertebrate cells, or as multiciliary bundles. Cilia are involved in various processes like signal transduction of several pathways (Wnt, sonic hedgehog), sensing of fluid flow (inner ear, kidney) or simply as motile organelle for cleaning of cell surfaces (lung). Cilia consist of a skeleton build of acetylated α-tubulin. The 'classical' cilium harbors nine outer tubulin doublets and one central doublet (9+2), whereas other cilia lack the central doublet (9+0) or some even display two inner doublets (9+2). Cilia assembly depends on motor proteins, more precisely on kinesins, which are necessary for building up the cilium, and on dyneins which transport cargo from the cilia tip back to the cell. Additionally, dyneins localized as outer and inner arms attached to the outer tubulin doublets are involved in cilia motility (Basu et al. 2008; Berbari et al. 2009; Satir et al. 2010).

A first evidence that cilia function is linked to LR development came from Afzelius in 1976 who described a human disease caused by immotile cilia lacking dynein arms, called the Kartagener syndrome. Multiple symptoms are the consequence, like defective mucociliary transport in the lung, immotile sperm of male patients and s*itus inversus totalis* in 50% of the patients (Afzelius 1976). In 1994, Sulik and colleagues described, based on scanning electron microscope studies and video microscopy analysis, a pit-like structure which was located at the distal tip of the mouse egg cylinder. In 7-9-day old mice, each cell in these structure exposed one single cilium which was motile (Sulik et al. 1994). Targeted disruption of the kinesin genes *KIF3A* or *KIF3B* led to loss of the pit cilia accompanied by LR defects (Marszalek et al. 1999; Nonaka et al. 1998). Also mouse mutants for the LR dynein (*lrd*) displayed LR defects demonstrating that LR axis determination in mouse depends on motility of the murine pit cilia (Okada et al. 1999; Supp et al. 1997). The LR cilia are tilted posteriorly, rotate in a clockwise fashion consequently producing an extracellular fluid flow towards the left side (Nonaka et al. 2005). The posterior polarization of the cilia is a PCP pathway-dependent process (Wang et al. 2011; Hashimotoa et al. 2010; Song et al. 2011). In an elegant experiment Nonaka and colleagues could show that the cilia-driven leftward flow is necessary for LR development. Therefore, they rescued LR defects of mouse

mutants lacking cilia by applying an artificial flow towards the left side. Remarkably, artificial rightward flow induced right-sided *Nodal* expression and inverted *situs* development which nicely confirmed the dependence of Nodal cascade induction on cilia-driven flow (Nonaka et al. 2002).

In 2007, our group could show that the ciliated pit-like structure in the mouse, formerly known as 'node', is part of the notochord and clearly distinguishable from the organizer/node. Consequently, this very structure was renamed posterior notochord (PNC). Interestingly, examination of the PNC homologous tissue in rabbit revealed existence of monocilia of all three subtypes (9+0/2/4) (Blum et al. 2007a). Also in zebrafish and medaka ciliated structures (Kupffer's vesicle, KV) involved in LR development were described, supporting the idea of conservation of cilia-dependent symmetry breakage in all vertebrates (Kramer-Zucker et al. 2005; Essner et al. 2002; 2005). However, in *X. laevis* a different cilia-independent mechanism was proposed to initiate symmetry breakage, which was commented by Cliff Tabin in 2005 as follows: '*The thorn in the side of the cilia model that just won't go away.*' (Tabin 2005). In the next chapter, the two models for symmetry breakage in *X. laevis* are presented.

III.3 Symmetry breakage: Two models for symmetry breakage in *Xenopus laevis*

In *X. laevis* the time point of symmetry breakage is highly controversial. Two quite different mechanisms are proposed for left side determination: (1) the 'ion-flux' model and (2) the leftward flow hypothesis. It seems to be a good reason for studying symmetry breakage in the model organism in which both mechanism have been investigated.

III.3.1 'Ion-flux'-hypothesis: Symmetry breakage during early cleavage

The first factor found to be necessary for LR determination in early development of *X. laevis* was cell-cell communication via gap junctions in 1998. During the following eight years other components have been added to the model: $H^{+/}K^{+}$-ATPase in 2002,

serotonin signaling in 2005 and the V-ATPase in 2006 (Levin et al. 1998, 1999, 2002; Fukumoto et al. 2005; Adams et al. 2006). All these components are combined in the 'ion-flux' hypothesis. Based on this model, the cells of the early cleavage stage embryo are linked via gap junctions (GJ) with exception of the ventral blastomeres which are isolated from each other. Shortly after fertilization maternal provided protein and mRNA encoding ion pumps ($H^{+/}K^{+}$-ATPase, V-ATPase) get localized asymmetrically which was proposed to represent the symmetry breaking event. Presumably, this is achieved by the transport along LR-asymmetric organized microtubules. The asymmetric ion pump activity results in an electrochemical gradient. Driven by this gradient, small molecules can distribute through GJ and accumulate on one side. The candidate molecule which is able to pass gap junctional channels and is known to be involved in LR axis determination is the neurotransmitter serotonin (Levin 2004, 2006; Adams et al. 2006).

Gap junctional cell-cell communication

GJ are widely distributed in the animal kingdom. Gap junctional channels link the cytoplasm of neighboring cells which allows fast molecule exchange. Molecules with a maximum size of 1000 Dalton can pass GJ, whereas also the 17 kDa large calmodulin protein was described to go through these channels (Curran et al. 2007). GJ are arranged in so-called plaques in the apico-lateral cell membrane. Each channel consists of two hemichannels (connexons), and each connexon of six subunits (connexins, Cx). Cx are four transmembrane-spanning proteins with both terminal ends reaching into the cytoplasm. GJ can form homo- or heteromeric structures, and gating properties and size of passing molecules depend on the composition of the subunits. Gating has been shown to be regulated by second messengers, e.g. cAMP, Ca^{2+}, or phosphorylation status of the Cx (Rackauskas et al. 2010; Sosinsky et al. 2005; Laird 2006a). Experimentally, gap junctional cell-cell communication (GJC) can be visualized using small dyes, e.g. Lucifer yellow which was used to analyze ventral and dorsal blastomere connectivity in the early embryo of *X. laevis* (Guthrie et al. 1988; Levin et al. 1998).

Serotonin signaling

Serotonin (5-HT) is the so-called 'happiness-hormone' because it contributes good feelings as neurotransmitter in the brain. 5-HT is a monoamine which is synthesized from the amino acid tryphtophan in two steps via the enzymes tryptophan hydroxylase (TPH) and amino acid decarboxylase (DDC). 5-HT in the cytoplasm gets degenerated very fast by monoamine oxidase (MAO) activity. To prevent degradation, it gets packed into vesicles. Therefore H^+ ions are pumped into vesicles by ion pumps like the H^+/K^+-ATPase. Along the proton gradient, the vesicular monoamine transporters (VMAT) translocate 5-HT into the vesicular lumen. After release of the vesicular content into the extracellular space, 5-HT can bind to its receptors. Transporters located at the membrane (SERT) are necessary for re-uptake of 5-HT into the cell to terminate signaling. In vertebrates about 20 receptor subunits have been described which are classified into seven subgroups ($5\text{-}HT_{1\text{-}7}$). The receptors are G-protein coupled receptors except for $5\text{-}HT_3$ which is a ligand-gated ion channel (Barnes et al. 1999). Receptor inactivation in different model organisms results in a variety of developmental defects like gastrulation, neurulation, heart and bone patterning defects (Yadav et al. 2008; Gaspar et al. 2003; Moiseiwitsch 2000; Lauder et al. 1981).

III.3.2 Leftward Flow: Symmetry breakage in neurula embryos

In *X. laevis*, a ciliated structure marked by expression of the motor protein LR dynein was already found in 2002 (Essner et al. 2002). In addition, Shook and Keller examined and described the development of a ciliated structure in gastrula and neurula stage embryos (Shook et al. 2004). In gastrula stage embryos, the mesodermal marginal zone is covered by an endodermal cell layer. However, on the dorsal side the superficial layer will develop into mesodermal tissue. This could be shown by labeling of the cells located on the outer surface at blastula stages and tracking cell migration during development. The authors found that the dorsally located superficial cells (superficial mesoderm, SM) end up in somites, notochord and form the hypochord in tadpole stage embryos.

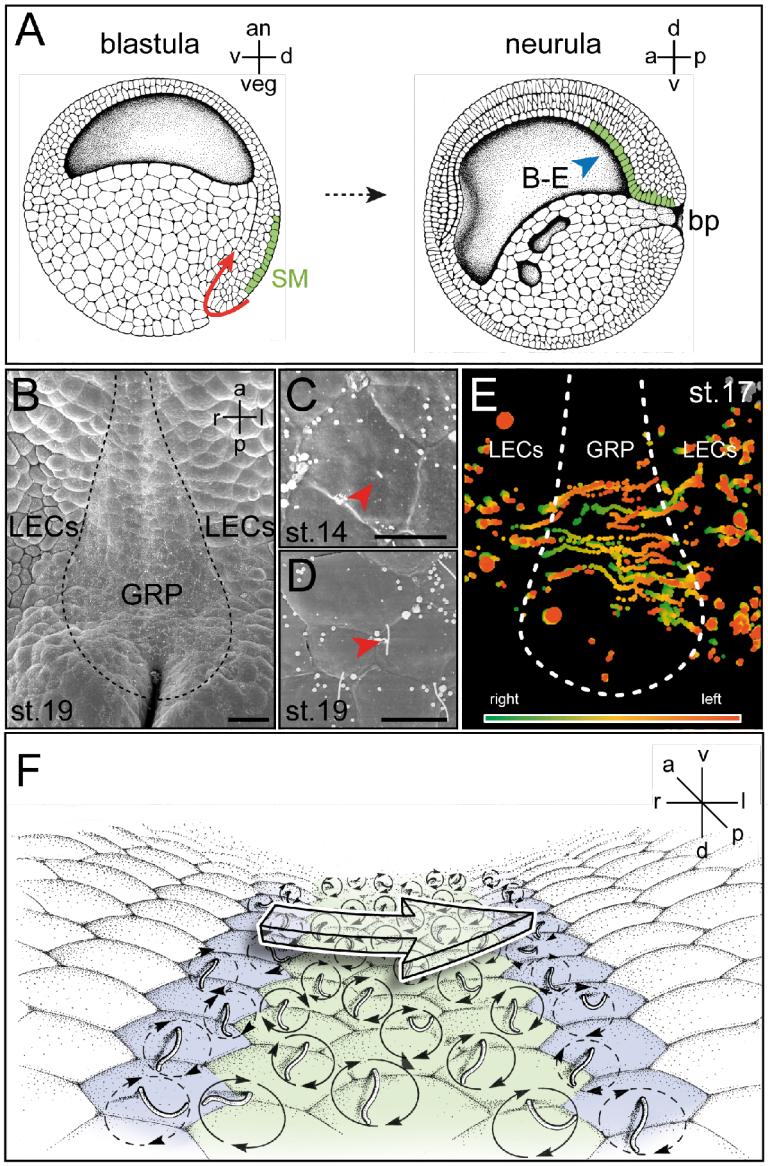

Figure 2: Leftward flow in *X. laevis*.
(A) GRP development. In the blastula stage SM cells (green) are located at the dorsal marginal zone. During gastrulation SM cells invaginate into the embryo (direction indicated by red arrow). In neurula stages SM cells can be found at the posterior part of the gastrocoel roof (gastrocoel roof plate, GRP). Blue arrowhead indicates ventral view used in **B-E**.
(B-D) SEM of the GRP. In st.17 the GRP displays a triangular shape (indicated by dashed line) and is surrounded by large endodermal cells (lateral endodermal crests, LECs). In st.14 short cilia located in the middle of the cell can be found **(C)**. In st.19 about 5µm long cilia are polarized to the posterior pole **(D)**. Cilia are indicated by red arrowheads, scale bars represent 50µm **(B)** and 10µm **(C, D)**.
(E) Visualization of flow. Fluorescent beads were added to GRP explants followed by particle tracking using time-lapse movies. Particle movement was visualized using a color gradient ranking from green (time 0s) to red (time 25s). In the GRP region a leftward flow occurred.
(F) Schematic presentation of cilia-driven extracellular fluid flow towards the left side (scheme modified from Blum et al. 2009).
a, anterior; an, animal; bp, blasopore; d, dorsal; l, left;p, posterior; r, right; SM, superficial mesoderm; st., stage; v, ventral; veg, vegetal.

Interestingly, at neurula stages the SM cells of the blastula/gastrula are located in the posterior part of the gastrocoel roof forming the gastrocoel roof plate (GRP; Fig. 2A). Nearly every cell of the GRP exposes one single cilium. A similar structure was described for *X. tropicalis*, a closely related species (Shook et al. 2004). In 2007, our group analyzed the GRP function in detail in the context of LR development. To describe the GRP development during neurulation, morphological analysis by scanning electron microscopy (SEM) was performed. Directly after gastrulation (stage 13) only a few very short cilia were found which were positioned in the center of the cell. During ongoing neurulation cilia number and length increased and more cilia were shifted

towards the posterior pole of the cell. At stage 17/18 most cells exhibited monocilia which were localized to the posterior pole (Fig. 2B-D). Thus, the GRP qualifies as a structure to establish a cilia-driven leftward flow in much the same way as described for other vertebrates.

To visualize directed extracellular movements above the GRP, fluorescent beads were added to dorsal explants. Particle motion was analyzed using a semi-automated tracking method of time-lapse movies. A strong leftward flow above the GRP of stage 17/18 embryos was detected, matching the timing of cilia development described by SEM (Fig. 2E, F). To prove that leftward flow was really necessary for LR axis determination, the viscosity of the extracellular fluid was increased by injecting 1.5% methylcellulose into the gastrocoel towards the GRP. This treatment resulted in absence of left-sided Nodal cascade induction, leading to the conclusion that cilia-driven leftward flow above the GRP is essential for LR development in X. laevis (Schweickert et al. 2007).

IV. Working hypothesis

The focus of this work was on LR axis development of the African clawed frog *X. laevis.* Two diverging models exist about the initiation of symmetry breakage in the frog, i.e. the 'ion-flux' and leftward flow hypotheses. Experimental manipulation of 'ion-flux' or the cilia-driven leftward flow, respectively, results in disturbance of the wildtypic left-sided Nodal cascade. However, the time point of symmetry breakage proposed for these models differs as the 'ion-flux' is supposed to take place during early cleavage stages and the leftward flow occurs in neurula embryos. Consequently, the question arose whether these mechanisms are redundant or acting in parallel to each other - or if the 'ion-flux' represents a prerequisite for proper leftward flow establishment. To investigate a potential connection, two components of the 'ion-flux' model, gap junctions and serotonin, were re-examined in the context of leftward flow development.

Therefore, the following main issues have been addressed in the present PhD thesis:

(1) When and how is gap junctional communication involved in LR development?

Inhibition of GJC at different time points and its influence on left-sided Nodal cascade induction was used to reveal the developmental stages in which GJC was relevant for LR development. If GJC was involved in leftward flow establishment, experimental inhibition of GJC should lead to altered morphogenesis of the GRP and disturbance of cilia-driven fluid flow. Therefore, GRP morphology and marker gene expression analysis was performed to investigate such a relationship.

(2) What is the consequence of loss of function of the serotonin signaling pathway?

Serotonin is thought to be distributed during early cleavage and to accumulate unilaterally. By pharmacological inhibition the serotonin receptor 3 class was identified as a LR-relevant factor. However, the downstream target of early serotonin signaling is not yet described. By specific knock-down of one subunit of the receptor 3 family followed by leftward flow analysis a possible role of this receptor for cilia function was assessed.

Results

I. Leftward flow: evolutionary conservation and downstream events

During previous analysis of the ciliated epithelium of the gastrocoel roof (gastrocoel roof plate; GRP) of *X. laevis*, we could prove the necessity of the GRP for left-right (LR) axis development (Schweickert et al. 2007). During the last four years follow-up studies have been performed to examine downstream signaling events in *X. laevis* and GRP homologous structures in other species.

I.1 Leftward flow in fish, amphibians and mammals

In 2007 our group compared the LR-relevant ciliated structures in *X. laevis*, rabbit and mouse neurula embryos. In mouse, analysis of *gsc* which is expressed within the organizer of 8-day old embryos, revealed clear distinction between the organizer tissue and the ciliated epithelium (PNC). Furthermore, the bilateral expression pattern of *Nodal* in all three species analyzed for this publication confirmed that the PNC/GRP was not part of the organizer but was found to be located more anterior to it (Blum et al. 2007a). As the description of such a ciliated epithelium in *X. laevis* in the context of LR determination was a quite new finding, comparative studies of two other amphibian species were performed to prove the conservation of the GRP (Fig. 3).

First, in addition to *X. laevis*, two other amphibians, i.e. the closely related anuran *X. tropicalis* and the urodele axolotl *Ambystoma mexicanum,* were examined for a GRP by scanning electron microscopy (SEM; Fig. 3A-C; see MM, I.1.5 and Schweickert et al. 2007; Beyer 2006). In high magnification pictures cilia were analyzed for length, position and number. In the GRP of *X. laevis* about 260 (st.18), in *X. tropicalis* about 150 (st.15/16) and in *A. mexicanum* 1000 ciliated cells (st.17/18) were present (Fig. 3D). In all three species a mean cilia length of 5µm was measured, most cilia were polarized to the posterior pole and cilia-driven flow showed a leftward direction (data not

shown and Thumberger 2011). Based on this analysis and on published data, an overall comparison of cilia number and size/shape of the ciliated structures in different vertebrate species is depicted in Fig. 3D (Okada et al. 2005; Blum et al. 2009; Feistel 2006).

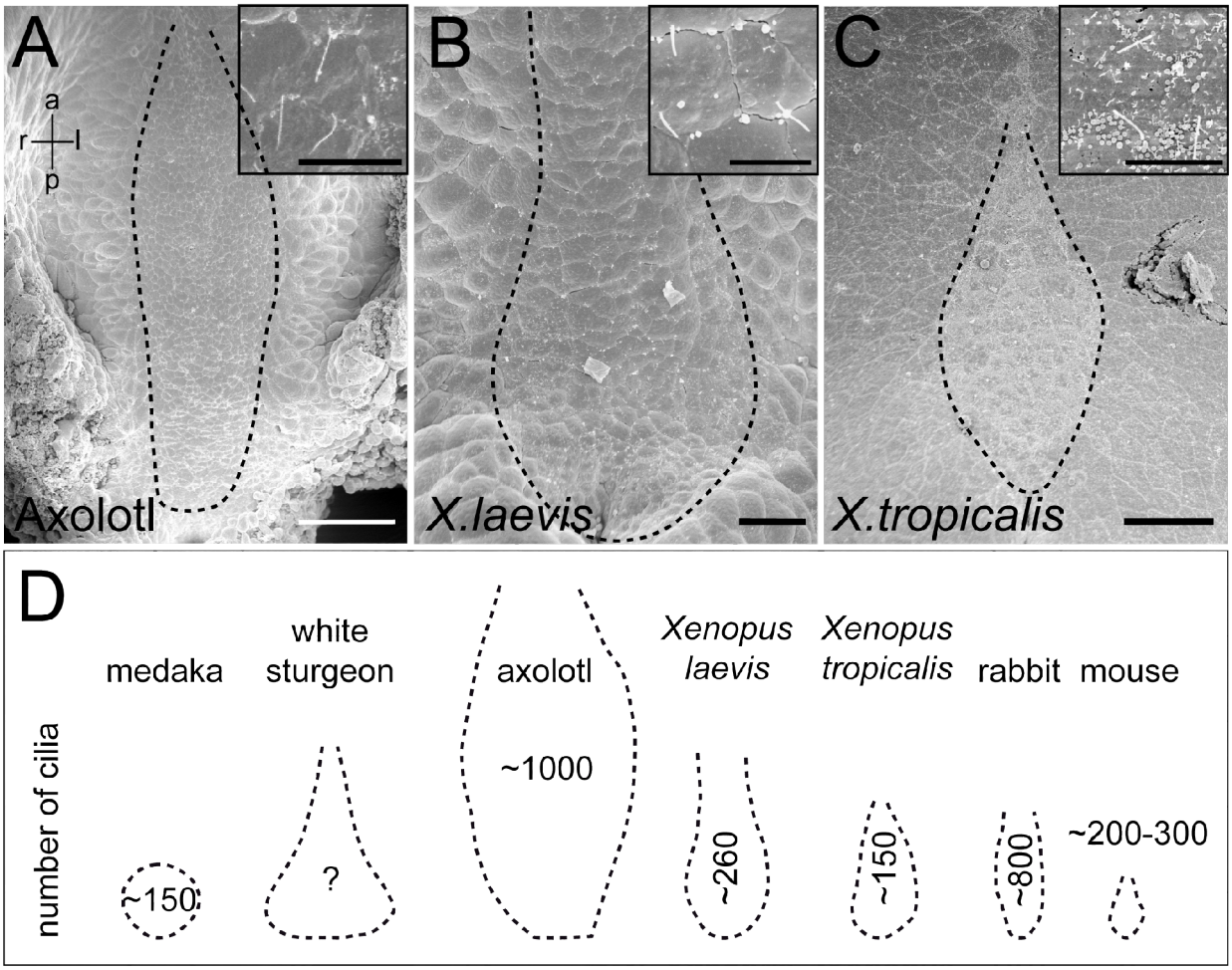

Figure 3: Comparison of the amphibian GRPs and homologous structures in fish and mammals
(A-C) SEM pictures (ventral view, anterior up) of the GRP of the anuran *Ambystoma mexicanum* (axolotl, st.17/18, **A**) and the urodeles *Xenopus tropicalis* (st.15/16, **B**) and *Xenopus laevis* (st.18, **C**).Insets show GRP cilia in detail. Scale bars represent 200µm **(A)**, 50µm **(B,C)** and 10µm (insets).
(D) Cilia number and KV/GRP/PNC size by comparison (medaka/rabbit numbers adapted from Okada et al. 2005). Dashed lines indicate ciliated region.
a, anterior; l, left; p, posterior; r, right.

I.2 Nodal cascade induction depends on *Xnr1* and *Coco* regulation in the midline

In mouse it has been shown that *Nodal* is transcribed in a bilateral fashion at the border of the ciliated PNC before asymmetric Nodal signaling occurs in the left LPM. This earlier *Nodal* expression domain is a crucial prerequisite for asymmetric *Nodal* induction. For example, mouse embryos in which the *Nodal* promoter element for PNC expression was mapped and knocked out, the left Nodal cascade failed to be activated (Brennan et al. 2002; Saijoh et al. 2005). In *Xenopus*, a homologous expression of *nodal-related 1* (*Xnr1*) was found in the posterior gastrocoel roof of neurula embryos. However, the exact nature (cell fate) or function of these *Xnr1* positive cells was not clear. Data addressing this questions are summarized in this chapter as a result of a collaboration of our group. Experiments were done by Philipp Vick, Thomas Thumberger, Melanie Eberhardt, Maike Getwan, Isabelle Schneider and Anke Pachur (see also acknowledgment; Pachur 2007; Vick 2009; Schweickert et al. 2010; Vick et al. 2009; Thumberger 2011). I performed the SEM analyzes of the GRP structure of treated an untreated *Xenopus* embryos.

As a first step the *Xnr1*-expressing cells were analyzed in detail during neurula stages to identify their relative position to ciliated GRP cells. For this, embryos labeled for *Xnr1* by whole-mount *in situ* hybridization (WMISH) were post-fixed for SEM. An overlay of the SEM pictures and photos of the *Xnr1* pattern was created to gain single cell resolution. Thereby, it was shown that *Xnr1*-expressing cells indeed are lateral-most monociliated GRP cells. In addition to that, vibratome-sections of the GRP of *Xnr1*-labeled embryos were compared to sections of embryos stained for the somitic marker gene *MyoD* (Steinbach et al. 1998; Hopwood et al. 1989). The two mRNA patterns clearly showed overlapping transcription in somitic GRP cells (Fig. 1 in Schweickert et al. 2010).

Second, analyzes of the expression patterns of *Xnr1* and *Coco* in neurula stage embryos pre-, during and post-flow were performed. Coco, a member of the Cerberus/DAN family, was described to be involved in LR axis development and can bind directly to *Xnr1* (Vonica et al. 2007). It was expressed in the same cells which displayed bilateral *Xnr1* expression. Loss of Coco function yielded bilateral induction of all three LPM markers, *Xnr1*, *Pitx2c* and *XLefty-A*. Over-expression of *Coco* on the left

side of the embryo led to absence of the Nodal cascade in the left LPM. These observations indicated an inhibitory function of Coco on left-sided *Nodal* induction, most likely by binding to Xnr1 (Vonica et al. 2007). Interestingly, no robust, statistically significant asymmetry of *Xnr1* was seen in the posterior midline at all neurula stages examined. In contrast to that, *Coco*-mRNA distribution was found to be asymmetric, namely predominantly on the right side of the GRP, suggesting that flow acts on *Coco* expression (Fig. 2,3 in Schweickert et al. 2010; Vonica et al. 2007). To analyze the relationship between *Coco* expression and leftward flow, the pattern was further analyzed in leftward flow-impaired embryos.

Flow can be inhibited either mechanically (see Introduction, III.3.2) by injection of 1.5% methylcellulose (MC) into the gastrocoel of neurula stage embryos, or it can be down-regulated by impairment of ciliary motility at the molecular level. Therefore, the *Xenopus dynein heavy chain 9* (*dnah9*), which is part of the motor driving cilia motility, was inhibited by injection of antisense morpholino oligonucleotides (MO; see MM, I.1.4). The GRP was targeted by dorsal marginal zone (DMZ) injections in 4-8-cell embryos where knock-down (KD) of *dnah9* resulted in absence of flow. In *X. laevis*, descendants of single blastomeres do not mix and the first cleavage splits the left and right side (see Introduction, II.2), enabling injections targeting only the left or the right half of the embryo and the GRP, respectively. When performed unilaterally, only KD on the left but not the right side led to LR defects (Vick et al. 2009; Vick 2009; Schweickert et al. 2007). These two techniques, MC and *dnah9*-KD, were used to interfere with leftward flow followed by analysis of the bilateral *Coco* expression. Remarkably, the *Coco* asymmetry found in wildtype stage 19-22 embryos was not seen in flow-impaired specimens. As *Coco* and *Xnr1* expression were found in the same bilateral domain but were differently regulated upon loss of leftward flow, epistatic experiments were performed to clarify the interplay of both components and cilia function. Loss of *Xnr1* on the left side or inhibition of leftward flow resulted in loss of *Pitx2c* in the left LPM, KD of *Coco* on the right side in induction of *Pitx2c* in the right LPM. Right-sided induction of *Pitx2c* upon *Coco*-KD was not influenced by additional impairment of leftward flow. *Coco* loss of function on the left side rescued *Pitx2c* expression in the left LPM of flow-ablated embryos. However, absent left-sided *Pitx2c* upon *Xnr1*-KD could not be restored by *Coco*-MO co-injection (Fig. 4 in Schweickert et al. 2010).

Taken together, impairment of leftward flow by *dnah9*-KD on the left side or MC injection into the gastrocoel led to loss of Nodal cascade induction in the left LPM and was rescued by parallel left-sided *Coco*-KD. *Xnr1*-KD resulted in absent *Pitx2c* expression but was not restored by parallel loss of *Coco* function. Consequently, the data revealed that leftward flow, *Xnr1* and the down-regulation of *Coco* were indispensable for left-sided Nodal cascade induction. This conclusion for symmetry breakage was strengthened by experimental evidences in other model organisms like fish and mouse (Hashimoto et al. 2004; Brennan et al. 2002; Belo et al. 2009; Hojo et al. 2007).

However, in *X. laevis* several factors were identified to play a role in LR axis formation at pre-flow stages (see Introduction, III.3.1). Two of them, gap junctions and the neurotransmitter serotonin, have been analyzed in detail with the results presented in the following chapters.

II. Gap junctional communication and LR development

The establishment of left-sided identity via asymmetric *Nodal* induction is well understood, but the initial symmetry breaking event is still under discussion. Since in *X. laevis* both models for symmetry breakage are described, i.e. 'ion-flux' and leftward flow, *Xenopus* is the only organism to clarify this contentious issue (see also introduction, III.3). Two specific questions are addressed in this chapter. First, at what time point is gap junctional cell-cell communication (GJC) crucial for LR axis development and does „early“ gap junctional activity act on leftward flow or downstream events.

II.1 Inhibition of gap junctional communication using long-chain alcohols

GJC in the 16-32-cell embryo is thought to be necessary for LR development. This was shown, among other approaches, by using the long-chain alcohol heptanol (HepOH) which consists of a seven carbons (7-C) containing chain and is known to inhibit GJC between cells, presumably by squeezing channels closed after membrane intercalation (Guan et al. 1997; Juszczak et al. 2009; Chanson et al. 1989). Short-chain alcohols, i.e. less than 6-C, or alcohol molecules longer than 9-C do not have the ability to block GJC and can be used as controls (Chanson et al. 1989). For clarifying the stages in which HepOH affects LR axis development, incubation experiments covering different developmental stages were performed. HepOH treatment was carried out either from early cleavage (4-16-cell) up to midblastula (stage 9) or, in a second setup, early blastula (stage 6) up to late neurula (stage 19/20). In both cases, HepOH-containing culture medium (0.1xMBSH) was used and embryos were transferred into fresh medium at the indicated time points (Fig. 4). Besides that, control incubation using ethanol (EtOH) were performed. A concentration of EtOH of 1% and higher was shown to interfere with the retinoic acid signaling pathway which has been clearly implicated in organizer specification in the frog (Yelin et al. 2005; 2007). Because of that, it was important to test whether HepOH treatment was able to influence the retinoic acid pathway like EtOH. Indeed, high doses of HepOH (>0.1%) resulted in the disruption of

blastopore closure or a shortened AP axis (not shown). Consequently, in this analysis only low concentrations (0.01%) excluding severe side effects were used, and embryos displaying normal dorsal axis development (DAI=5; dorso-anterior index) were assessed for LR development (Examples shown in Fig. 4B, C). After washing out the alcohol, the embryos were cultivated up to stage 30 for assessment of *Pitx2c* expression or stage 45 for organ situs analysis (Fig. 4A). After HepOH treatment the effect primarily observed was loss of left-sided *Pitx2c* in the LPM, verifying a role of GJ in LR development. The incubation with HepOH from early blastula up to late neurula resulted in about 70% of embryos with absent *Pitx2c* expression, which was a very highly significant effect compared to controls. This effect on *Pitx2c* was much stronger than after treatment from 4-8-cell up to midblastula with only about 20% of absent *Pitx2c* (Fig. 4B). The observation that late HepOH incubation was more efficient was confirmed by the analysis of the organ situs. 30% of late treated embryos exhibited heterotaxia whereas early incubation only resulted in 12% of specimens with laterality defects (Fig. 4C). However, also early HepOH applications led to significant increase of laterality defects when compared to controls (*Pitx2c*, $p=0.001$; organ situs, $p<0.001$; Fig. 4B, C). Control embryos (EtOH for *Pitx2c*, untreated for organ situs) showed less than 5% LR axis defects in both cases.

Taken together, these experiments confirm the published role of GJC in LR axis formation (Levin et al. 1998). However, the data presented here indicated that GJ activity was required rather in late blastula stages or during neurulation for left-sided determination than in early cleavage embryos. Interestingly, after the end of gastrulation and when the cells which will give rise to the ciliated GRP had migrated inside the embryo, HepOH treatments had no or only little effect on LR development (see Introduction, III.3.2 and data not shown). To investigate whether the tissue targeted by HepOH incubation was not efficiently penetrated by simple incubation, injection experiments were performed (Fig. 4A'). Thereby, the developmental stages in which GJC was required should be determined more precisely.

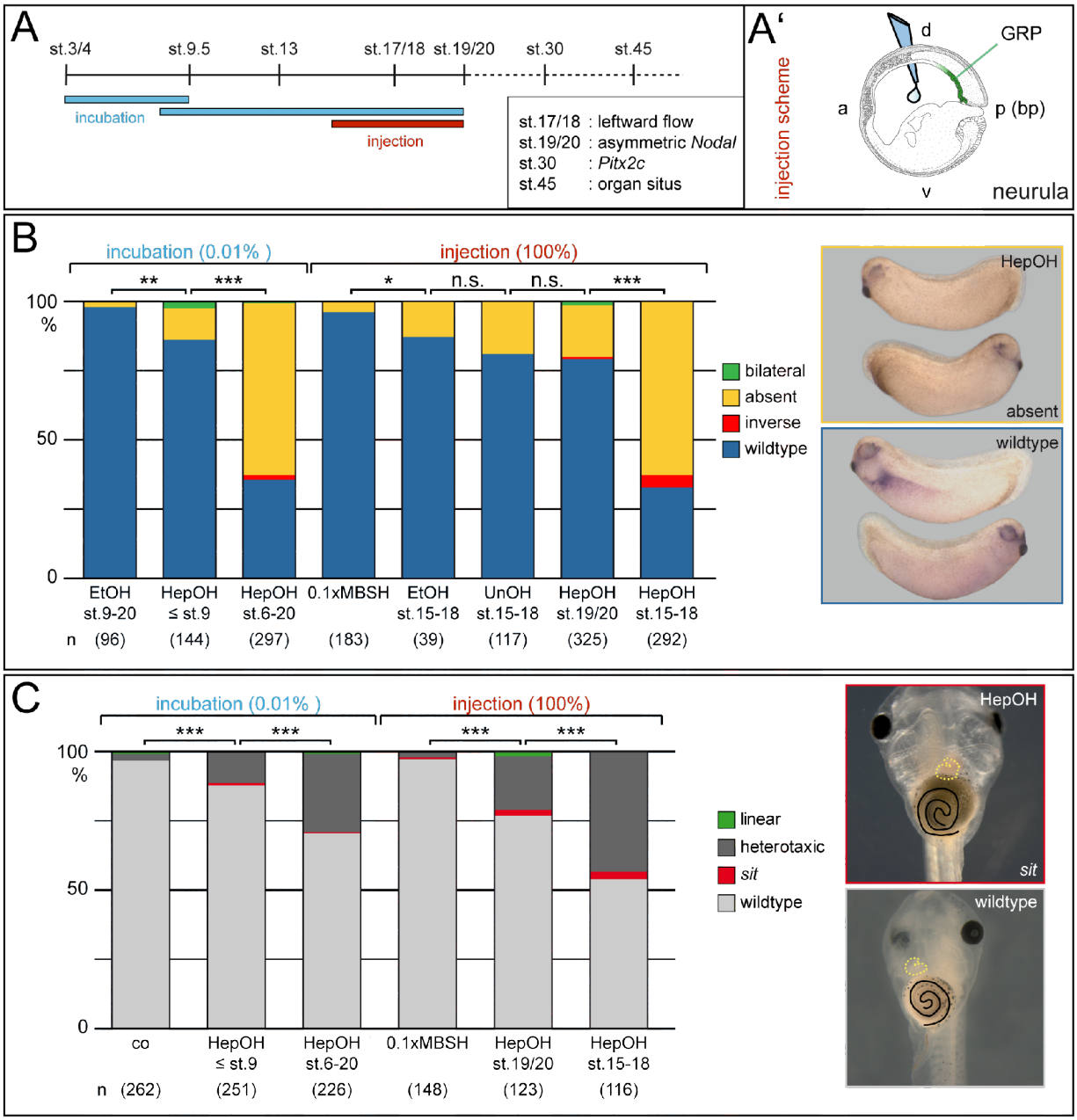

Figure 4: Laterality defects in heptanol-treated embryos

(A) Time scale of *X. laevis* development. LR-relevant stages are lettered. Incubation has been done between 4/8-cell and midblastula or between early blastula and late neurula. Injections were applied in neurula stage embryos.

(A') Gastrocoel injection scheme. A small amount (blue) of 100% alcohol or 0.1xMBSH was injected. GRP epithelium is indicated in green.

(B) Graph of *Pitx2c* analysis. LR axis development was evaluated after alcohol treatments by *Pitx2c* marker gene expression. Examples for HepOH-incubated and control embryos are shown.

(C) Graph of organ situs analysis. Organ morphogenesis of treated embryos was analyzed by assessing heart and gall bladder orientation and gut coiling. Examples for a *sit* and a wildtypic organ situs are shown. Yellow dashed line indicate heart, black line gut coiling.

a, anterior; d, dorsal; co, control; EtOH, ethanol; GRP, gastrocoel roof plate; HepOH, heptanol; p, posterior; *sit*, situs inversus totalis; st.,stage; UnOH, undecanol; v, ventral.

Because lipophilic long-chain alcohols and aqueous solutions like MBSH dissociated very fast in the injection needle a small amount (roughly 20nl) of 100% alcohol was injected. As control 100% undecanol (UnOH, 11-C) which is lipophilic like HepOH but does not influence GJC, and 100% EtOH which is hydrophilic, were used. Unlike suggested by the incubation experiments, *Pitx2c* expression was lost in about 70% of embryos injected with HepOH into the gastrocoel of neurula embryos at pre- or flow stages (stage 15-18). Injections into the gastrocoel of late neurula stages (19/20) led to 23% embryos with absent *Pitx2c* which was not significantly different compared to the control treatments with 22% (UnOH vs. HepOH, stage 19/20; p=0.096) or 14% (EtOH vs. HepOH, stage 19/20; p=0.089) inhibited *Pitx2c* expression (Fig. 4B). These observations were confirmed by assessment of organ situs. Treatments at flow stages (15-18) led to heterotaxia in 45% of cases and to 24% heterotaxia post-flow (19/20), injections of UnOH or EtOH, however, were not done for this analysis (Fig. 4C).
Taken together, inhibition of GJC using the long-chain alcohol HepOH in gastrula and/or neurula stage embryos led to LR defects. Because blocking of GJC at flow stages induced LR defects very efficiently, an interplay of GJC and leftward flow appeared likely to happen. Therefore, the next step was to find connexin (Cx) encoding candidate genes displaying expression patterns in neurula/flow stage embryos. In such a scenario, a GJC-independent activity would be excluded on the one hand, and the subunit composition of GJ which are relevant for LR patterning would be elucidated on the other hand. Consequently, a more specific approach for targeted loss of function should be established for further analysis.

II.2 Expression analysis of *connexin* genes in neurula stage embryos

For *X. laevis* nine gap junctional subunits (*Xenopus* connexins; *xCx*) were described (De Boer et al. 2005; 2006). To find candidates for LR axis development the literature was scanned for potentially interesting *xCx* expression patterns. *XCx40.4* was found to be expressed in somitic tissue (De Boer et al. 2005). As somitic cells represent the lateral-most part of the GRP (see Introduction, III.3.2) an analysis by WMISH for this very gene was performed. No expression in the GRP itself but in more anterior tissue

was detected (data not shown). As no obvious overlapping expression pattern with tissues involved in LR development was visible, *xCx40.4* was not further analyzed.

Two other GJ subunits, *xCx26* and *xCx32*, were described to be expressed in a similar pattern in neurula stage embryos. Interestingly, the human homologous subunits were shown to form heterotypic channels indicating that expression domains in the same tissues could be an evidence for redundant or complementary functions (Bevans et al. 1998; De Boer et al. 2006). Therefore, an in depth expression analysis using RT-PCR and WMISH was performed for each gene (for PCR see MM, I.2.2 and 3).

RT-PCR primer sequences were designed in such a way that amplification of genomic DNA, present as contamination, was not possible. To do so, primers should cover the sequence of two neighboring exons. In the closely related species *X. tropicalis* the homologous sequences of *xCx26* and *32* each displayed an intron located in the 5'UTR region (Ensembl: *xtCx26*, XB-GENE-955798; *xtCx32*, XB-GENE-481038). Because of the high homology of *X. tropicalis* and *X. laevis* sequences (Pubmed: *xCx26,* NM_001087009.1; *xCx32,* NM_ 001101749.1) a putative intron site was assumed for both *xCxs* coding genes (Fig. 5A and data not shown). For testing the existence of intron sequences in *X. laevis* two different forward primers were designed, one located in the 5'UTR in front of the putative intron site (xCx_5'UTRfor) and one in the coding region (xCx_codfor) (Fig. 5A and data not shown). As negative control total RNA probes without prior reverse transcription reaction were used (-RT). The amplified PCR products were separated by size using gel-electrophoresis and visualized by adding the DNA-intercalating fluorescent substance ethidium bromide. As seen by PCR with primers only binding to the coding region, PCR products in both samples were present revealing genomic contamination in the negative control (-RT). In contrast, using the 5'UTR primer only yielded in the +RT probe in an amplified product whereas no specific fragment was observed by using the -RT probe (Fig. 5B, C). These observations supported the notion that the intron site described for *X. tropicalis* in the 5'UTR region is conserved in *X. laevis*. Thus, the problem of genomic contamination of total RNA could be excluded for the following expression analysis by using the 5'UTR primers.

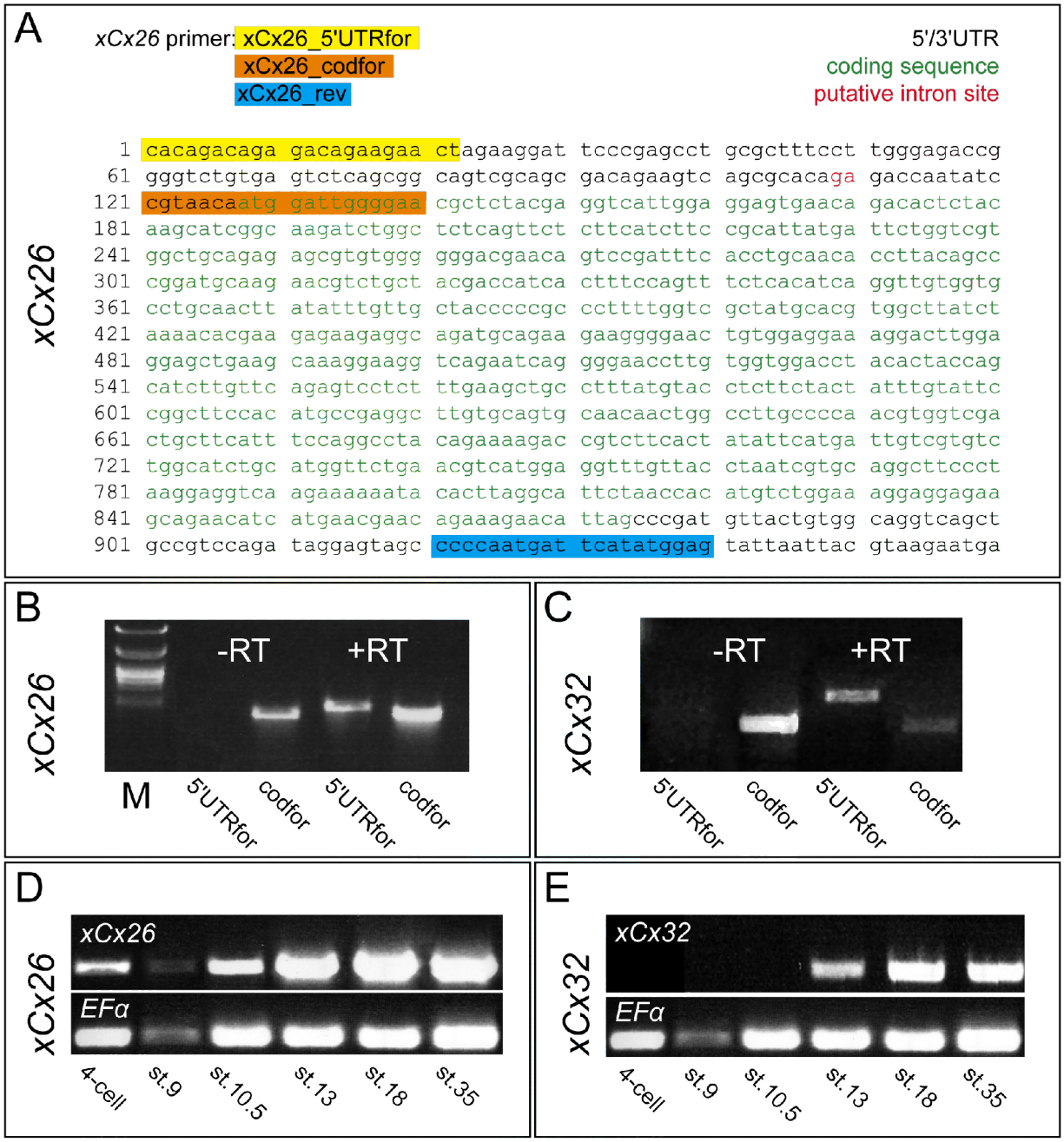

Figure 5: Developmental expression of *xCx26* and *32* by RT-PCR
(A) DNA sequence (5'-3') of *xCx26*. Primer binding sequences are highlighted in yellow, orange (forward primers) and blue (reverse primer). Coding sequence is depicted in green, UTR regions in black and the two bases directly adjacent to the putative intron site in red letters.
(B,C) PCR for *xCx26* and *xCx32*. Two primer pairs were used: **(B)** xCx26_5'UTRfor or xCx26_codfor, each paired with xCx26_rev and **(C)** xCx32_5'UTRfor or xCx32_codfor, each together with xCx32_rev. Two probes were tested: isolated total RNA (-RT) and cDNA (+RT) of tadpole stages. PCR products were detected in all four cases using the codfor primers (*xCx26*, 820bp; *xCx32*, 742bp). Only in +RT probes a PCR product was seen using the 5'UTR primers (*xCx26*, 940bp; *xCx32*, 1057bp).
(D,E) Expression of *xCx26* **(D)** and *32* **(E)** at different developmental time points using 5'UTR primers. *Elongation factor α* (*EFα*) was used as loading control. *xCx26* was expressed in all stages examined. *xCx32* expression was not detected before early neurulation.
xCx, *Xenopus connexin*; M, Marker; RT, reverse transcription; st., stage; UTR, untranslated region; .

Applying a series of cDNA samples of different developmental stages, expression of *xCx32* was detected specifically in early neurula stage and tadpole embryos (Fig. 5E). *XCx26* was found in all analyzed stages (Fig. 5D). To identify the spatial expression of the two GJ subunits WMISH was used.

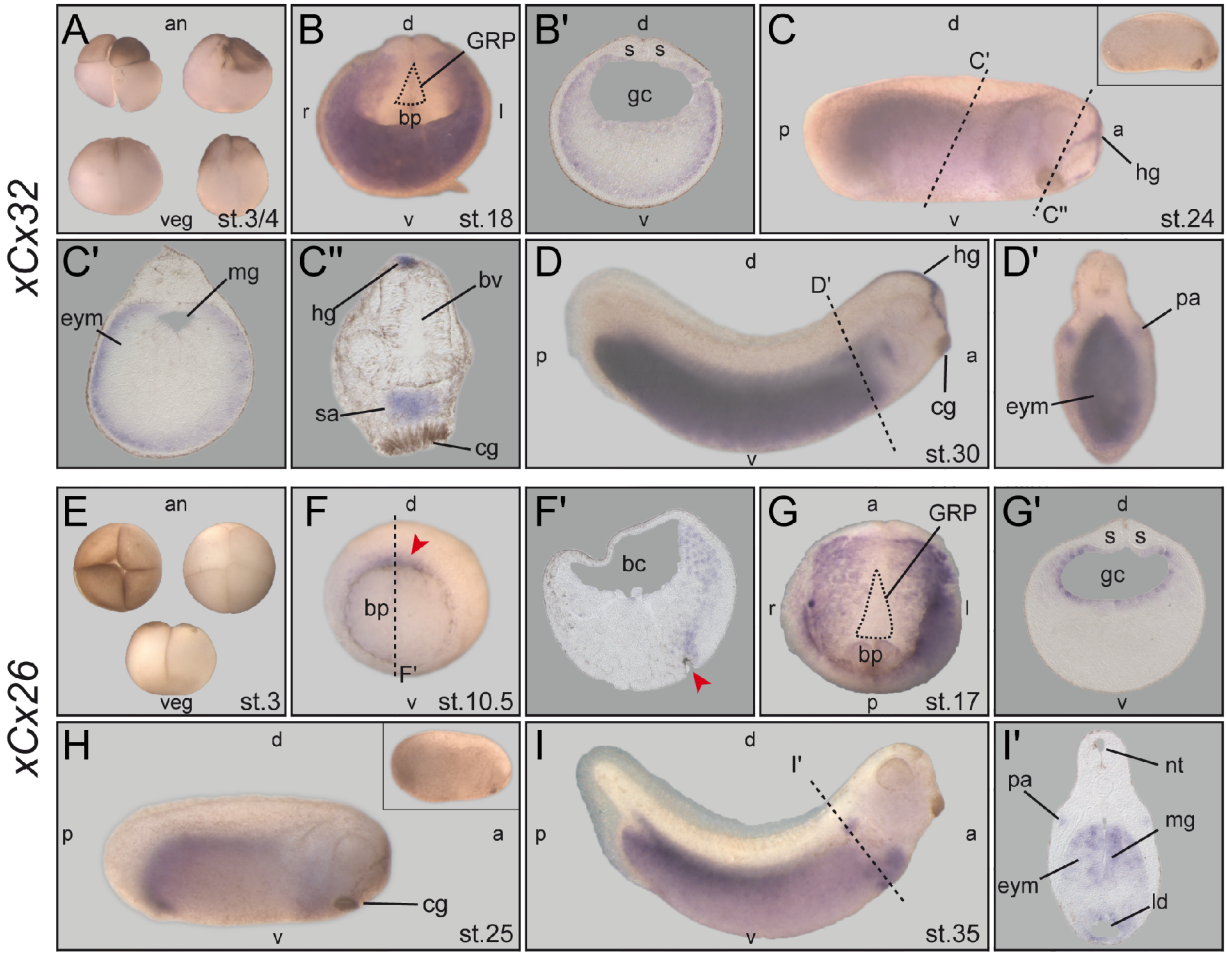

Figure 6: Expression patterns of *xCx26* and *32*

(A-D') Expression of *xCx32*. No expression was detected in st.3/4 embryos (**A**, lateral view, animal to the top). Endodermal expression was seen in neurula stage specimens excluding the GRP tissue (**B**, anterior view, dorsal up, GRP indicated by dashed line, and **B'**). Staining in the endoderm and hatching gland was found in all tadpole stage embryos **(C, C"-D')**. Additionally, *xCx32* mRNA was detected in the stomodeal anlage **(C")** and the pronephros **(D')**. In **C, D** lateral view, dorsal up, anterior to the right. Inset in C shows a sense control embryo.

(E-I') *XCx26* expression. No staining in st.3 embryos **(E)**. At gastrula stages, a faint signal was seen in involuting endodermal cells (**F, F'**, red arrowhead indicate dorsal lip formation). Endodermal staining only in the gastrocoel lining but not in more ventral tissue was found in neurula specimens (**G**, ventral view, anterior up, GRP indicated by dashed line, and **G'**). At tadpole stages *xCx26* expression was detected in dorsal endoderm (**H, I**, lateral view, dorsal up, anterior to the right, and **I'**), in the liver and the pronephros **(I, I')**.

Dashed lines indicate sectional planes **(C, D, F, I)**. a, anterior; an, animal; bc, blastocoel; bp, blastopore; bv, brain ventricle; cg, cement gland; d, dorsal; eym, endodermal yolk mass; gc, gastrocoel; GRP, gastrocoel roof plate; hg, hatching gland; ld, liver diverticulum; mg, midgut; nt, neural tube; p, posterior; pa, pronephric anlage; s, somites; sa, stomodeal anlage; st., stage; v, ventral; veg, vegetal.

There was no staining of *xCx32* in early cleavage stage embryos (Fig. 6A). In neurula stages expression of *xCx32* was found to be restricted to the endoderm including gastrocoel lining surrounding the GRP (Fig. 6B, B'). Additional domains were found in the hatching gland, stomodeal anlage and the pronephros of tadpoles (Fig. 6C-D'). WMISH for *xCx26* differed from the results of the RT-PCR. No staining was detected in pre-gastrulation stage embryos (Fig. 6E). At early gastrula stages expression was found at the forming dorsal blastopore in cells that had already involuted (Fig. 6F, F'). In neurula stage embryos *xCx26* mRNA was detected in the whole gastrocoel except the mesodermal tissue of the GRP. Notably, the expression was restricted to the gastrocoel lining and was not present in more ventral endodermal tissue (Fig. 6G, G'). In tadpole embryos mRNA staining was detected in the pronephros, the liver and the endoderm as previously described in literature (Fig. 6H-I' and De Boer et al. 2006).
Based on these data it was concluded that gap junctional subunits were expressed in overlapping domains in the endodermal lining of the gastrocoel of neurulae with no expression in the GRP proper. A co-expression at tadpole stages was found in the endoderm and primitive kidney tissue, the pronephros, as well. However, no staining was detected in tissues described to be relevant for LR development, i.e. GRP or the LPM. But the expression in kidney tissues, which represents a ciliated structure, indicated that a link between cilia function (sensing or generating extracellular fluid flow) and GJC was conceivable. To further analyze a possible role of *xCx26* and *32* for LR establishment, gain of function experiments were performed.

II.3 Gain of function of *xCx26* and *xCx32*

Levin and Mercola (1998) used in their studies constructs either for loss of function by the dominant-negative *H7* dorsally or for gain of function by *xCx26*, *xCx43* and *xCx37* mRNA injection ventrally. In all four approaches they obtained heterotaxic embryos (Levin et al. 1998). However, it was not clear if the *xCx26* construct used by the authors represented the same sequence as taken for the here presented work as the subunit was renamed recently (formerly *xCx29*). Because of this, effects upon *xCx26* and *xCx32* misexpression were (re-) investigated. Therefore, *xCx* over-expression

constructs were cloned to examine (1) subcellular (co-) localization at the membrane of both subunits for testing the functionality of the constructs used in this study and (2) LR development in injected specimens. *XCx* constructs were subcloned into the Cs^{2+} vector, *xCx26* fused to *green fluorescent protein* (*eGFP, xCx26::eGFP*) and *xCx32* was tagged with the sequence of *red fluorescent protein* (*RFP, xCx32::RFP*). The fluorescent protein coding sequences were attached to the C-terminal end of the respective *xCxs* (Bukauskas et al. 2001; Lauf et al. 2001).

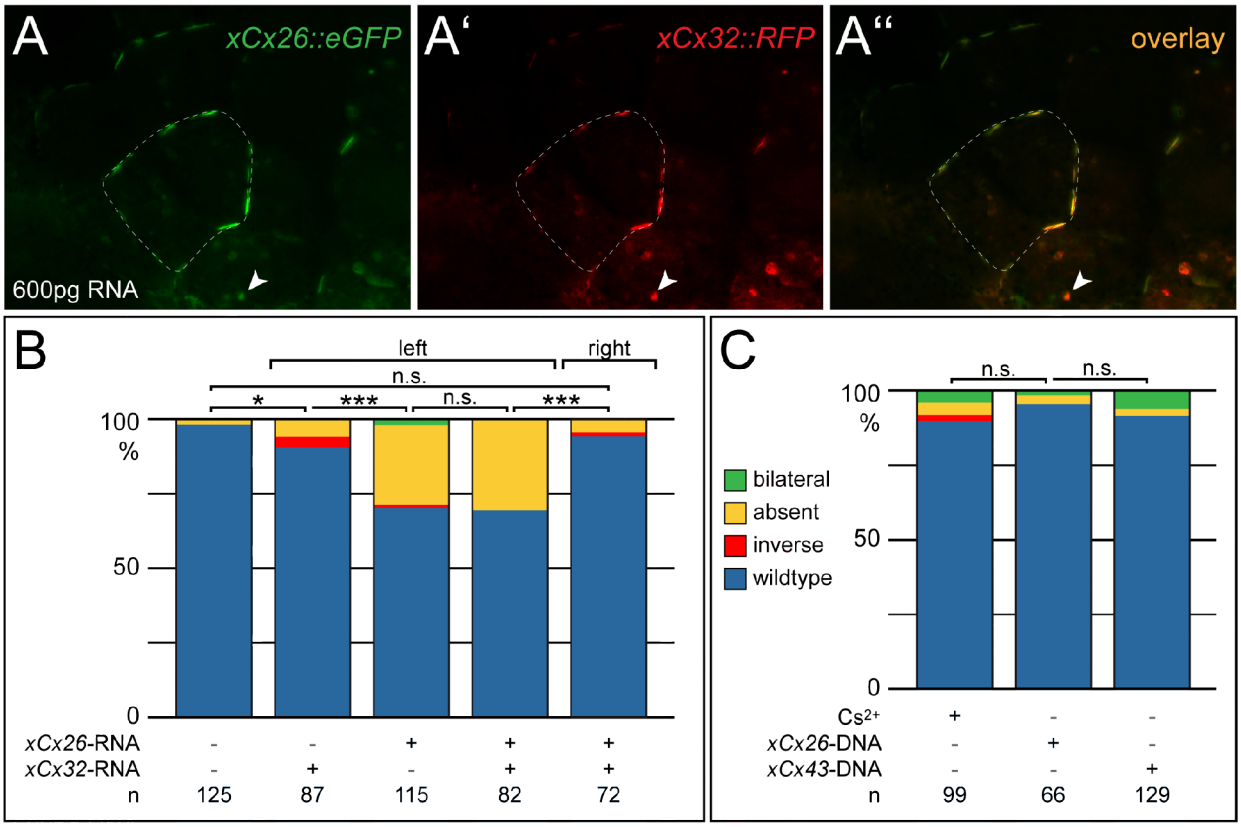

Figure 7: Over-expression of single GJ subunits
(A-A") Subcellular *xCx* localization. 600pg mRNA of two fluorescent fusion constructs (*xCx26::eGFP* (A); *xCx32::RFP* (A')) were co-injected animally in 4/8-cell embryos. Protein localization was examined in blastula/gastrula stages. Both *xCx* were detected co-localized at the cell membrane and in vesicles.
(B) Injection of *xCx*-mRNA. Left-sided over-expression of *xCx26* (400pg) led to LR defects in a very highly significant manner compared to the control, whereas *xCx32* had only a weak effect (p=0.013). The results by co-expression of both *xCx* compared to *xCx26* single injections were not significantly different (p=0.124). Also right-sided over-expression had no effect (vs. co, p=0.131).
(C) Injection of *xCx-D*NA. Injection of the empty expression vector $Cs2^{+}$ (1pg) was used as control. Over-expression of *xCx26* and *xCx43* had no effect on LR development ($Cs2^{+}$ vs. *xCx26*, p=0.107; $Cs2^{+}$ vs. *xCx43*, p=0.427).
n, number of embryos analyzed; n.s., not significant.

For analysis of subcellular localization, 600pg mRNA of *xCx26::eGFP* and *xCx32::RFP* were injected into one cell of the animal pole in 4-8-cell embryos and fluorescence was analyzed at blastula/gastrula stages. Each fusion protein was detected intracellularly mostly in vesicular structures and attached to the cell membrane. In specimens in which both constructs were co-injected, a clear overlaying membrane localization of eGFP and RFP was visible (Fig. 7A-A"). Because Cxs were described to be unaffected by proteins fused to the C-terminus and, in addition, based on the subcellular distribution shown here which is typical for GJ, it was concluded that the fusion constructs could be used for functional studies (Fig. 7A-A" and Bukauskas et al. 2001; Lauf et al. 2001). For the second step, the analysis of LR axis defects provoked by misexpression of GJ subunits, mRNAs for *xCx26* and *32* were injected into 4-8-cell embryos either ventrally or dorsally into the MZ followed by examination of *Pitx2c* expression at tadpole stages (for the injection scheme see also Fig. 8A). Left-sided co-injection of the *xCx* constructs inhibited induction of *Pitx2c* in a very highly significant manner whereas right-sided misexpression had no effect (Fig. 7B). Both, left ventral and left dorsal injections had the same outcome (not shown). To answer the question if both subunits were needed to alter laterality, each *xCx* was overexpressed individually. Interestingly, *xCx32* injection affected LR development only slightly (co vs. *xCx32*, p=0.013). However, *xCx26* left-sided misexpression led to 27% embryos lacking *Pitx2c* which was very highly significant different to the control (2% absent *Pitx2c*) but not to over-expression of both *xCx'*s with 30% absent marker gene expression (p=0.124, Fig. 7B). This indicated that *xCx26* represented the crucial factor for induction of laterality defects by Cx gain of function. To confine the timing of effectiveness of ectopic *xCx* misexpression, *xCx26*-DNA was injected, which should not be transcribed before MBT (stage 8/9). Levin and Mercola (1998) got laterality defects by over-expression of another GJ subunit, i.e. *xCx43.* Thus, also DNA of this very subunit was tested. No significant increase of *Pitx2c* alteration was seen in *xCx*-injected specimens using DNA compared to control injections performed with the expression vector Cs^{2+} alone (Fig. 7C).

These results showed that tagged proteins of *xCx26* and *32* were co-localized at the cell membrane and in vesicles. However, only misexpression of *xCx26*- but not *xCx32*-mRNA on the left side resulted in laterality defects.

II.4 Knock-down of *xCx26* and *xCx32* induced laterality defects

To analyze the endogenous role of *xCx26* and *xCx32* for establishment of the LR axis loss of function experiments using MOs were performed. The sequence of each *xCx* which was targeted by the MO spanned the ATG start codon region (*xCx26*-MO, *xCx32*-MO). Upon MO binding, translation of mRNA encoding these GJ subunits should be inhibited. A mixture of *xCx26*- and *xCx32*-MO (1-1.5pM each) was injected either dorso-laterally or ventro-laterally into the left blastomeres of the 4-cell embryo (Fig. 8A). Accurately injected embryos were detected by co-injection of *eGFP*-mRNA (Fig. 8B-D). Dorsal injections targeted the dorsal midline tissues (Fig. 8C), i.e. the dorsal lip at gastrula and the neural tube, hypochord, notochord, part of the somites, intermediate mesoderm and the GRP of neurula stage embryos. Ventro-lateral injections led to KD in more lateral tissues (Fig. 8D) comprising skin, LPM and blood forming tissue in neurula stage embryos. Dorsal loss of xCx function resulted in a phenotype which was characterized by small eyes, small heads (Fig. 8E, left dorsal) and sometimes bending towards the injected side (not shown), while ventral injections did not reveal abnormal axis development (Fig. 8E, left ventral). Expression analysis of *Pitx2c* was used as read-out for LR development in uninjected control embryos, control-MO (co-MO) and *xCx*-MO-injected specimens. In untreated control and right-sided *xCx*-MO-injected embryos, no effect on LR development was observed. However, the number of embryos with reduced or absent *Pitx2c* expression increased very highly significant upon left ventral or left dorsal *xCx*-KD, as compared to controls (Fig. 8F). In 70% of embryos which were dorsally injected and 30% of ventrally injected specimens *Pitx2c* expression was inhibited (Fig. 8F). To test whether function of these GJ subunits was needed upstream or downstream of Nodal signaling for *Pitx2c* induction in the left LPM, *Xenopus nodal-related 1* (*Xnr1*)-DNA was co-injected with the *xCx*-MO. *Xnr1*-DNA (4pg) instead of mRNA was used to avoid endoderm and mesoderm induction/patterning by early Xnr1 protein function. *Xnr1*-mRNA would be translated before MBT and thus would have caused early developmental defects. The co-injection of *Xnr1*-DNA restored *Pitx2c* expression in 46% of embryos. Also, ventral *xCx* loss of function (30% absent) was rescued upon *Xnr1* over-expression (7% absent) in a very highly significant manner (Fig. 8F).

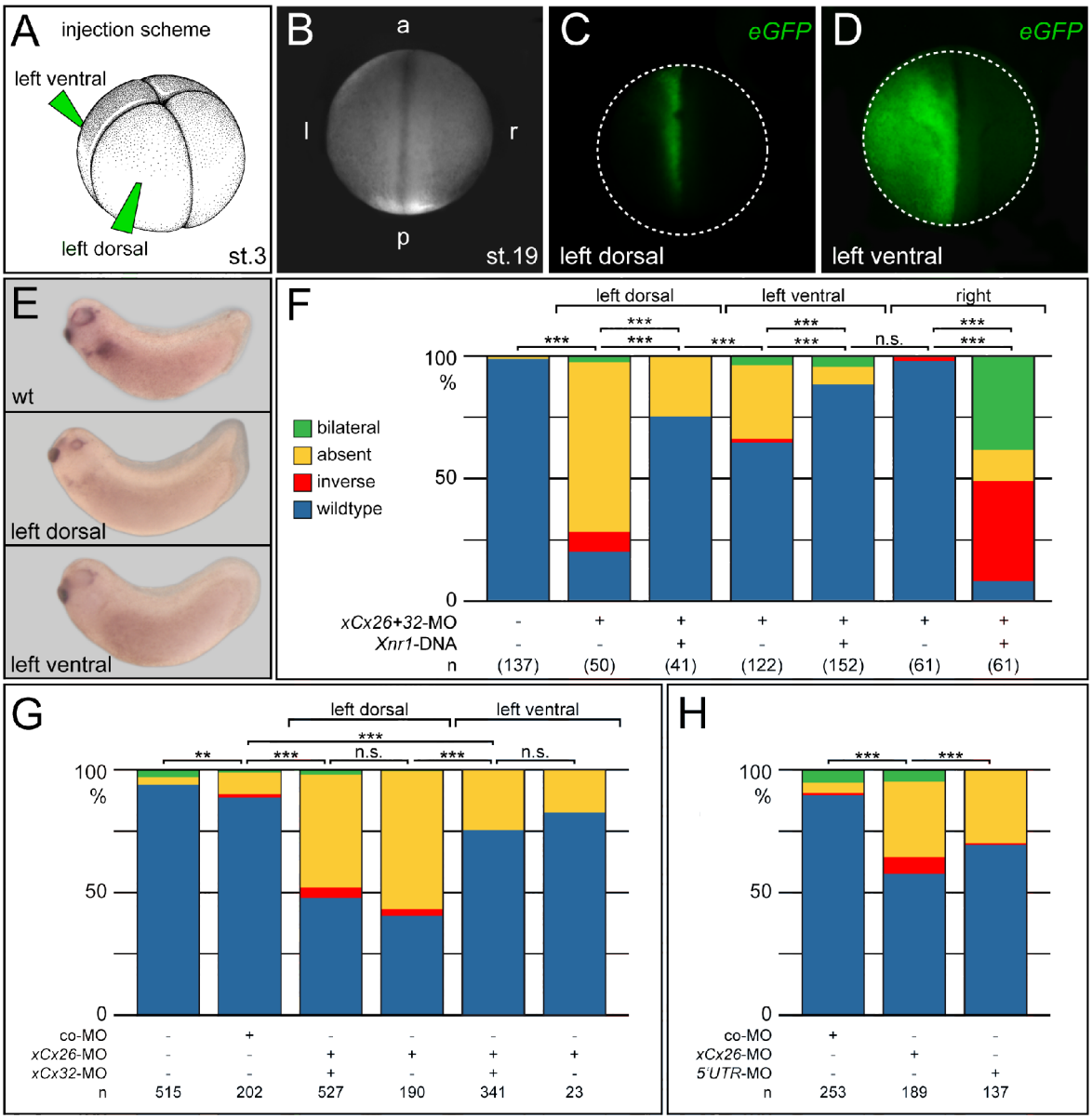

Figure 8: *Connexin* knock-down led to laterality defects

(A) Injection scheme of the 4-cell embryo (dorso-lateral view).

(B-D) Targeted tissue in st.19 embryos. *eGFP*-mRNA was used as lineage tracer and analyzed in st.19 embryos **(B)**. Dorsal injections targeted the dorsal midline **(C)**, left ventral injections left lateral tissue **(D)**.

(E) *Pitx2c* expression analysis. WMISH for *Pitx2c* revealed absent staining in injected embryos whereas the wt displayed normal left-sided expression. Dorsal injections led to small heads and eyes on the targeted side.

(F) Graph of *Pitx2c* analysis. *XCx26* and *xCx32* double KD (each 1-1.5pM) inhibited *Pitx2c* expression significantly when injected into the left but not into the right side (p=0.428). This effect could be rescued in a very highly significant manner by *Xnr1*-DNA (4pg) co-injection.

(G) Evaluation of *xCx26* single KD compared to *xCx*-MO co-injection. The defects induced by both *xCx*-MOs was not significantly different to *xCx26*-MO single injection (dorsal: *xCx26+32*-MO vs. *xCx26*-MO, p=0.057; ventral: *xCx26+32*-MO vs. *xCx26*-MO, p=0.159). Co-MO injection led to high significant increase of embryos displaying laterality defects compared to the uninjected control (p=0.007).

(F) *XCx26*-MO specificity. Injection of a second MO, which bound to the *xCx26* 5'UTR-region, increased the number of embryos lacking *Pitx2c* very highly significant compared to co. The same was shown for *xCx26*-MO. Each MO (1pM) was injected into the left dorsal and ventral blastomere laterally.

n, number of embryos analyzed; n.s., not significant; st., stage; wt, wildtype.

As mentioned above, injection of *xCx*-MO into the right side had no effect on LR development. *Xnr1*-DNA co-injection led to right-sided *Pitx2c* induction in about 90% of embryos, resulting in Nodal signaling which was not prevented by parallel *xCx*-KD (Fig. 8F). These results suggested that GJC had a role for left-sided Nodal cascade induction upstream of the core factor Nodal.

Next, the LR relevance of homotypic channels consisting of only one subunit was tested by single *xCx*-KD. *XCx32* loss of function resulted in a weak effect on LR axis determination when injected dorsally (not shown). In contrast, *xCx26*-MO injections (1-1,5pM) inhibited *Pitx2c* expression in a very highly significant manner (dorsal, 56%; ventral, 17%). These effects were not significantly different from those induced by *xCx26*- and *xCx32*-MO double KD (dorsal, 46%; ventral, 25%; Fig. 8G). These results indicated that only xCx26 was necessary for LR development and was therefore used for further analyzes. The specificity of the *xCx26*-MO was tested using a second MO which was designed to bind to a sequence of the *xCx26* 5'UTR-region (*5'UTR*-MO), non-overlapping with the *xCx26*-MO binding site. The *5'UTR*-MO and the *xCx26*-MO were each injected into the left dorsal and ventral blastomeres of 4-cell embryos. Loss of function using the *5'UTR*- or the *xCx26*-MO resulted in an increase of embryos with absent *Pitx2c* expression compared to co-MO injected specimens ($p<0.001$; Fig. 8H).

In summary, this part of the present study showed that left-sided KD of *xCx* inhibited the induction of *Pitx2c* expression, and this phenotype was rescued by *Xnr1*-DNA co-injection. Interestingly, only the endogenous function of xCx26 but not of xCx32 seemed to mediate the effect on LR determination. The specificity of the effect observed upon *xCx26*-KD was proven by using a second MO which was complementary to a sequence of the *xCx26 5'-UTR*.

II.5 Effects of *xCx* loss of function on GRP development

Because *xCx26* expression was found in gastrula stage embryos at the dorsal lip of the blastopore (see results, II.2), an effect of *xCx26*-KD on GRP development was examined by marker gene expression and morphology analysis. A disturbed GRP morphology would also provide an explanation for loss of left-sided Nodal cascade

induction (Vick et al. 2009).

For the investigation of the GRP, a batch of embryos was injected with 1pM *xCx26*-MO unilaterally into the left side. At stage 18, one half of the batch was fixed for SEM preparation. The remaining embryos were cultivated until they reached stage 30 for *Pitx2c* analysis to evaluate, if the KD was effective in this experiment. As *Pitx2c* was inhibited efficiently compared to the co-MO-injected specimens (not shown), SEM analysis was performed. SEM pictures at a magnification of 1000-fold were taken and the central region of the GRP was evaluated for ciliation rate, cilia length and cell surface area (see MM, I.1.5 and Schweickert et al. 2007). Co-MO-injected specimens were compared to the uninjected right side and the *xCx26*-MO-targeted left side, respectively. No significant change of the ciliation rate was observed (Fig. 9A). However, the *xCx26*-MO-injected side revealed a highly significant decrease in cilia length when compared to the uninjected side ($p=0.002$) and a very highly significant decrease when compared to co-MO-injected specimens (Fig. 9B). Surprisingly, also the uninjected control side showed a significant decrease in cilia length when compared to co-MO embryos ($p=0.0276$). The slightly shorter cilia observed on the untreated right side of *xCx26*-MO left-side-injected embryos indicated that these specimens were fixed at earlier developmental stages than the co-MO-injected ones. Furthermore, the cell size changed upon *xCx26*-KD compared to co-MO ($p=0.005$) and uninjected right side ($p=0.004$, Fig. 9C).

In addition to the SEM analysis, marker gene expression of the lateral-most GRP cells was investigated. Specimens injected unilaterally into the left DMZ were examined by WMISH for bilateral expression of *Xnr1*. In these experiments co-injection of *xCx26*- and *32*-MO were performed because they were done before ruling out a significant role of *xCx32* for LR development (see results, II.3). Again, the effectiveness of the experiment was controlled by *Pitx2c* expression analysis. In 51% of embryos *Pitx2c* was inhibited (Fig. 9D). *Xnr1* expression was classified into three categories: normal bilateral expression (R=L), stronger expression on the right side (R>L) or no expression at all (absent). *Xnr1* analysis revealed a very highly significant increase of embryos with diminished left-sided expression upon *xCx*-KD (Fig. 9E). The efficiency of the KD was comparable whether *Xnr1* or *Pitx2c* were analyzed.

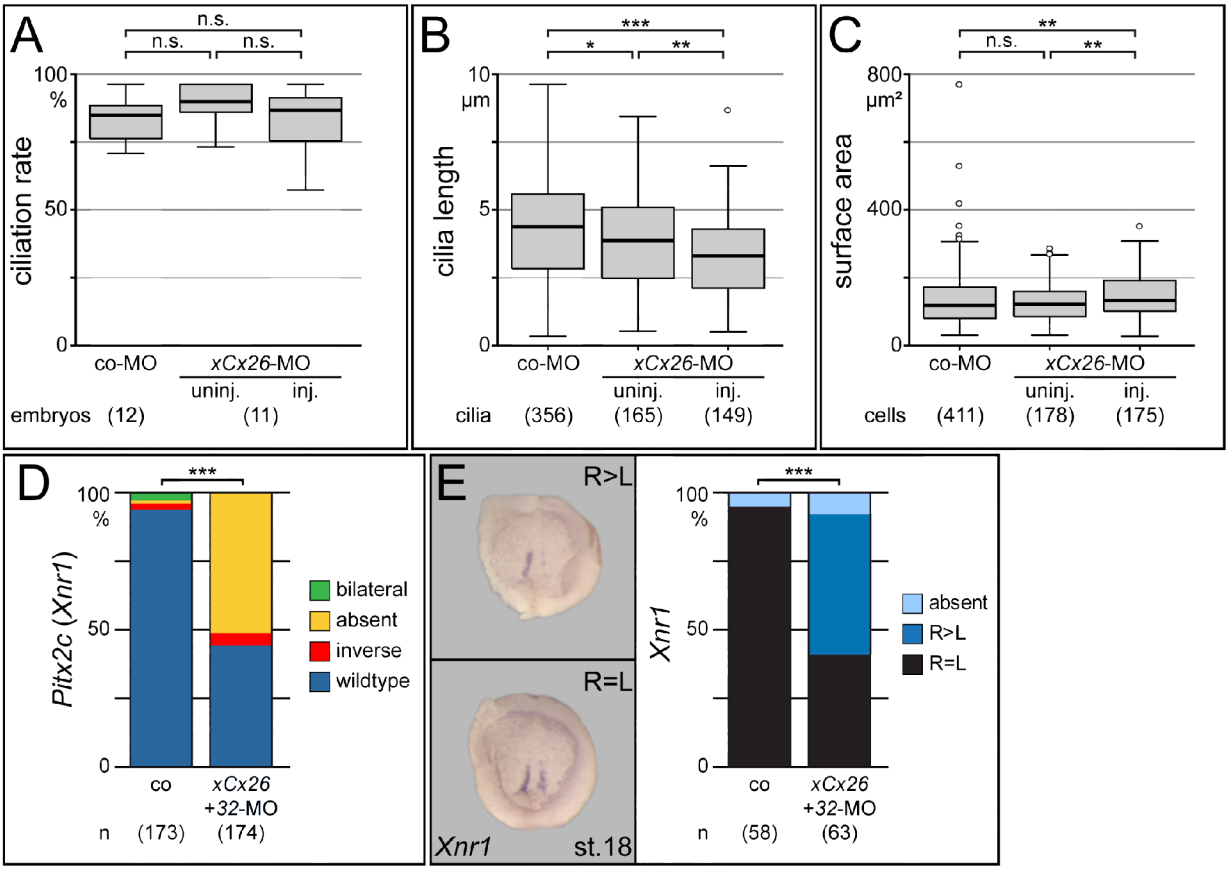

Figure 9: Analysis of GRP morphology and *Xnr1* expression in GJC-impaired embryos
(A-C) Analysis of SEM pictures. The GRP of st.18 embryos (unilateral left injection with *xCx26*- and *32*-MO into 4-cell embryos) was examined by SEM. Ciliation rate **(A)**, cilia length **(B)** and cell surface area **(C)** was measured in ImageJ and data have been assessed using statistical-R (see MM, I.1.5). Co-MO and uninj. side have been compared to the *xCx26*-MO inj. side. This analysis was done in collaboration with Thomas Thumberger.
(A) No significant difference of ciliation rate was seen (co-MO, 85.92% ± 8.16; uninj. side, 92.63% ± 7.44; inject. side, 86.23% ± 12.37; uninj. side vs. co-MO, p=0,0584; inject. vs. uninj. side, p=0.268; co-MO vs. inject. side, p=0.665).
(B) Cilia length was highly significant (p=0.002) decreased in the inject. (3.27µm ± 1.17) compared to the uninj. side (3.75µm ± 1.41) and very highly significant compared to co-MO-injected specimens (4.05µm ± 1.46). Also the uninj. side displayed significantly shorter cilia as against the co-MO-injected specimens (p=0.028).
(C) Cell surface area was enlarged highly significant in the *xCx26*-MO-inject. side (136.52µm^2 ± 70.12) as against co-MO (122.43µm^2 ± 80.69; p=0.005) or the uninj. side (116.93µm^2 ± 59.63; p=0.004). Co-MO and uninj. side showed no significant difference (p=0.8).
(D, E) *Xnr1* expression. *XCx26*- and *32*-MO have been injected unilaterally (left dorsal blastomere of 4-cell stage embryos) and either fixed at st.18 for *Xnr1* **(E)** or at st.30 for *Pitx2c* expression **(D)** analysis. Examples for *Xnr1*-stained embryos are shown in **E** (ventral view onto the gastrocoel roof, anterior up). *Xnr1* patterns were categorized as follows: bilateral expression (R=L), stronger staining on the right side (R>L) and no expression (absent). A reduction of *Xnr1* on the left side was found in very highly significant more embryos compared to the control **(E)**.
inj., injected side; n.s., not significant; st., stage; uninj., uninjected side.

In summary, these experiments showed that the marker gene expression of *Xnr1* in the lateral-most GRP cells was reduced upon *xCx*-KD. Furthermore, alterations of the GRP morphology were detected in *xCx26*-MO-injected specimens. This was an unexpected

result as this very subunit was not expressed in the GRP cells. Nevertheless, inhibition of GJC using the long-chain alcohol HepOH-induced laterality defects even when injected into the gastrocoel of neurula embryos (see results, II.1). In these specimens bilateral expression of *Xnr1* and GRP development was already established which strongly suggested a dual role for GJC during LR development. In early stages, GJ activity was required for development of the GRP including *Xnr1* marker gene expression. In later stages but before left-sided Nodal cascade induction it is reasonable to assume that GJC has a role for the transfer of a signal from the midline towards the left side.

II.6 Visualization of subcellular localization of Xnr1 protein

How the initial left-sided signal, which is released or induced by the leftward flow, gets transferred to the LPM is still not resolved. One hypothesis postulates that Nodal itself represents this mediator but its diffusion has not been proven yet. As antibodies are not available, experiments in mouse were performed using Myc-tagged Nodal (Oki et al. 2007). Again, no clear result was obtained as to asymmetric diffusion of Nodal. To be able to address this issue in *Xenopus* on the one hand and, on the other hand, as GJC probably had a role in the transfer of the midline signal, i.e. Nodal distribution to the left LPM, an assay should be established using tagged Nodal protein to visualize this process *in vivo*.

Members of the TGFβ protein family are secreted molecules. They regulate gene expression in a concentration and time-dependent manner at a distance from the protein source (morphogens; see Introduction, III.1; Wolpert 1969). In chick the distribution of GFP-tagged Nodal and Lefty was measured and found at distances up to 500µm (Sakuma et al. 2002). In *Xenopus*, a *Xnr2::GFP* fusion construct was used which made it possible to follow protein movement in animal cap experiments (Williams et al. 2004). Based on these findings, a *Xnr1::eGFP* and different tagged deletion constructs have been designed to examine protein domain function and movement under changing conditions.

II.6.1 Cloning of *Xnr1::eGFP* fusion constructs

The Nodal proprotein consists of three main domains, namely the signal peptide, the pro- and the mature protein domain (Fig. 10). The secreted proprotein gets cleaved in the extracellular space by proprotein convertases at the -RXXR- cleavage site. The prodomain is thought to inherit protein stability and/or diffusion range. The mature domain is needed for activation of downstream signaling by receptor binding (see introduction, III.1.1 and Shen 2007). To analyze the subcellular Xnr1 localization dependent on specific protein domain function, four constructs were designed. Based on published data for *Xnr2::GFP,* the *eGFP* coding sequence was inserted right behind the cleavage site and in front of the mature protein domain (Fig. 10). Besides the full-length *Xnr1* sequence (*Xnr1::eGFP*), a deletion construct for the cleavage site (*Xnr1ΔF::eGFP*) was used which was thought to be more stable because of defective protein processing *in vivo* (Shen 2007). Additionally, one construct lacking the mature domain (*Xnr1ΔM::eGFP*) and one lacking the prodomain and the cleavage site (*Xnr1ΔP::eGFP*) were cloned (Fig. 10 and MM, I.2.3, *Xnr constructs*).

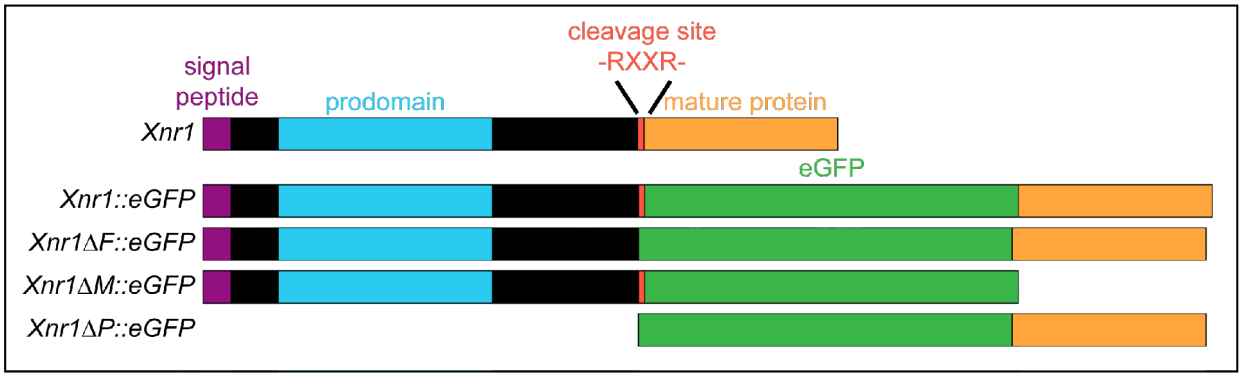

Figure 10: *Xnr1::eGFP* fusion constructs
Xenopus nodal-related 1 (*Xnr1*) fused with *enhanced green fluorescent protein* (*eGFP*). Full-length *Xnr1* (*Xnr1::eGFP*) and deletion constructs lacking the cleavage site (*Xnr1ΔF::eGFP*), the mature domain (*Xnr1ΔM::eGFP*) or the prodomain and the cleavage site (*Xnr1ΔP::eGFP*) with *eGFP* inserted between the RXXR-site and the mature domain were cloned. In black sequences with unknown functions are depicted.

II.6.2 Over-expression of *Xnr1* fusion constructs

Nodal activity can be directly detected by the induction of target gene expression like *Xbra* or by ectopic bottle cell formation (Kurth et al. 2000). To test whether the various constructs were capable to activate Nodal signaling, mRNA of each fusion construct was injected animally into one cell of 8-16-cell embryos. *Xnr2::GFP* misexpression was used as positive control. At gastrula stages, the embryos were fixed for examination of the phenotypic consequences and for *Xbra* expression.

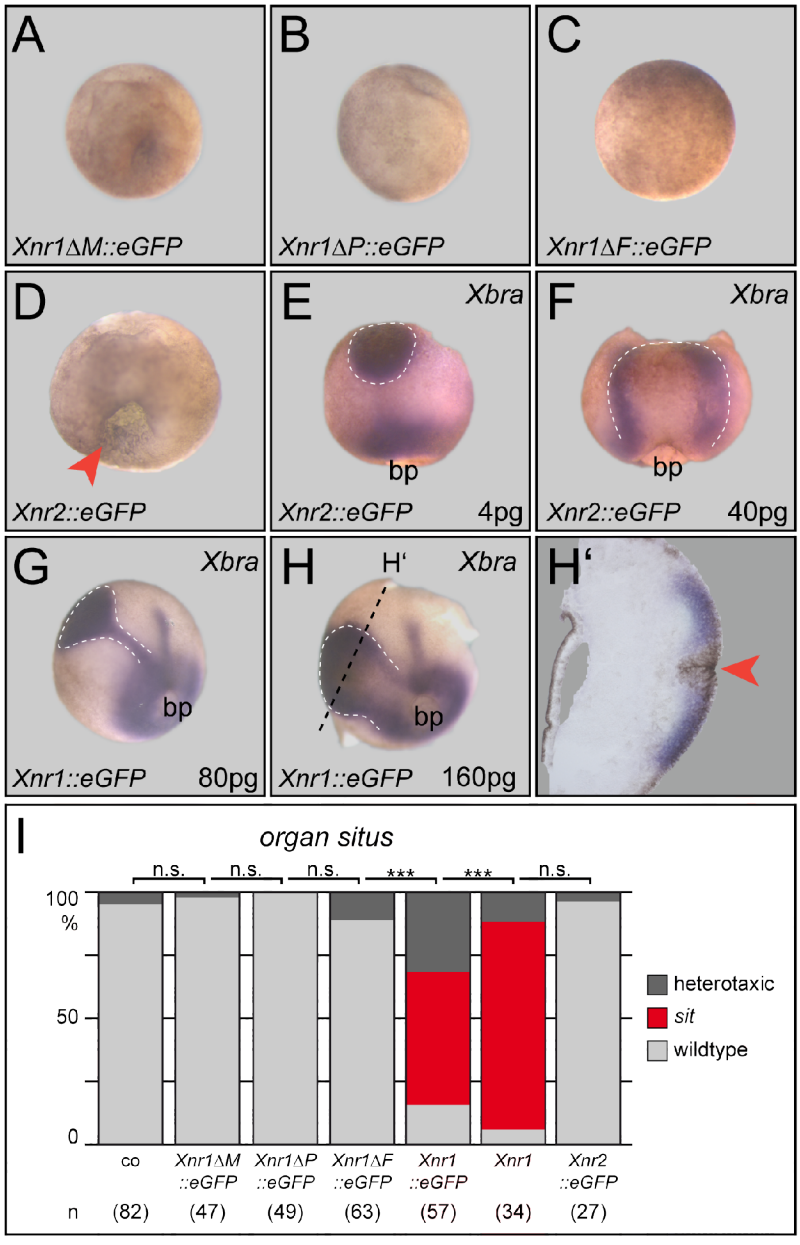

Figure 11: Bottle cell formation and *Xbra* induction upon Xnr fusion gain of function
(A-C) Deletion constructs induced neither *Xbra* expression nor bottle cell formation (animal view).
(D-F) Cell invagination (animal view, **D**) and *Xbra* expression (bp to the bottom, **E, F**) were induced by *Xnr2::GFP* over-expression. Dependence of the resulting *Xbra* pattern on mRNA concentration was observed (4pg in **E**, 40pg in **F**).
(G-H') Dot-like induction of *Xbra* after injection of 80pg *Xnr1::eGFP*-mRNA **(G)** and ring-like induction after injection of high concentrations (160pg in **H**) was achieved. Sectioning revealed bottle cell formation (red arrowhead) surrounded by *Xbra* expression **(H')**.
(I) Right-sided injection of each fusion construct was followed by organ situs analysis at st.45. over-expression of 4pg DNA resulted in laterality defects in *Xnr1::eGFP*- and *Xnr1*-injected siblings.
White dashed line indicate indicate *Xbra* expression in **E-H**. bp, blastopore; n.s. not significant; *sit*, *situs inversus totalis.*

The deletion constructs did not induce *Xbra* or bottle cell formation (Fig. 11A-C). In contrast, both full-length clones, the positive control *Xnr2::GFP* and *Xnr1::eGFP,* led to ectopic invagination of cells in the animal region (Fig. 11D, H') and to *Xbra* induction (Fig. 11E-H'). Low concentrations resulted in a dot-like *Xbra* pattern, which was sometimes connected to the endogenous expression domain surrounding the blastopore via a thin line (Fig. 11E, G). Higher mRNA concentrations induced a ring-like expression pattern which was fused to the blastopore *Xbra* domain (Fig. 11F, H). Additionally, endogenous notochordal staining was seen in some of these embryos (Fig. 11G, H). Sections revealed bottle cell formation by high pigmentation and cell invagination surrounded by *Xbra* expression (Fig. 11H'). Thus, the full-length clones *Xnr2::GFP* and *Xnr1::eGFP* were fully functional while the deletion constructs caused no phenotypic consequences.

Next, the effect of each construct on LR development was examined. As Nodal/Xnr1 represents the key factor of the left side determining cascade, right-sided misexpression is known to affect laterality development (Nonaka et al. 2002; Hirokawa et al. 2006; Capdevila et al. 2000). Therefore, 4pg DNA of each construct was injected into the right dorsal blastomere of 4-cell embryos followed by analysis of the organ situs in stage 45 (see also results II.4). Neither one of the deletion constructs nor *Xnr2::GFP* had an effect on LR development. However, the untagged *Xnr1* and *Xnr1::GFP* resulted in laterality defects in a very highly significant manner. In most cases, a *situs inversus totalis* was observed, in addition to some heterotaxic embryos (Fig. 11I).

II.6.3 Detection of fluorescent Xnr protein

Further, mRNA-injected embryos were examined for fluorescent staining and thus for subcellular localization. 4-8-cell embryos were injected animally and cultivated until they reached blastula/gastrula or tadpole stages. The fluorescence was recorded 2-48 hrs after fixation, as longer storage resulted in faint or lost GFP signal. Embryos were co-injected either with rhodamine-B-dextran (blastula/gastrula) or with mRNA coding for *membrane localized RFP* (*mRFP,* tadpoles) to visualize the injected cell lineage, and, in the case of *mRFP*, membranes and skin cilia bundles.

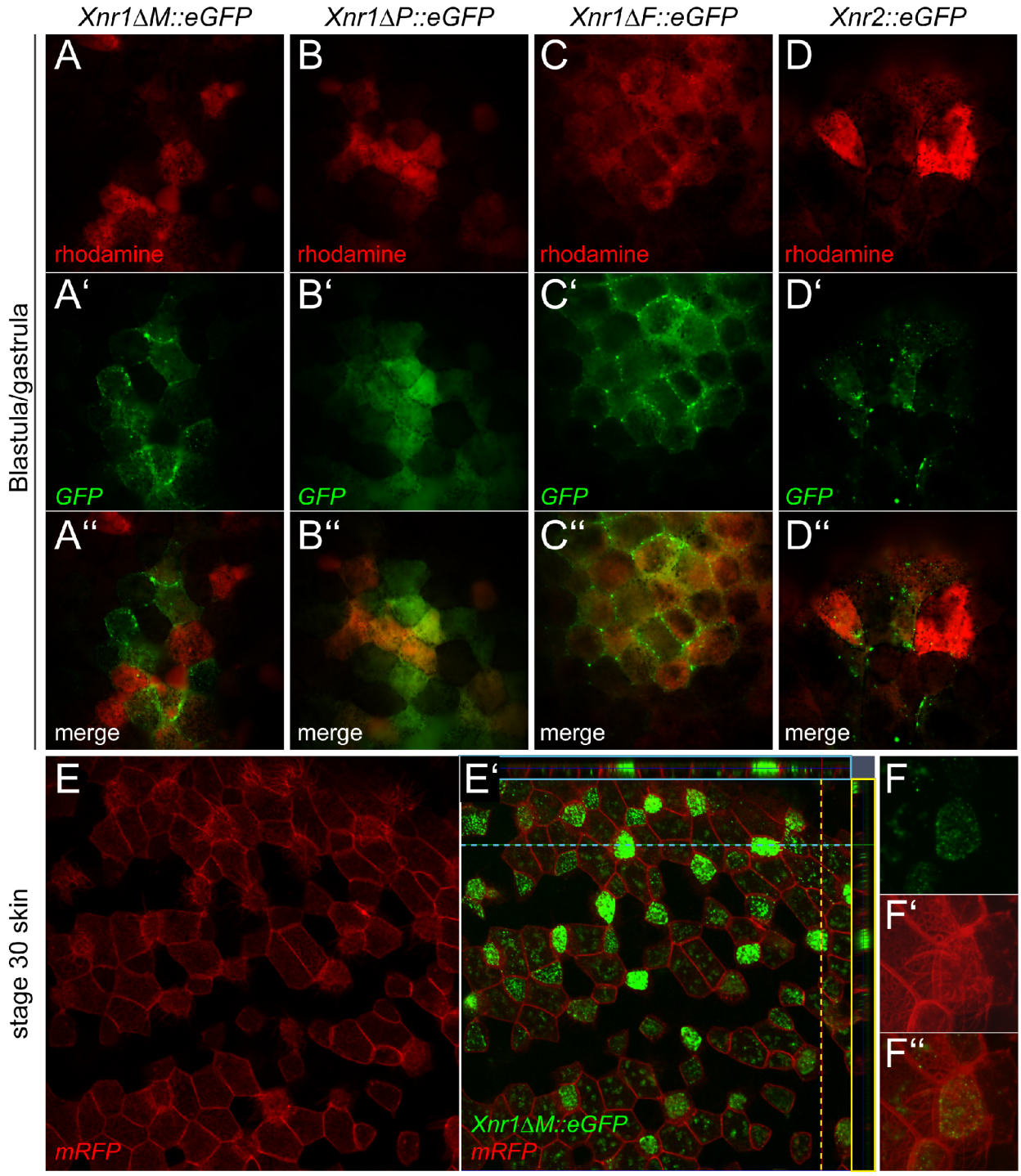

Figure 12: GFP signal in embryos injected with *Xnr* fusion constructs
(A-D) Blastula/gastrula stage embryos injected either with *Xnr1ΔM::eGFP* **(A-A")**, *Xnr1ΔP::eGFP* **(B-B")**, *Xnr1ΔF::eGFP* **(C-C")** or *Xnr2::GFP* **(D-D")**. Each of them was co-injected with rhodamine-B-dextran for detection of targeted cell lineage (red). In green fluorescence of GFP is shown. The merge displays the overlay of red and green channel **(A"-D")**. All GFP-tagged proteins were detected by green staining either in the extracellular space **(A', C')**, as vesicle-like structures **(A', C', D')** or in the cytoplasm **(A'-D')**.
(E-F) Skin of a st.30 embryo injected with *Xnr1ΔM::eGFP* and *mRFP*. Apical accumulation of vesicles containing GFP **(E')** especially in multiciliated cells was observed **(F-F")**. st., stage.

The protein lacking the mature domain (Xnr1ΔM::eGFP*)* was found in rhodamine-

positive cells in the cytoplasm and at the membrane but also in rhodamine-negative cells and in the extracellular space, respectively (Fig. 12A-A''). The deletion protein consisting of the eGFP and the mature protein domain only (Xnr1ΔP::eGFP) showed fluorescence exclusively in the injected cells. As the green and red staining did not show a similar intensity in all cells (Fig. 12B, B'), an irregular merge of both fluorescent markers was observed (Fig. 12B''). In contrast to that, *Xnr1ΔF::eGFP* injections resulted in a GFP pattern in the cytoplasm and the extracellular space/at the cell membrane which exactly overlapped with the targeted cell lineage (Fig. 12C-C''). Also the tagged Xnr2 protein was detected but, compared to the deletion proteins, only a weak signal was seen in the cells (Fig. 12D-D''). However, each fusion product except the Xnr1ΔP::eGFP was detected in vesicle-like structures. Similarly, in the skin of tadpole embryos which were injected ventral-animally at the 4-8-cell stage with *Xnr1ΔM::eGFP,* GFP-containing vesicles were observed. Surprisingly, apical accumulation of these vesicles was seen especially in multiciliated skin cells compared to low level fluorescence in neighboring non-ciliated cells (Fig. 12E-F''). Focusing on one cell, the overlay clearly demonstrated vesicular GFP staining in the ciliated cell compared to weak green fluorescence in the surrounding cells (Fig. 12F-F''). As the deletion constructs were shown to be non-functional and revealed a high diversity in fluorescent staining, the GFP-tagged full-length construct was analyzed next.

The over-expression of *Xnr1::eGFP* strongly induced target gene expression of *Xbra* and bottle cell formation (see results, II.6.2) indicating that functional protein was produced. Unexpectedly however, almost no specific fluorescence was detected. Rarely, in some embryos, probably due to a higher amount of injected *Xnr1::eGFP*-mRNA, signals were visible in enlarged cells (Fig. 13A-A'). Two reasons could be envisaged for the difficulty to visualize the functional Nodal fusion protein: (1) Nodal protein is a very competent morphogen, already inducing downstream signaling in low concentrations and (2) the turn-over of Nodal is quite fast as it gets internalized and degraded immediately after receptor binding (Shen 2007; Beck et al. 2002). Both features could lead to a level of GFP-tagged protein too low to be detectable by this method. If this assumption was true, signaling and concomitant fast turn-over of Xnr1::eGFP might be prevented by co-expression of the Nodal binding protein *Coco* to stabilize Nodal-eGFP and thereby facilitate detection.

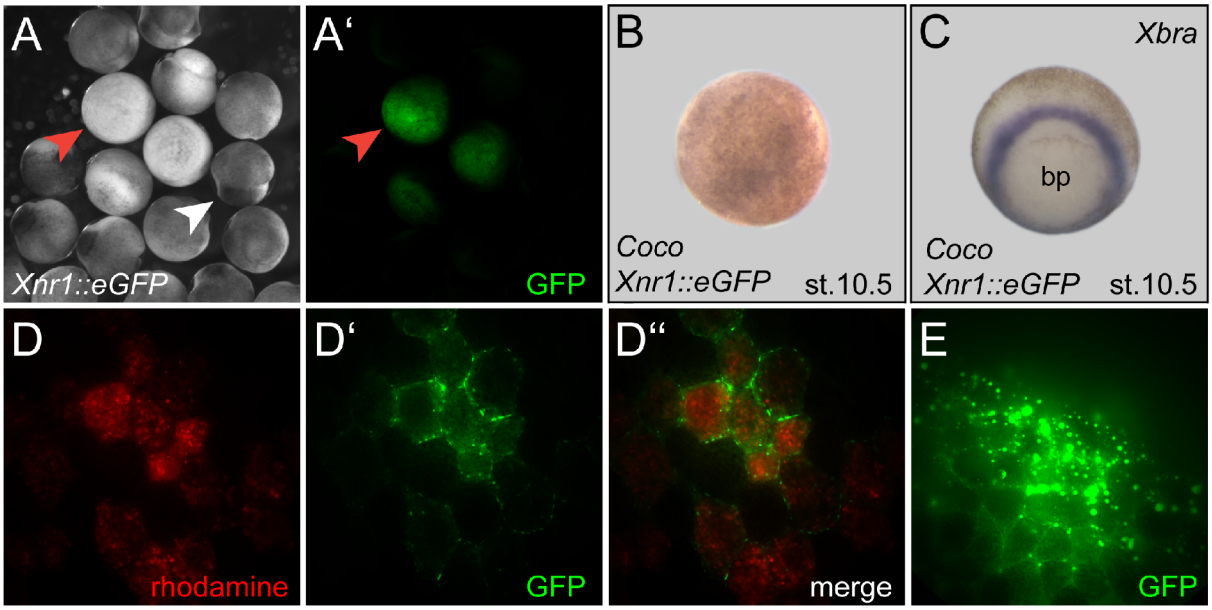

Figure 13: Over-expression of *Xnr1::eGFP* and *Coco*
(A) Injection of 400pg *Xnr1::eGFP*-mRNA-induced bottle cell formation (white arrowhead) in late gastrula stages. In very few embryos GFP fluorescence was detected (red arrowhead, **A'**).
(B, C) Co-injection of *Xnr1::eGFP* and *Coco* (160pg each into 4-8-cell embryos animally) neither resulted in bottle cell formation (animal view, **B**) nor in induction of *Xbra* expression (vegetal view, **C**). Only wildtypic *Xbra* expression was seen. bp, blastopore; st., stage.
(D-E) Fluorescent GFP signal was detected in the cytoplasm, in the extracellular space **(D', D")** and in vesicles **(E)**. Rhodamine-B-dextran was used as lineage tracer **(D-D")**.

Co-injection of *Xnr1::eGFP*- and *Coco*-mRNA into the animal hemisphere of 4-8-cell embryos did not induce bottle cell formation or ectopic *Xbra* expression at gastrula stages, which confirmed the inhibitory activity of Coco on Nodal (Fig. 13B, C and Bell et al. 2003). However, examination of embryos for fluorescence revealed GFP staining in the extracellular space/at the membrane and in vesicular structures (Fig. 13D-E"). Interestingly, rhodamine-B-dextran co-injection showed the same distribution as seen for the GFP protein suggesting that no diffusion occurred (Fig. 13D-D").

Taken together, fluorescence of non-functional GFP-tagged *Xnr1* deletion constructs and protein localization could be detected *in vivo*. Remarkably, *ΔM* displayed non-overlapping staining with the co-injected lineage tracer rhodamine-B-dextran which implied distribution of the protein. The full-length fusion construct *Xnr1::eGFP* was detected after co-expression of the inhibitor *Coco*, i.e. mainly in the extracellular space or at the membrane, but only in cells targeted by injection. Up to now, non of these applications seemed to be viable to visualize Nodal distribution *in vivo*, but interesting patterns of the protein domains have been observed which could represent useful tools for further studies.

III. Serotonin signaling and LR development

Serotonin (5-HT) signaling was first described to be involved in LR axis determination by Fukumoto et al. in 2005. This study identified, among other 5-HT signaling factors, receptors of the subtype 3 (5-HT_3) to be necessary for correct LR development. 5-HT receptors are usually G-protein coupled receptors except for 5-HT_3, which act as ligand-gated ion channels. 5-HT_3 consist of five subunits (HTR3) which form a proton channel, e.g. for Ca^{2+} or K^+ (Thompson et al. 2006). As in *Xenopus* leftward flow was described to be necessary for LR axis determination recently, the main focus in this study was on the development of the GRP in 5-HT signaling-impaired embryos (Schweickert et al. 2007).

III.1 Loss of serotonin signaling induced laterality defects

In order to address the role of 5-HT signaling in LR development at the molecular level, the expression pattern of the 5-HT_3 subunit *xHtr3* during *Xenopus* development was analyzed by RT-PC. Expression of the housekeeping gene *EFα* served as loading and positive control. No *xHtr3* mRNA was found in pre-MBT stage embryos. The first expression was detected in gastrula stages and was present in neurula and tadpole embryos (Fig. 14A). The expression pattern could not be confirmed by WMISH in gastrula and neurula stages most likely caused by a low expression level. To interfere with the function of 5-HT signaling two approaches were used. First, two MOs for specific knock-down (KD) of *xHtr3* were designed which targeted non-overlapping sequences. *XHtr3*-MO1 spanned the ATG start codon region whereas *xHtr3*-MO2 was directed to the 5'UTR region (Fig. 14B).
Two controls were used to test MO specificity. First, the co-MO was injected in the same concentration as MO1 and 2. Second, a fusion construct combining the *xHtr3*-MO1/2 targeting and the *eGFP* coding sequence (*MOsite::eGFP*) was co-injected together with MO1 and 2 (see MM, I.2.3, *Serotonin*; Fig. 14B). Specific binding of the MOs was confirmed indirectly by a decrease of green fluorescence (Fig. 14C, C2-C2" and data not shown) compared to co-MO co-injected controls (Fig. 14C, C1'-C1").

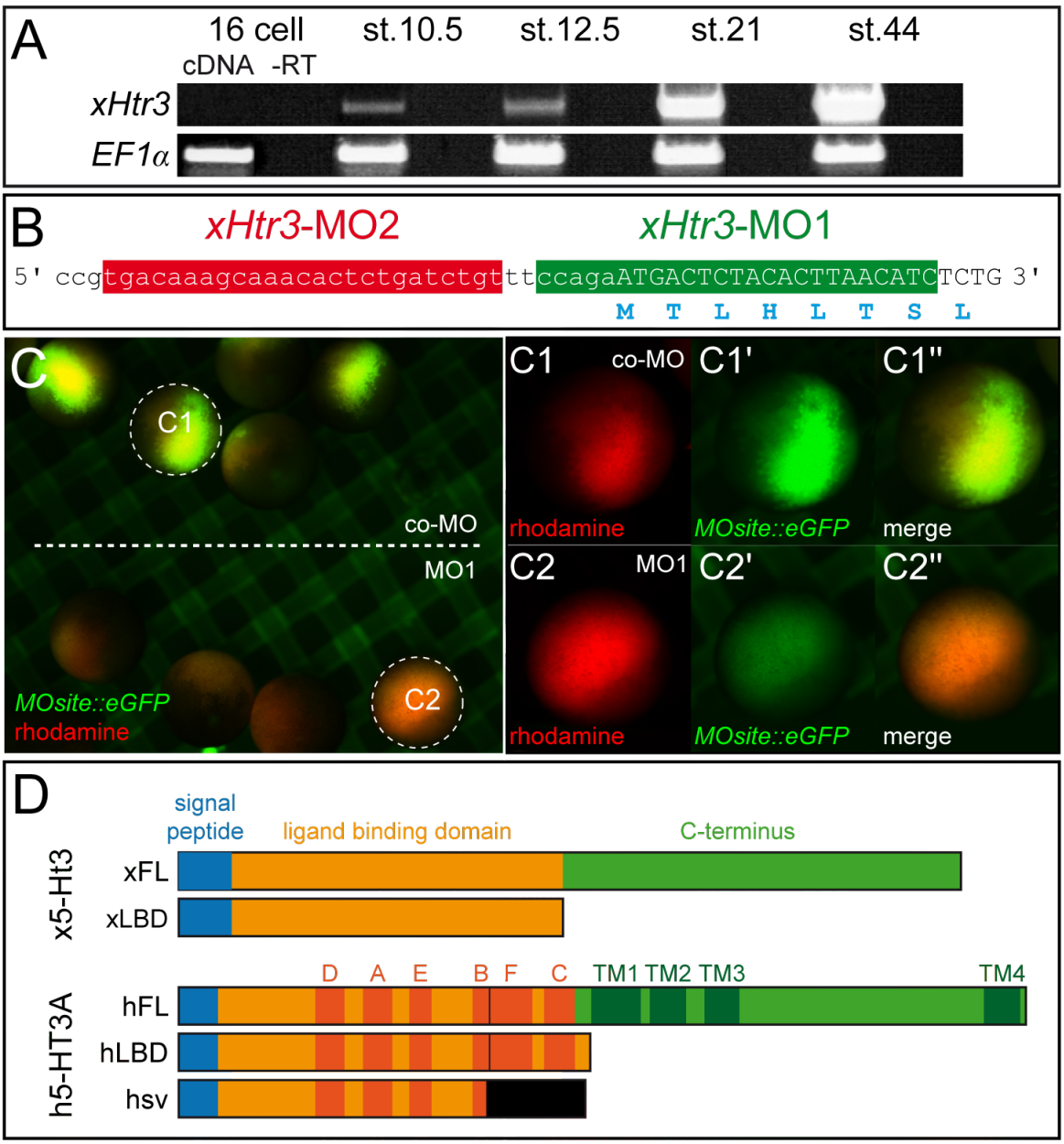

Figure 14: *xHtr3* and *HTR3A*

(A) RT-PCR for *xHtr3*. *EFα* was taken as loading control and -RT probes as test for genomic contamination. cDNAs of 16-cell up to st.44 were used to examine *xHtr3* expression. *xHtr3* could be detected in st.10.5 and older specimens.

(B) MO sequences. *xHtr3*-MO1/2 were designed to bind non-overlapping to the 5'UTR (MO2) or to the ATG start codon region (MO1).

(C) MO specificity. Specific MO-binding was evaluated by co-injecting co-MO or MO1 with the MO-binding site **(B)** fused to the *enhanced green fluorescent protein* (*MOsite::eGFP*). A decrease of GFP staining was observed upon MO1 **(C, C2-C2")** but not in co-MO co-injections **(C, C1-C1")**. Rhodamine-B-dextran was used as injection control.

(D) Receptor constructs. The *Xenopus* 5-Ht3 and the human 5-HT3 consist of a signal peptide (blue), a ligand binding domain (LBD, orange) and a C-terminus (green). The human subunit is more specified in the literature with the C-terminal end containing four transmembrane domains (TM1-4) and the LBD consisting of six loops (A-F, Thompson et al. 2006). Constructs lacking the C-terminal end were cloned (*xLBD* and *hLBD* see MM, I.2.3, *Serotonin*). In addition, a construct lacking the loops F and C, which are necessary for 5-HT binding, was used (*hsv,* Niesler 2011; Brüss et al. 2000).

FL, full-length; hsv, human splive variant; MO, morpholino; st., stage.

In addition to the KD by MO1 and 2, a second approach was used to interfere with 5-HT signaling independent of specific receptor activity. To that end, experiments using a deletion construct of *xHtr3* (*xLBD*) which lacked the C-terminal domain including the transmembrane coding regions were performed. To take advantage of the well described human homologous subunit receptor 3a (h5-HT3A, Thompson et al. 2006), a similar human deletion construct (*hLBD*) was used for comparison. Thereby, it was possible to control the specificity by over-expression of a splice variant (*HTR3AT*, here *hsv*) which was no longer capable for 5-HT binding due to a deletion of loops F and C (Niesler 2011; Brüss et al. 2000b).

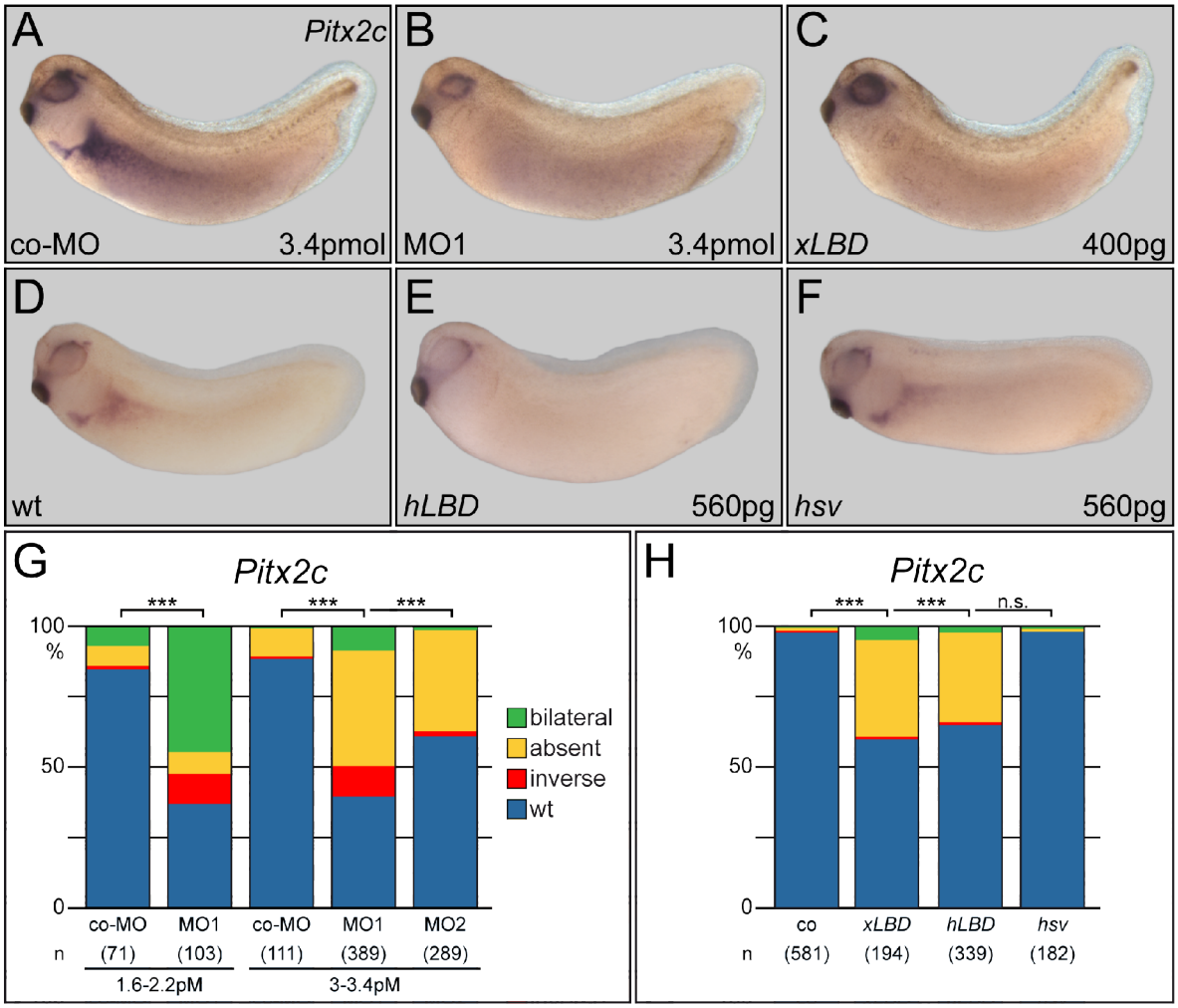

Figure 15: *Pitx2c* expression is altered in 5-HT-impaired embryos
(A-F) *Pitx2c* pattern. Expression of the left-sided marker *Pitx2c* was analyzed in wt embryos **(D)** and co-MO- **(A)**, MO1- **(B)**, *xLBD*- **(C)**, *hLBD*- **(E)** and *hsv*-injected **(F)** specimens.
(G, H) Quantification of results. The graphs summarize either MO1/2 induced phenotypes **(G)** or resultant patterns observed upon dorsal misexpression of receptor deletion constructs **(H)**. MO1/2, *xLBD* and *hLBD* injection led to laterality defects in a very high significant manner. No influence was seen in *hsv*-injected specimens (p=0.225). wt, wildtypic left-sided expression.

MOs (co-MO, MO1/2) and receptor constructs (*LBDs*, *hsv*) were injected into the DMZ in 4-8-cell embryos to target the GRP (Vick et al. 2009). LR development was analyzed at tadpole stages by WMISH for *Pitx2c* expression. Examples of treated and untreated tadpole stage embryos are shown in Fig. 15A-F. Only embryos exhibiting normal axis AP/DV development (dorso-anterior index; DAI=5) were evaluated for LR axis determination. Low doses of MO1 resulted in 64% laterality defects with bilateral *Pitx2c* expression as prevailing phenotype (45%). Higher concentrations of MO1 and MO2 led to 41% and 36% absent *Pitx2c* expression, respectively, which was a very highly significant effect compared to co-MO injections (Fig. 15G). Dorsal misexpression of the *LBDs* prevented left-sided *Pitx2c* induction in 34% (*xLBD*) or 32% (*hLBD*) of embryos. In contrast to that, *hsv* injection did not result in laterality defects in a significant manner (Fig. 15H). That indicated that the ability of the LBDs to bind 5-HT was required to influence LR development.

III.2 Loss of serotonin signaling affected GRP morphogenesis

Injections into the DMZ of 4-8-cell embryos target, according to the cell lineage, dorsal tissues like neural tube, notochord and the epithelium of the ciliated GRP (Vick et al. 2009). As both, loss of cilia-driven leftward flow and loss of 5-HT signaling led to absent *Pitx2c* expression, the morphology or function of the GRP could be affected in 5-HT signaling-impaired embryos. To reconsider this assumption, stage 17/18 embryos which were injected with co-MO, MO1/2 or *LBDs*, were prepared for SEM analysis (see MM, I.1.5). For comparison of cilia length, polarization and cell size, SEM pictures of GRPs were analyzed using the same central region of the GRP directly anteriorly to the blastopore (Fig. 16A-C, white box). The region was marked by a square of 1000x1000 pixel and cilia and cells were measured using the open source program ImageJ (Sbalzarini et al. 2005). Quantification of results and calculation of significances were done in Statistical-R (R developmental core team 2008). In Fig. 16 examples of a wildtype (A), MO1- (B) and *xLBD*-injected (C) GRPs are shown.

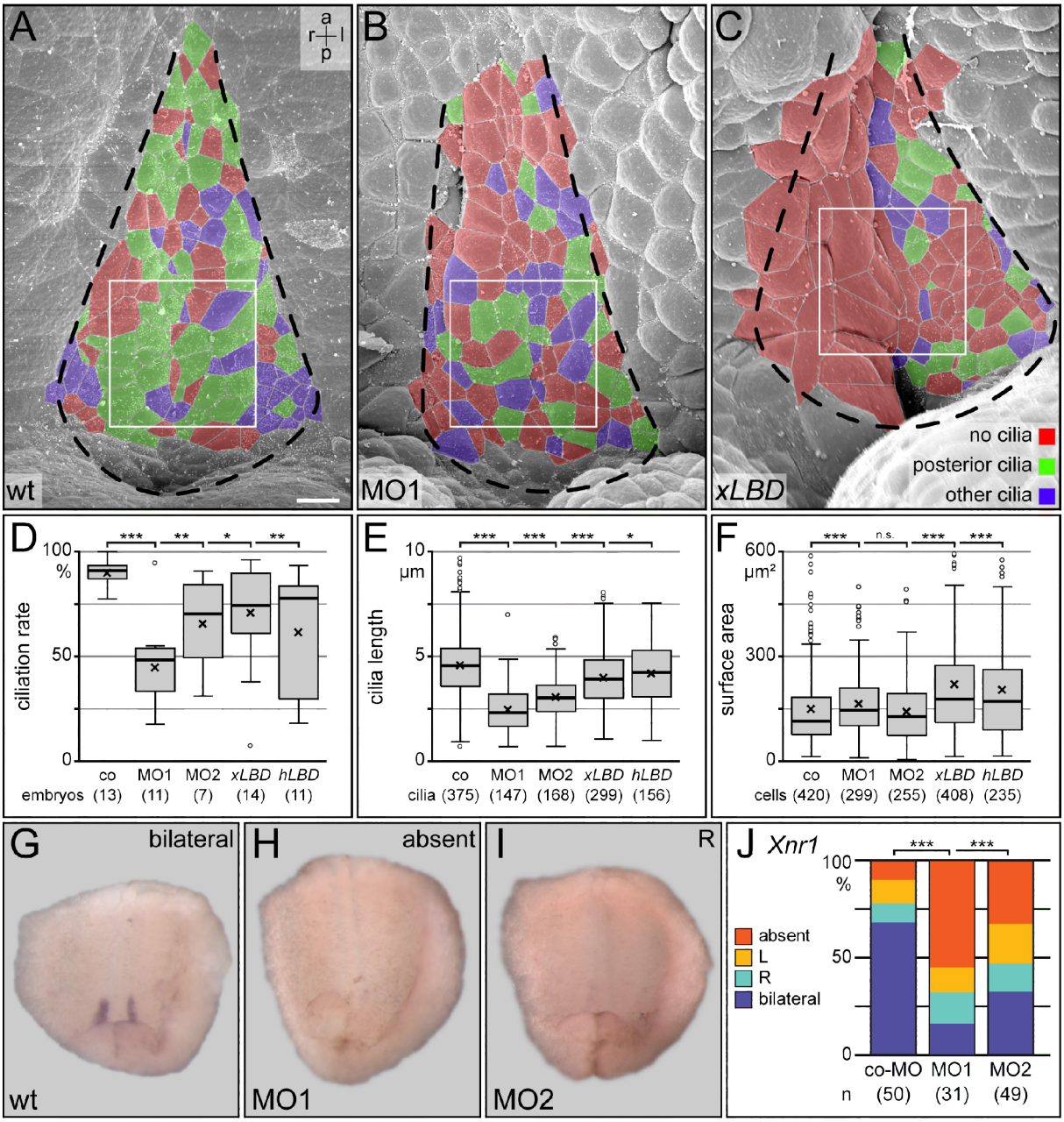

Figure 16: GRP morphology and marker gene expression after 5-HT signaling impairment
(A-C) SEM of the GRP. SEM pictures revealed disturbance of the GRP morphology in MO1- **(B)** and *xLBD*-injected specimens **(C)** when compared to the wt **(A)**. Cells with no cilia are indicated in red, with posteriorly polarized cilia in green and with cilia, which are not polarized to the posterior pole in purple.
(D-F) Quantification of SEM analysis. Ciliation rate **(D)**, cilia length **(E)** and cell size **(F)** were measured in 5-HT morphants (MO1/2) and *LBD*-injected specimens using ImageJ (MM, I.1.5). **(D)** Ciliation rate dropped significantly upon MO1 (45% ± 21), MO2 (66% ± 23, p=0.009), *xLBD* (71% ± 25, p=0.019) and *hLBD* injection (62% ± 29, p=0.004) vs. co (90% ± 7). **(E)** Cilia length decreased significantly: MO1 (2.47µm ± 1.08), MO2 (3.07µm ± 0.98), *xLBD* (4µm ± 1.37), *hLBD* injection (4.21µm ± 1.45, p=0.027) vs. co (4.6µm ± 1.54). **(F)**. The cell size increased except in MO2-injected specimens: MO1 (165.36µm^2 ± 101.13), MO2 (142.95µm^2 ± 88.94,p=0.073), *xLBD* (221.53µm^2 ± 169.16), *hLBD* injection (205.53µm^2 ± 178.05) vs. co (150.64µm^2 ± 127.10). SEM analysis was done in collaboration with Thomas Thumberger.
(G-I) *Xnr1* expression observed in wt **(G)**, MO1- **(H)** and MO2- **(I)** injected specimens.
(J) Quantification of *Xnr1* analysis. *Xnr1* expression was lost in 5-HT morphants.
a, anterior; co, control; l, left; L, left-sided expression only; p, posterior; r, right; R, right-sided expression only; vs., significant versus; wt, wildtype;.

Colored cells indicate the observed phenotypes. Green color marks cells with posteriorly polarized cilia, purple cells with non-polarized cilia and red cells possessed no cilia. Ciliation rate and cilia length were significantly decreased in 5-HT signaling-impaired embryos (Fig. 16D, E). Additionally, MO1 and *LBD* injections resulted in an increase of cell size (Fig. 16F). Taken together, interference with 5-HT signaling led to morphogenetic defects of the GRP structure which resulted in disturbed leftward flow and subsequently in LR defects (Thomas Thumberger, personal communication and Thumberger 2011) and subsequently in LR defects.

The most lateral cells of the GRP harbor *Xnr1* expression in a bilateral pattern (see results I.2). To test if not only GRP cell appearance but also marker gene induction was affected upon KD of *xHtr3*, the *Xnr1* pattern was analyzed by WMISH (examples are shown in Fig. 16G-I). In MO1- and MO2-injected specimens *Xnr1* expression was decreased or even lost in a very highly significant manner compared to co-MO-injected embryos (Fig. 16J). As this bilateral expression was proposed to be required for left-sided Nodal cascade induction, this observation indicated that the absence of *Pitx2c* expression could be a result not only of disturbed leftward flow but also of inhibition of the bilateral *Xnr1* domain upon 5-HT signaling down-regulation (Kawasumi et al. 2011; Saijoh et al. 2005).

Taken together, it was shown that interference with 5-HT signaling resulted in morphological defects of the GRP, alteration of leftward flow and decreased *Xnr1* expression in the most lateral cells. Therefore, the assumption was that 5-HT signaling was required for GRP specification. Thus, for further analysis gastrula stage embryos were examined because the tissue which will give rise to the GRP proper is already specified at these stages.

III.3 *Foxj1* expression in the superficial mesoderm was disturbed

The master regulator gene for motile cilia, i.e. the forkhead transcription factor *Foxj1,* was described to be expressed in a specific pattern above the forming dorsal lip in the SM cell layer (Stubbs et al. 2008). In this study *Foxj1* was used to analyze SM specification in gastrula stages of 5-HT impaired embryos.

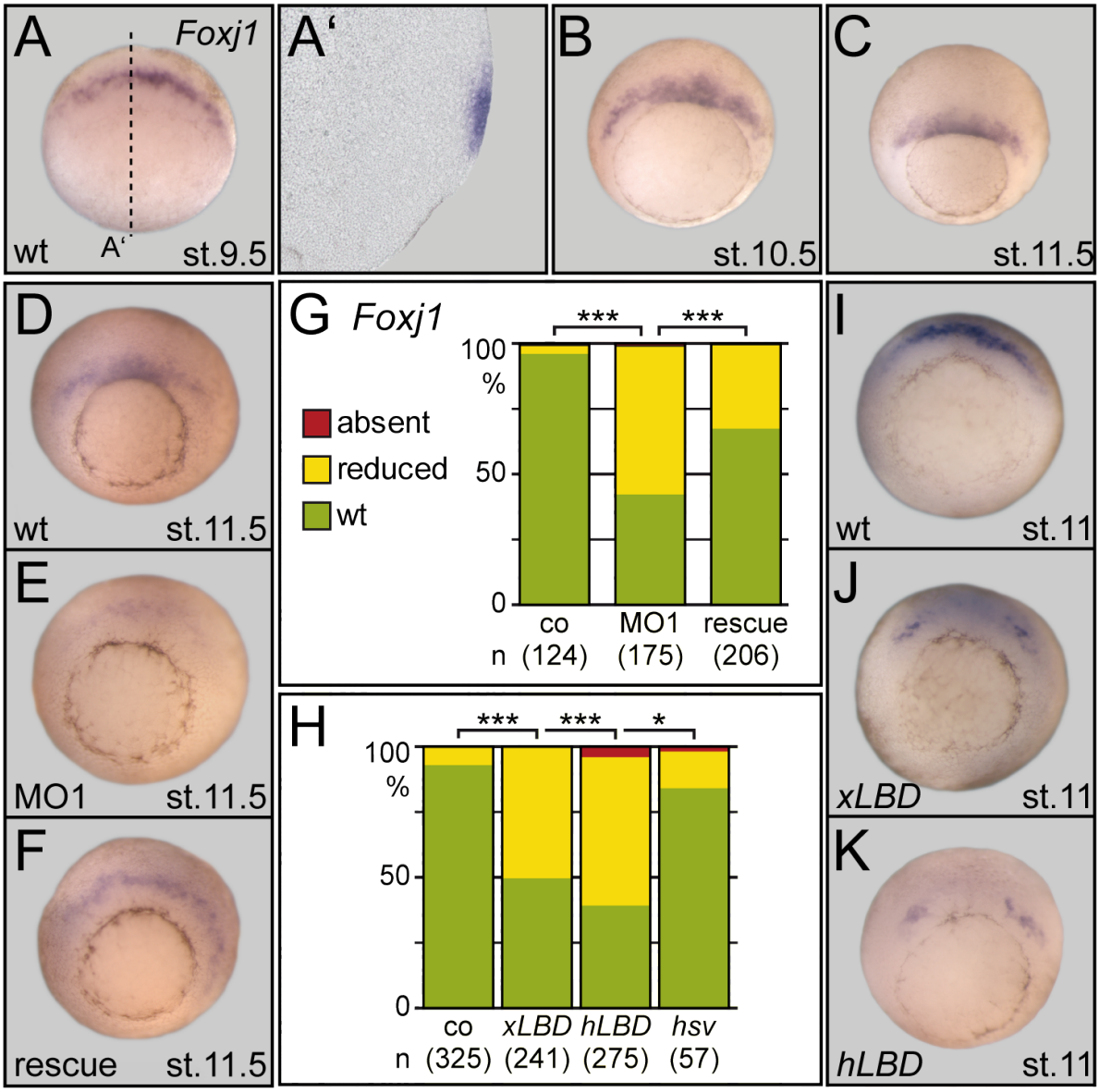

Figure 17: *Foxj1* expression in wt embryos and after disturbance of serotonin signaling
(A-C) Wildtypic *Foxj1* expression in gastrula stage embryos. Staining for *Foxj1* was first detected in st.9.5 embryos in the superficial mesoderm (SM, **A, A'**). Expression stayed restricted to the region above the dorsal lip during gastrulation **(B, C)**. Dashed line indicates sectional plane in **A'.**
(D-G) *Foxj1* in MO1-injected embryos. MO1 injection led to reduction of *Foxj1* staining **(E)** which was rescued by co-expression of the full-length sequence clone harboring a changed MO-binding site (*xFL,* **F**) in a very high significant manner. Quantification of the results is shown in **G**.
(H-K) *Foxj1* in *LBD*-injected embryos. Over-expression of each *LBD* caused very highly significant reduction of *Foxj1* expression **(J, K)**. Injection of the *hsv* inhibited in 16% of the embryos *Foxj1* (p=0.022). The graph in **H** summarizes the results.
Embryos are shown in a vegetal view, dorsal up. st., stage; wt, wildtype.

First, an overview of wildtypic expression of gastrula stages was prepared to examine whether the staining varies between different gastrula stages (Fig. 17A-C). *Foxj1* was first detected in stage 9.5 embryos restricted to the SM on the dorsal side (Fig. 17A). During gastrulation the expression domain got more concentrated to the dorsal lip and

Foxj1-positive cells started to ingress (Fig. 17B, C). The intensity of staining varied slightly between stages and experiments (Fig. 17A-D, I), but expression patterns performed in the same WMISH and with embryos of the same batch displayed comparable staining in all gastrula stages (Fig. 17A-C, D-F and G-I). The expression of *Foxj1* in 5-HT morphants and *LBD*-injected embryos was therefore examined to investigate if 5-HT was required for SM specification or not. MO1 injections resulted in down-regulation of *Foxj1* expression in 58% of embryos (Fig. 17D, E, G). This effect could be rescued in a very highly significant manner by co-expression of a mixture of mRNA and DNA encoding the *Xenopus* full-length *xHtr3* harboring a mutated MO-binding site (rescue, Fig. 17F, G). Also, dorsal misexpression of the *LBDs* led to reduction of *Foxj1* expression (Fig. 17H-K; *xLBD,* 50%; *hLBD,* 61%). In contrast, injection of *hsv* affected *Foxj1* expression only slightly (*hsv*, 16%, p=0.022, Fig. 17H).
In summary, this analysis showed that *Foxj1* expression was down-regulated and SM patterning was disturbed in 5-HT morphants and *LBD*-injected embryos. This resulted in morphogenetic defects of the GRP, disturbed leftward flow and thus in LR defects. However, interference with 5-HT signaling did not only alter LR determination but also resulted in more severe phenotypes which suggested a more general function of 5-HT during development.

III.4 Dorsal axes defects in serotonin-impaired embryos

Although assessment of LR axis determination was only performed in embryos displaying normal axis development (see results, III.1), higher doses of MO1/2 or the *xLBD* construct resulted in additional defects. Injection of high doses of MO1/2 led to inhibition of cement gland formation and neural tube closure defects (NTD), which was visible in rhodamine-B-dextran co-injected specimens (Fig. 18A-D). A similar phenotype was seen in early tadpole embryos (stage 22) injected with *LBDs*. Cement gland formation was reduced or even absent and the neural tube did not close completely (Fig. 18E-G). In stage 28-32 embryos dorsal bending, small heads, thickening along the DV axis and NTDs were observed in 5-HT morphants and *LBD*-injected specimens (Fig. 18H-M).

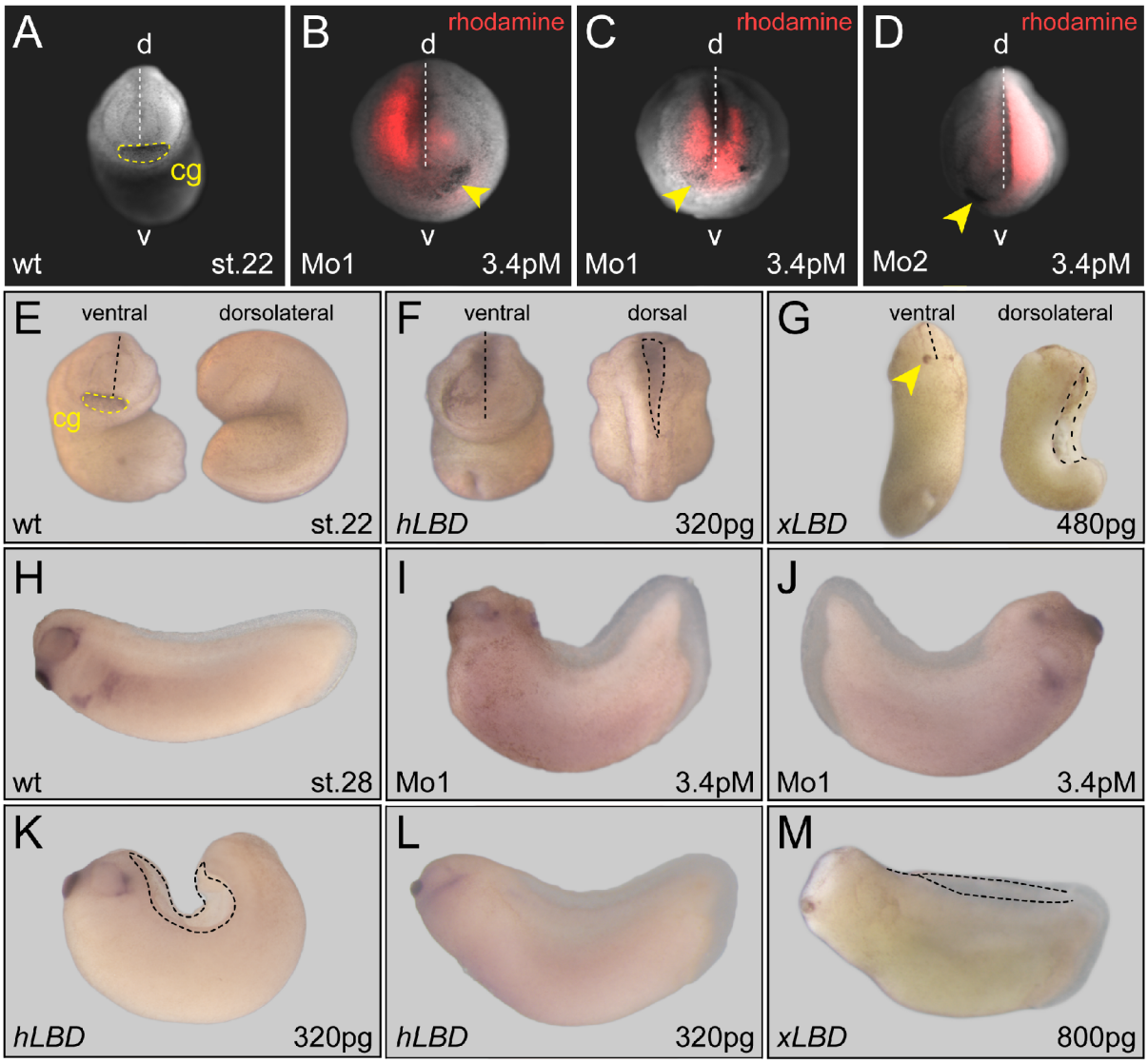

Figure 18: Phenotypes upon loss of 5-HT signaling
Phenotypes induced by MO1/2/*LBD* injections. Targeted tissue was visualized in MO-injected specimens by co-injection of rhodamine-B-dextran **(A-D)**. Inhibition of 5-HT signaling led to NTDs and reduction of the cement gland in early tadpole stages **(B-D, F, G)**. In older stages head structures were reduced **(I, J, I, M)** and embryos displayed dorsal bending **(I-L)** and NTDs **(K, M)**. Embryos are shown in an anterior view **(A-D)**, ventral/dorsal/dorsolateral view anterior up **(E-G)** or lateral view anterior to the left **(H ,I , K-M)** or right **(J)**. Cement gland is indicated by yellow dashed lines and yellow arrowheads **(A-E, G)**. Anterior midline and NTDs are marked by white **(A-D)** or black **(E-G, K, M)** dashed lines.
cg, cement gland; d, dorsal; NTDs, neural tube closure defects; st., stage; v, ventral; wt, wildtype.

These results indicated that 5-HT signaling was involved not only in *Foxj1* patterning and LR axis development but also in dorsal axis development in general. Consequently, a second dorsal marker was analyzed in gastrula stage embryos. For this, the *Xenopus nodal-related gene 3* (*Xnr3)* was chosen which is known to be a direct target gene of Wnt signaling (Smith et al. 1995; Glinka et al. 1996).

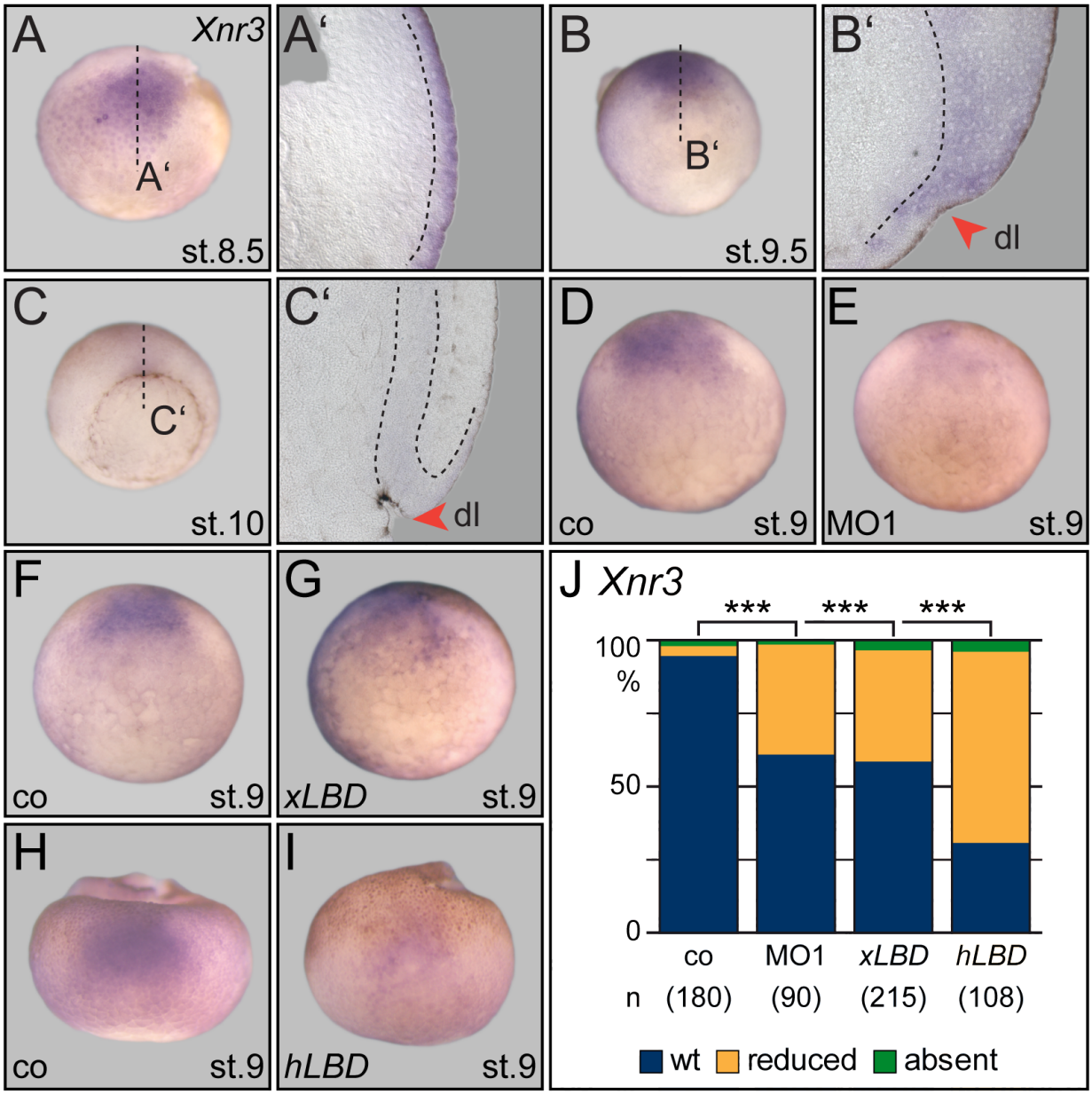

Figure 19: *Xnr3* expression in untreated and injected specimens
(A-C) *Xnr3* expression in gastrula stage embryos. Expression was observed in st.8.5 **(A)**, st.9.5 **(B)** and st.10 embryos **(C)**. Sections revealed expression restricted to the superficial epithelium in st.8.5 **(A')** and staining in deeper tissue in st.9.5 embryos **(B')**. Weak expression above the dorsal lip could be detected in st.10 **(C')**. Red arrowhead mark invagination of cells at the dorsal lip region, dashed lines indicate sectional plane **(A, B, C)** and *Xnr3* expression domain **(A', B', C')**.
(D-I) *Xnr3* expression analysis of treated embryos. *Xnr3* staining was reduced in 5-HT signaling-impaired embryos (MO1, **E**; *xLBD*, **G**; *hLBD*, **I**) compared to the control **(D, F, H)**.
(J) Quantification of results. *Xnr3* expression is very high significantly reduced in MO1- (39%) or *LBD*-injected specimens (x*LBD*, 41%; *hLBD*, 70%).
Embryos are shown either in dorsal view, animal up **(A, H, I)** or in vegetal view, dorsal up **(B-F)**.
st., stage; dl, dorsal lip; co, control; wt, wildtype.

Expression of *Xnr3* was found already at stage 8 and 8.5, respectively. *Xnr3* mRNA was restricted to the dorsal superficial cell layer including the SM (Fig. 19A, A'). In early

gastrula stage embryos *Xnr3* staining was also observed in deeper mesodermal tissue, but the signal faded at late gastrula stages (Fig. 19B-C'). Interestingly, upon impairment of 5-HT signaling the expression of *Xnr3* was reduced in a very highly significant manner with 39% embryos displaying disturbed staining in MO1-, 41% in *xLBD*- and 70% in *hLBD*-injected embryos (Fig. 19D-I).

Taken together, in 5-HT signaling-impaired embryos dorsal axis defects were observed when higher concentrations either of the MO1/2 or of the *LBDs* were used. In addition, *Xnr3* staining was diminished at midgastrula of 5-HT morphants and *LBD*-injected embryos. As 5-HT loss of function had an influence on the direct Wnt target *Xnr3*, a role for 5-HT in Wnt signaling was suspected and further investigated.

III.5 Serotonin is involved in Wnt signaling

Wnt-dependent dorsal axis induction can be analyzed in *X. laevis* by using the classical double axis induction assay (Moon et al. 1998). Injection of canonical Wnt signaling components into one ventral blastomere of a 4-cell embryo induces a second organizer and thereby a complete secondary axis. In this study mRNA either for the ligand *XWnt8*, the cytoplasmic factor *XDsh* or the downstream target gene *XSia* were injected ventrally.

Double axis formation was evaluated in late neurula or tadpole stage embryos. Three categories for secondary axis induction were used: no secondary axis, partial axis induction displaying short trunk structures without heads and complete secondary axes (Fig. 20A). First, *XWnt8*-mRNA was used to induce secondary axes which was the case in 80% of the injected embryos. This value dropped very highly significant when embryos were co-injected with MO1/2 (54%, MO1; 56%, MO2) or the *LBDs* (*xLBD*, 57%; *hLBD* 47%, Fig. 20B). In contrast, *XDsh*-induced secondary axes were not influenced by parallel KD of *xHtr3* (*XDsh*, 69%; +MO1, 68%; p=0.472). However, co-injections with the *LBDs* prevented the development of additional axes in a very highly significant manner (*XDsh*, 73%; +*xLBD*, 27%; +*hLBD* 20%, Fig. 20C).

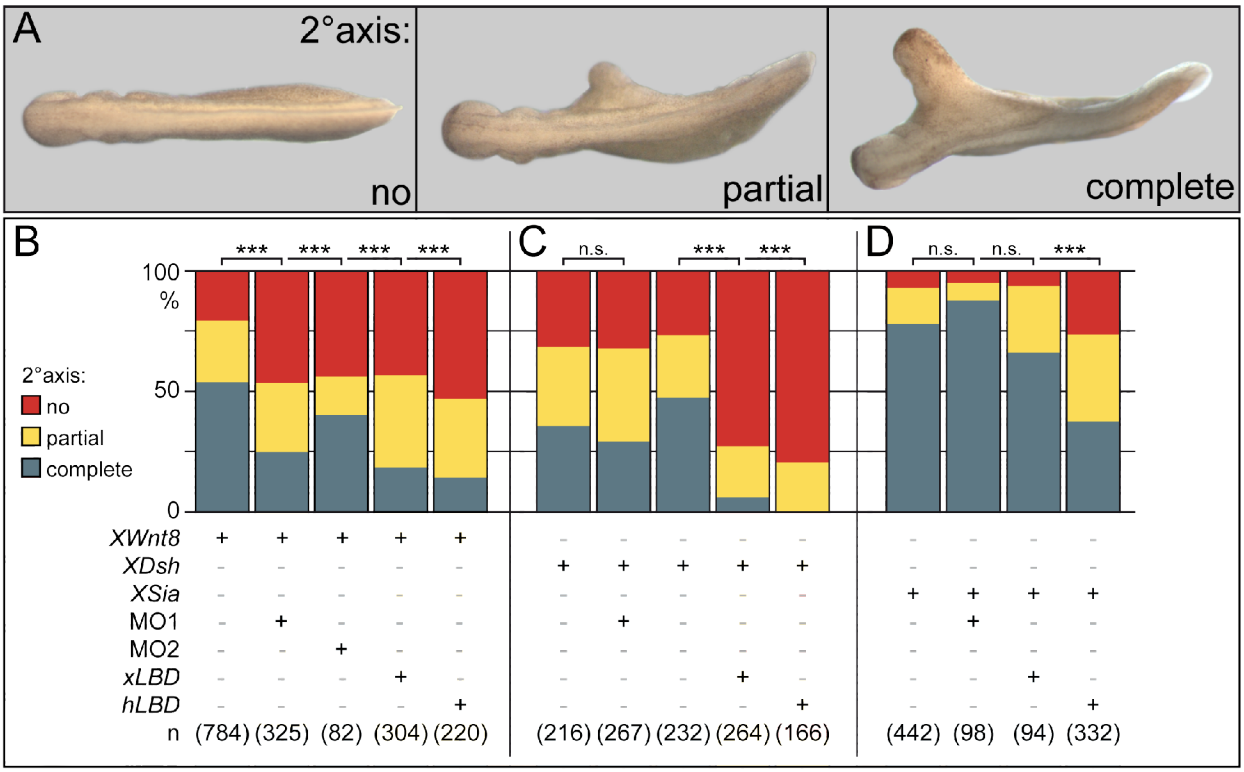

Figure 20: Epistasis of Wnt signaling components and loss of 5-HT signaling
(A) Evaluation of double axes. Secondary (2°) axis induction was categorized as follows: no 2° axis formation, partial double axis displaying trunk structures and complete 2° axis including trunk and head. Embryos are shown in a dorsal view, anterior to the left.
(B-D) Quantification of results. Induction of double axes was achieved using *XWnt8* **(B)**, *XDsh* **(C)** and *XSia* **(D)**. In all cases double axis formation was inhibited by co-expression of *hLBD*. Co-injection of *xLBD* prevented 2° axis induction when *XWnt8* and *XDsh* were used. KD of *xHtr3* with the MO1/2 reduced only the efficiency of *XWnt8* induced double axis formation. n.s., not significant.

Ventral misexpression of *XSia* resulted in double axis formation in 93% of embryos. MO1 or *xLBD* co-injection was not effective to interfere with secondary axis induction by the latter (MO1, 95%, p=0.151; *xLBD* 94%, p=0.177). Nevertheless, *hLBD* misexpression also prevented secondary axis induction by *XSia* (Fig. 20D). These results indicated an interplay of 5-HT and Wnt signaling.

III.6 Wnt and serotonin signaling were required for dorsal *Foxj1* expression

The double axis assay revealed an interplay of 5-HT and canonical Wnt signaling during development of the dorsal axis. But up to date it was not shown if the canonical Wnt pathway was required for LR determination in *X. laevis*. To address this issue, loss of function of the *Xenopus frizzled receptor 8* (*Xfz8*) was performed. *Xfz8* represented a

good candidate for the KD because (1) it was expressed in the DMZ at midblastula in deep mesodermal tissue and, more importantly, in the superficial cell layer, (2) KD did not inhibit gastrulation movements, (3) ventral over-expression resulted in partial secondary axis induction and (4) morphants developed cysts which is a phenotype often observed upon impairment of LR relevant genes (Fig. 21A-C and Maisonneuve et al. 2009; Pazour 2004; Simons et al. 2005; Satow et al. 2004; Itoh et al. 1998).

A well characterized MO was used for the loss of function which had been tested for its specificity for translational inhibition of *Xfz8* (Satow et al. 2004). To investigate the function of Xfz8 in LR development, 2pM of the *Xfz8*-MO were injected into 4-cell embryos dorsally to target the dorsal lip of gastrula and the GRP of neurula stages. At tadople stages, analysis of *Pitx2c* expression revealed absent staining in 50% of the *Xfz8* morphants which was very highly significant different compared to the control (Fig. 21I). Next, it was tested whether leftward flow was affected by *Xfz8*-KD. Calculation of data obtained by the analysis of eight *Xfz8* morphants and four control specimens revealed severe inhibition of directed extracellular fluid flow above the GRP in a highly significant manner (Fig. 21H, see MM, I.1.6). To examine if this was due to morphological defects of the ciliated GRP, SEM analysis of *Xfz8* morphants was performed. Ciliation rate dropped and cell size increased upon *Xfz8*-MO injection when compared to control GRPs ($p=0.004$; Fig. 21D, E, G). However, no significant change of cilia length and polarization was seen (Fig. 21F and data not shown). These observations indicated that *Xfz8* was required for the development of the GRP, most likely by specification of the SM. To test the influence of *Xfz8*-KD on the SM, expression of the marker gene *Foxj1* was analyzed by WMISH (see also results III.3). A reduction of *Foxj1* was shown in *Xfz8*-MO-injected embryos which was a very highly significant effect compared to the control (Fig. 21J). Thus, impairment of Wnt signaling by loss of function of the receptor Xfz8 led to failure of SM specification, morphological defects of the GRP, disturbed leftward flow and, consequently, to laterality defects.

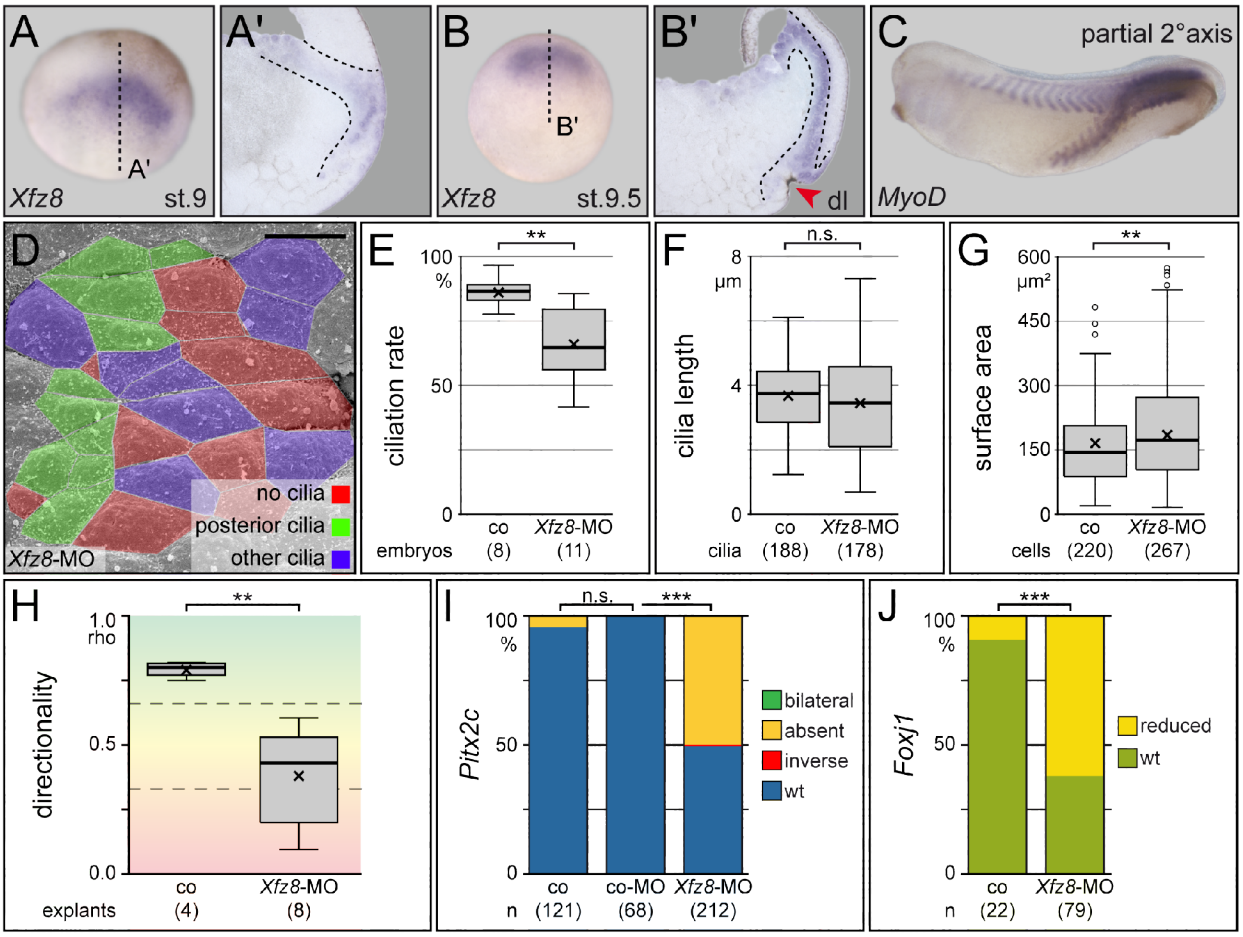

Figure 21: Loss of function of the *Xenopus frizzled receptor 8* inhibited left side determination
(A-B) *Xfz8* expression in gastrula stage embryos. In st.9 *Xfz8* mRNA was detected by WMISH in the dorsal mesoderm in superficial and deep cells **(A, A')**. At early gastrula, strong staining could be found in mesodermal cells which had involuted and migrated anteriorly and in superficial cells above the dorsal lip (dl, indicated by red arrowhead; **B, B'**). Embryos are shown in a vegetal view, dorsal up. Sectional planes **(A, B)** and *Xfz8* staining in sections **(A', B')** are depicted by dashed lines.
(C) Secondary (2°) axis induction. Ventral injection of 1300pg *Xfz8*-mRNA into the 4-cell embryo induced a partial 2° axis. Somites have been stained by *MyoD*. Embryo is shown in a lateral view, anterior to the left.
(D-G) SEM analysis. SEM pictures revealed morphological defects of the GRP in *Xfz8* morphants (scale bar=20µm). Ciliation rate **(E)**, cilia length **(F)** and cell surface area **(G)** was measured using the open source programs ImageJ and Statistical-R (see MM, I.1.5). Ciliation rate dropped from 86% ± 6 in control embryos to 66% ± 15 in *Xfz8* morphants (p=0.004). The cell surface area was increased highly significant from 165.75µm² ± 86.99 in controls to 184.49µm² ± 122.55 in *Xfz8*-injected specimens (p=0.001). No difference was seen in cilia length (co, 3.68µm ± 1.15; *Xfz8*-MO, 3.45µm ± 1.46; p=0.112).
(H) Leftward flow. Measurement of the extracellular fluid flow above the GRP revealed disturbance of the directionality (indicated by the rho-value, see MM, I.1.6) of the wildtypic leftward flow upon *Xfz8*-KD (p=0.008).
(I) *Pitx2c* expression. Left-sided *Pitx2c* staining was inhibited in *Xfz8*-MO-injected specimens in a very highly significant manner when compared to the uninjected co or co-MO injected embryos.
(J) *Foxj1* expression. In gastrula stages *Foxj1* was reduced in *Xfz8* morphants very highly significant compared to the co.
co, control; dl, dorsal lip; n.s., not significant; st., stage; wt, wildtype.

After studying the loss of function phenotype of Wnt signaling and its role in dorsal SM specification, it was tempting to speculate that Wnt gain of function was capable of

inducing *Foxj1* expression. This was tested by ventral injection of mRNA coding for either *XDsh*, *β-cat* or *XSia* followed by WMISH for *Foxj1* at gastrula stages. In all cases, ventral activation of the Wnt signaling pathway resulted in *Foxj1* induction above the ventral blastopore lip. Staining for *Foxj1* was only observed in the superficial epithelium rather than in deep tissue (Fig. 22A-C'' and data not shown). On the dorsal side endogenous *Foxj1* expression was detected (Fig. 22C').

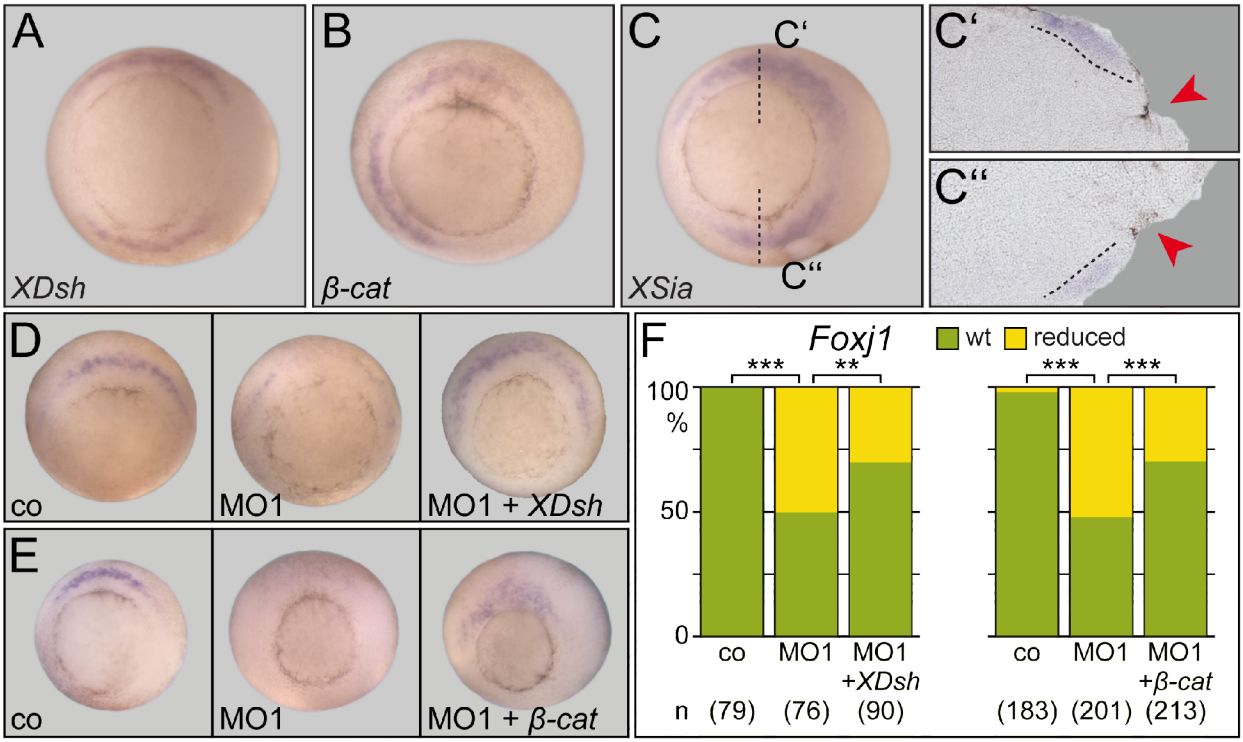

Figure 22: Rescue of *Foxj1* expression in 5-HT morphants
(**A-C**) *Foxj1* induction. By WMISH *Foxj1* expression was analyzed in embryos which were injected ventrally either with *XDsh* (**A**, st.10), *β-cat* (**B**, st.10.5) or *XSia* (**C**, st.10.5). Ventral *Foxj1* induction was observed in all cases. The staining of the endogenous *Foxj1* expression and upon injection on the ventral side was restricted to the superficial epithelium **(C', C'')**. Red arrowheads indicate dorsal **(C')** and ventral **(C'')** cell ingression.
(D-F) Rescue of 5-HT morphants. Embryos were either injected with the MO1 or co-injected with the MO1 and *XDsh* or *β-cat*, respectively (**D**, st.10; **E**, st.10.5-11). Quantification of results is shown in **F**. Reduced *Foxj1* expression in 5-HT morphants was very highly significant restored upon *XDsh* or *β-cat* co-expression.
Embryos are shown in a vegetal view, dorsal up **(A-B, D, E)**. Section plane is indicated by black dashed line **(C)**. co, control; st., stage; wt, wildtype.

Taken together, these results demonstrated that Wnt signaling was crucial for *Foxj1* expression. The Wnt loss of function resulted in a phenotype which was comparable to the effects observed in 5-HT signaling-impaired embryos (see results, III.1-3). This led to the assumption that 5-HT and Wnt signaling were both required for *Foxj1* induction,

comparable to dorsal axis development by the double axis assay. Experiments combining loss of 5-HT and induction of Wnt signaling were performed to elucidate epistatic correlation of both pathways like it was done for the double axis assay (see results III.5), here with regard to dorsal *Foxj1* expression. Therefore, dorsal co-injection of MO1 and *XDsh* or *β-cat* mRNA were conducted. About 50% of embryos injected with the MO1 showed reduced *Foxj1* expression. This effect was reversed in a very highly significant manner by co-expression of *XDsh* or *β-cat* mRNA (+*XDsh*/*β-cat*, 30%; Fig. 22D-F).

III.7 *Foxj1* induction by maternal signals

Foxj1 expression was associated with ciliated cells in the mouse PNC, the zebrafish KV and the *X. laevis* GRP structure but yet it is not clear how the expression pattern is initiated and regulated during development (Zhang et al. 2004; Stubbs et al. 2008; Pohl et al. 2004). In *Xenopus* the expression at gastrula stages is restricted to the SM above the dorsal lip and was induced upon over-expression of Wnt signaling components ventrally (see results, III.6). These results indicated that *Foxj1* was either a direct target of the Wnt pathway, like it is known for *Xnr3* and *gsc*, or its expression depended on downstream components. To address this question *Foxj1* expression was analyzed in embryos in which protein synthesis was down-regulated by treatment with cycloheximide (CHX) (Cascio et al. 1987, see MM, I.1.3). Target gene induction via activated downstream signaling requiring newly synthesized protein can thus be excluded. If *Foxj1* would be a direct target of the dorsal active canonical Wnt pathway, unilateral *Foxj1* staining by WMISH of CHX-treated embryos was to be expected.
Early blastula embryos were transferred into CHX-containing medium and cultivated until untreated control embryos developed to stage 10 which was followed by WMISH for the myogenic differentiation factor *MyoD*, the homeobox gene *gsc*, the transcription factor *Xbra* or *Foxj1*. *MyoD* was used as negative control as its expression does not represent a direct target of maternal pathways but depends on FGF and XWnt8 signaling (Hoppler et al. 1996; Fisher et al. 2002; Murai et al. 2007).

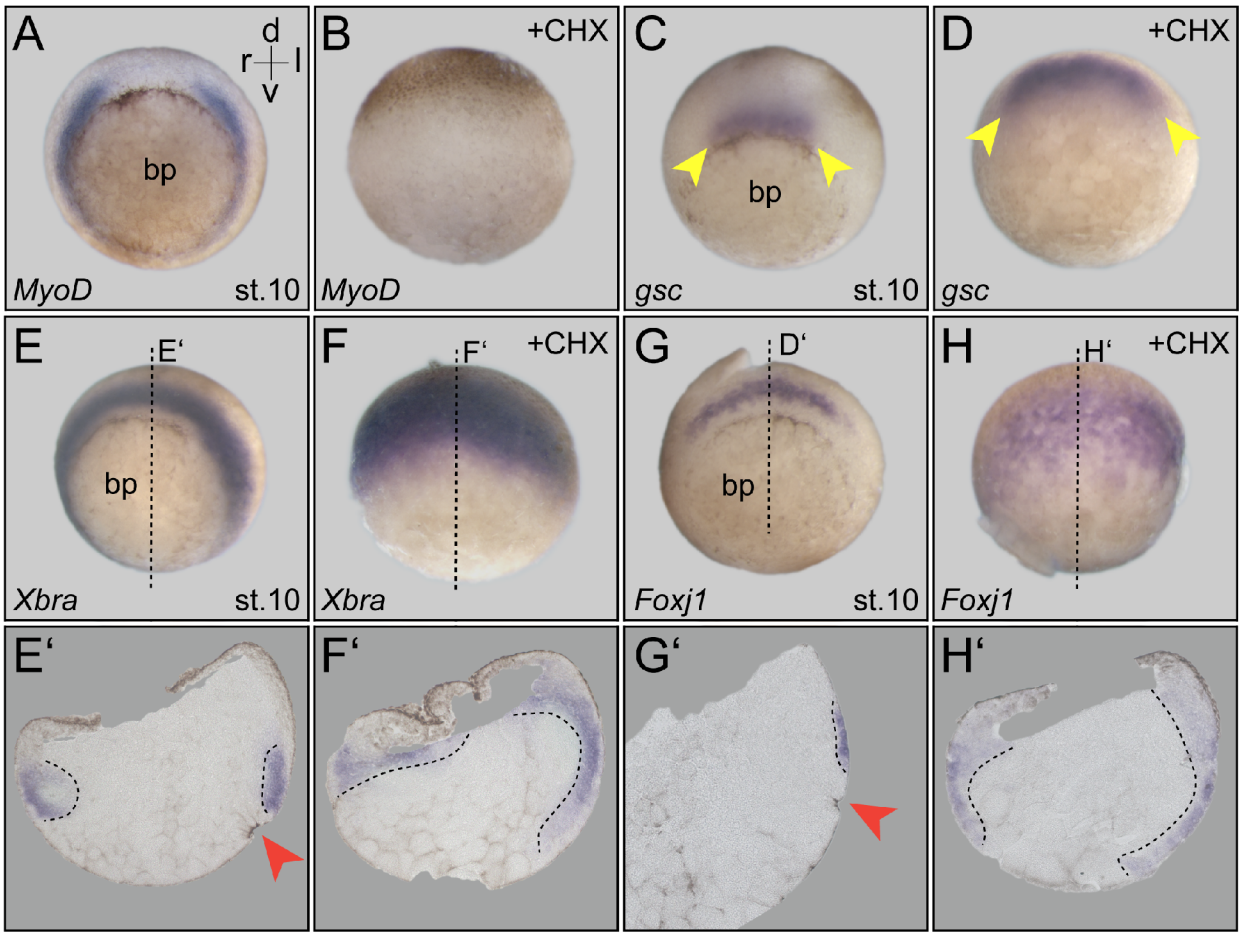

Figure 23: Expression patterns in CHX-treated embryos
Embryos were cultivated either in normal medium or in CHX-containing medium for inhibition of protein synthesis. Expression patterns have been examined when the controls have developed st.10.
(A, B) *MyoD* expression was prevented in CHX-treated embryos **(B)**. Wildtypic bilateral expression was observed in untreated controls **(A)**.
(C, D) *Gsc* expression appeared to be expanded ventrally in embryos cultivated with CHX **(D)** compared to the more narrow expression seen in wildtypes **(C)**. Expression is indicated by yellow arrowheads.
(E-F') *Xbra* expression was detected surrounding the blastopore **(E, E')**. Incubation with CHX caused additional staining of *Xbra* vegetally and animally on one side and medially on the opposing side **(F, F')**.
(G-H') Wildtypic *Foxj* expression was restricted to the superficial cells above the dorsal lip **(G, G')**. Sections of CHX-treated specimens revealed *Foxj1* staining in a ring surrounding the marginal zone of the embryo with additional expansion towards the animal and the vegetal pole and into deep tissue **(H, H')**.
All embryos are shown in a vegetal view, dorsal up. Dashed lines indicate either sectional planes **(E-H)** or expression patterns (E'-H'). Dorsal lip formation is highlighted by red arrowheads.
bp, blastopore; CHX, cycloheximide; d, dorsal; l, left; r, right; st., stage; v, ventral.

Gsc and *Xbra* were taken as positive controls because both are induced by maternal signals and showed an expansion of the expression domains after CHX treatment (Kurth et al. 2005). As expected *MyoD* expression was lost after treatment with CHX compared to the untreated control displaying normal bilateral staining (Fig. 23A, B). *Gsc* was found in a broader domain than in control embryos, in which expression was observed to be more restricted above the dorsal lip (Fig. 23C, D). The wildtype

expression of *Xbra* was found in a ring-like pattern surrounding the blastopore with a uniform staining dorsally and ventrally revealed by sectioning (Fig. 23E, E'). In contrast, the expression of *Xbra* in CHX-treated specimens was found to be expanded animally and medially (Fig. 23F, F'). *Foxj1* staining in untreated embryos was found in a restricted pattern above the dorsal lip (Fig. 23G, G'). Remarkably, the expression of *Foxj1* was expanded upon CHX treatment. *Foxj1* signal was ectopically observed in more vegetal and animal tissues as well as in deeper cell layers (Fig. 23H, H'). Surprisingly, *Foxj1* staining was found in a ring-like fashion, surrounding the embryo including the ventral half of the embryo. This pattern was reminiscent of *Xbra* transcription (Fig. 23F', H').

The CHX experiments, in which protein synthesis was prevented in embryos from blastula (stage 7/8) onwards, resulted in an expansion of *Foxj1* expression, i.e. staining was detected ectopically in ventral and dorsal cells. These results suggested that induction of *Foxj1* in the SM cells was achieved by maternally provided signaling pathways but could not depend exclusively on dorsally active Wnt signaling.

Discussion

The focus of this thesis work was on investigating so-called early determinants of the LR axis formation (Levin et al. 1998; Adams et al. 2006; Fukumoto and Levin 2005; Fukumoto et al. 2005). Specifically, two components of the 'ion-flux' hypothesis, namely serotonin (5-HT) and gap junctions (GJ), were analyzed in context of the conserved mechanism of leftward flow. Recently, in *X. laevis* a ciliated structure was described, called the GRP, which represents the homologue of the PNC of mouse and rabbit and of Kupffer's vesicle (KV) in bony fish (Schweickert et al. 2007; Hamada et al. 2002; Takeda et al. 1999; Shiratori et al. 2006; Blum et al. 2009; Hirokawa et al. 2006; Essner et al. 2002). A cilia-driven leftward flow of extracellular fluid above the GRP towards the left side was shown to be needed for left-sided Nodal cascade induction. In this study, the role 5-HT signaling and cell-cell communication via GJ (GJC) during LR development was elucidated. The results of the present work strongly suggest that both components act in the context of leftward flow, which renders the ‚ion-flux' hypothesis in the published version highly unlikely. In the following chapters the new role of 5-HT for GRP morphogenesis and a dual role of GJC for leftward flow and signal transfer towards the left lateral plate mesoderm (LPM) will be discussed.

I. Serotonin signaling

The early action of 5-HT signaling was proposed based on a pharmacological screen. (Fukumoto et al. 2005; Fukumoto and Levin 2005; Adams et al. 2006). However, in the work presented here it was shown that 5-HT signaling via the receptor 3 was indispensable during gastrulation for superficial mesoderm (SM) specification, leftward flow establishment and left-sided Nodal cascade induction. More precisely, determination of the SM and downstream events were disturbed in *xHtr3* morphants. These results were confirmed by interfering with 5-HT signaling in general upon misexpression of the ligand binding domain (*xLBD*) of *xHtr3* or of its human homologue (*hLBD*), and specifically in the GRP cell lineage (results, III). Due to these new

experimental evidences, a more specific role for 5-HT signaling in LR axis formation can be postulated.

I.2 Serotonin is symmetrically localized in early cleavage stage embryos

5-HT was thought to have a ventral function because of its specific LR asymmetric ventral localization (Fukumoto et al. 2005). The experiments presented here, however, did not meet this expectations, as only dorsal but not ventral loss of 5-HT signaling resulted in LR defects (results, III and Vick, 2009). To clarify this inconsistency, the distribution of 5-HT at early cleavage up to gastrula stages has been re-examined by Michael Danilchik[1] (OHSU, Portland, USA) for the 5-HT project. Some of the results are presented here to complete the data discussed for 5-HT signaling.

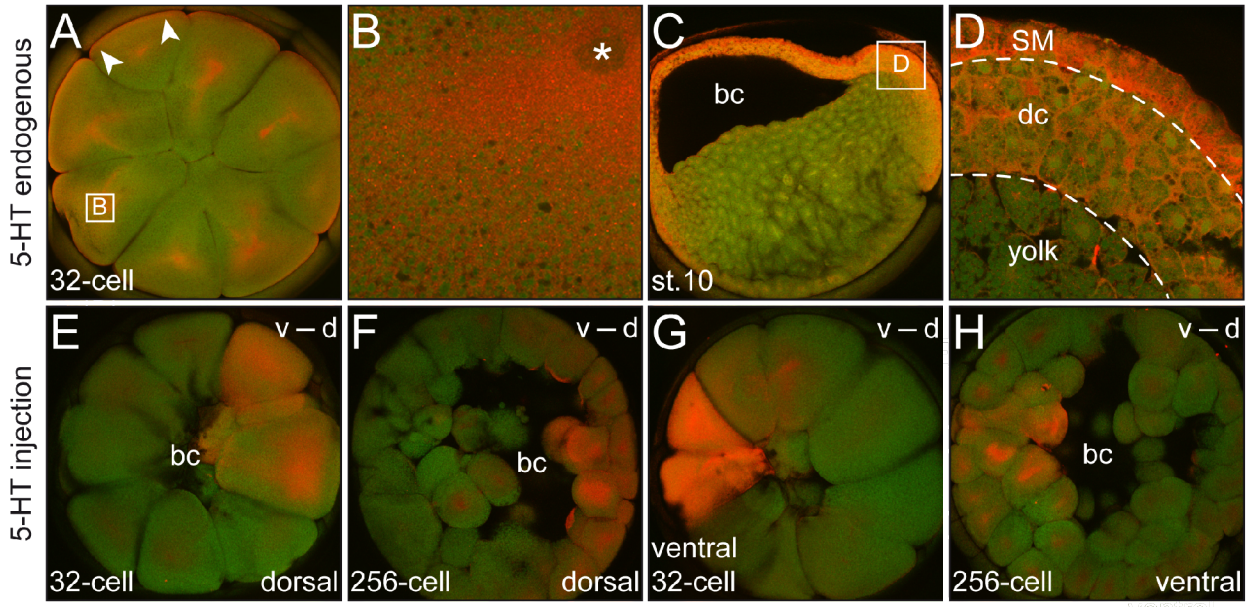

Figure 2[2]: Serotonin localization
(A-D) Endogenous 5-HT. In the 32-cell embryo 5-HT was evenly distributed in all blastomeres with accumulation below the membrane (white arrowheads) and in the perinuclear region **(A, B)**. A granular staining was seen in higher magnification **(B)**. At st.10, 5-HT appeared to be enriched animally compared to the vegetal region **(C)**. Strong staining was detected in the superficial cell layer **(D)**. Embryos are shown in an animal view **(A)** or a lateral view, dorsal to the right **(C)**.
(E-H) Exogenously applied 5-HT. 5-HT was either injected into the ventral **(E, F)** or the dorsal side **(G, H)**. Analysis of the 5-HT distribution in different stages revealed staining in blastomeres of the injected cell lineage **(F, H)**. Embryos are shown in an animal view, dorsal to the right.
bc, blastocoel; d, dorsal; dc, deeper cells; SM, superficial mesoderm; st., stage; v, ventral.

1 personal communication

2 Michael Danilchik, with permission

He visualized endogenous 5-HT distribution by antibody staining in equatorially bisected embryos using a confocal laser scanning microscope. Series of optical sections in defined intervals were performed to compare 5-HT appearance in several cell layers (Fig. 24). Through this analysis he could show that 5-HT was evenly distributed in 32-256-cell stages with strong staining around the nucleus and below the plasma membrane (Fig. 24A, B). This cytosolic 5-HT seemed to appear in a punctated pattern which most likely represented vesicular structures. At gastrula stages, 5-HT accumulation was observed in the superficial animal layer, more weak staining in deeper tissue and vegetal cells (Fig. 24C, D). Occasionally, he also detected strong signals in single blastomeres as it was described in the literature, but by comparison with adjacent sections this turned out to be an artifact (M. Danilchik, personal communication). In addition, functional analysis was performed by injections of 5-HT, followed by analysis of *Pitx2c* expression or the organ situs to investigate a potential influence on LR axis determination. In none of these injections a significant effect on laterality was observed (Mike Danilchik, personal communication and data not shown).
In addition, Danilchik investigated the distribution of exogenously applied 5-HT and found it to be almost exclusively restricted to the injected cell lineage with no differences between ventral and dorsal injections (Fig. 24E-H). Consequently, the suggested 5-HT diffusion by passage through GJ in 128-256-cell embryos could not be confirmed by these experiments (Levin et al. 1998). Supporting these findings, it was shown that inhibition of GJC in early cleavage stage embryos up to stage 9 induced only a low level of LR defects compared to the effectiveness obtained by treatment of older stages (see also below, discussion II.). However, the asymmetric localization and activity of ion pumps which, according to the 'ion-flux' hypothesis, displays the initial step of the symmetry breakage, remains to be investigated.

I.2 Serotonin signaling is necessary for superficial mesoderm specification

Using pharmacological inhibition of 5-HT signaling, receptors of the class 3 and 4 were reported to be involved in LR axis determination (Fukumoto et al. 2005). By WMISH, the receptor 4 was not found to be expressed earlier than in tadpole stages and did not

represent a good candidate for targeted KD (Susanne Bogusch, personal communication). However, expression of the receptor 3 subunit *xHtr3* was detected by RT-PCR from gastrulation onwards. The 5-HT receptor family 3 are ligand-gated ion channels for Ca^{2+}, K^{+} and Na^{+}, whereas receptors of all other classes represent G-protein coupled receptors (Barnes et al. 1999; Thompson et al. 2006). Because of the relatively late expression of *xHtr3* at gastrula, this subunit was a good target for loss of function experiments, as maternal effects could be excluded. Besides that, 5-HT-dependent Ca^{2+} influx was involved in ciliary motility what implicated that 5-HT signaling could be involved in generation of leftward flow (Doran 2004).

5-HT itself is maternally provided and newly synthesized 5-HT seemed not to be necessary for axis development. This was proven by Levin and his colleagues by performing incubation experiments using an inhibitor of tryptophane hydroxylase (tph). Tph is an enzyme involved in the synthesis of serotonin and its inhibition had no effect on LR development. Interestingly, interference with the 5-HT degrading enzyme monoamine oxidase (MAO) induced laterality defects, which led to the conclusion that a specific 5-HT level was needed for correct LR development (Fukumoto et al. 2005). However, this experiment was in contrast to 5-HT injections done by Mike Danilchick in which exogenously applied 5-HT was visible during development but had no effect on LR specification. In addition, overexpression of MAO or the second degrading enzyme catechol-O-methyl-transferase (COMT) did not affect LR determination in a reproducible manner, arguing that vesicular 5-HT was protected from degradation (Philipp Vick, personal communication and data not shown). For the stated reasons, the focus was on the *Xenopus* receptor 3 subunit (*xHtr3*) in this study.

The outcome that dorsal *xHtr3*-KD not only led to absent left-sided *Pitx2c* expression and loss of leftward flow but also to morphogenetic defects of the GRP, came as surprise (Figs. 15 and 16). These results were further supported by laterality defects induced by misexpression of the *xHtr3* truncated construct and the human homologous sequence, both consisting of the ligand binding domain only (*xLBD*, *hLBD*, Figs. 14-16). Analysis of *Foxj1* and *Xnr3*, two markers expressed in the SM, revealed disturbance of SM specification during gastrulation in *xHtr3* morphants (Figs17 and 19). These findings correlate with accumulation of 5-HT in the animal superficial cell layer and in the MZ, supporting a function of 5-HT on the dorsal rather than the ventral side at gastrula

stages. However, the importance of 5-HT signaling seemed not to be restricted to SM specification because, besides LR axis defects, more severe phenotypes were observed mostly upon injection of higher doses (Fig. 18). Interestingly, *Xnr3* expression in uninjected embryos was not restricted to the SM but staining could be found in deep tissues, as well. The strong reduction of this very marker in 5-HT signaling-impaired specimens suggested that also tissues other than *Foxj1*-positive cells were influenced in these experiments, although the expression was not analyzed in sections so far.

Further, in other model organisms, interference with 5-HT signaling led to divers developmental defects. For example, pharmacological inhibition of various 5-HT receptors in early sea urchin embryos was shown to block gastrulation movements (Buznikov et al. 2005). In mouse, loss of function of the receptor subunit 5-HT_{2B} resulted in heart and neural tube closure defects (NTDs; Nebigil et al. 2001; Choi et al. 2006). Interestingly, in mouse, as in frog embryos, 5-HT was supposed to be provided by the mother. Developmental defects only occurred in the offspring of tph knock-out mothers (Côté et al. 2007). All these findings support a role of 5-HT signaling for early (DV) axis development.

The molecular nature of 5-HT signaling for SM specification remains elusive but an involvement of the channel function and intracellular regulation of the Ca^{2+} appears attractive for the following reasons. Ca^{2+} represents a key player for early development and furthermore, its requirement for LR axis specification is well documented (Schneider et al. 2008; McGrath et al. 2003; Slusarski et al. 2007; Raya et al. 2004). In *Xenopus* for example, artificially provoked increase of the cytosolic Ca^{2+} concentration by thapsigargin treatment during gastrulation (SM stages) led to LR defects (Schneider et al. 2008). This observation suggests a function of Ca^{2+} for LR axis formation during gastrulation, albeit the exact timing is not yet clear. Besides that, the Ca^{2+} level regulates both ciliary beat frequency of motile cilia and sensing of extracellular fluid flow of primary cilia, e.g. in the kidney (Praetorius et al. 2001; Tabin et al. 2003; Davis et al. 2006; Satir 1980). However, due to the developmental defects observed at stages preceding leftward flow, a dysfunction of GRP cilia in 5-HT signaling impaired embryos could not be analyzed so far.

I.3 The role of Wnt signaling in LR axis determination

In *Xenopus*, maternally provided canonical Wnt signaling components on the dorsal side are necessary for axis development (Cha et al. 2008; Standley et al. 2006; Glinka et al. 1996; Rao et al. 2010; Heasman 2006a). In the same region the SM monolayer is specified, which is a prerequisite for GRP development and LR determination (Stubbs et al. 2008, Shook et al. 2004; Schweickert et al. 2007). But up to now, an involvement of dorsal Wnt signaling in SM patterning was not confirmed in the frog.

A connection between the canonical Wnt pathway and LR development was described for other model organisms. In mouse, loss of function of the canonical ligand Wnt3a resulted in LR defects, although in this case PNC cilia developed normally. The authors found that polycystein 1, the sensing component of polycystein complexes, was reduced in PNC cilia (Nakaya et al. 2005). This interpretation is difficult to reconcile with the fact that PKD1 knock-out mice revealed normal LR development (Karcher et al. 2005). Interestingly, PKD1-like 1, a new member of the polycystins family related to PKD1, was shown to be necessary for LR development in mouse and medaka recently (Kamura et al. 2011; Field et al. 2011). In fish, the development of the KV was affected by both, the loss and the gain of canonical Wnt activity in morphants. KV cilia were reported shorter, most likely resulting in disturbed flow, and *Wnt3/8* over-expression led to enlarged KVs (Lin et al. 2009).

Due to the missing proof in frog, loss of Wnt signaling and its effect on LR axis determination was analyzed by KD of the *Xenopus frizzled receptor 8* (*Xfz8*) in the work presented here. *Xfz8* was capable of inducing a 2° axis and is described to induce dorsal marker genes upon overexpression (Deardorff et al. 1998; Sokol 1998). *Xfz8* expression could be detected in the organizer region of gastrula stage embryos. Loss of *Xfz8* resulted in absent *Pitx2c* expression, leftward flow/GRP defects and *Foxj1* reduction, resembling the phenotypes observed in 5-HT signaling-impaired embryos (Fig. 21). These findings suggest a role of Xfz8-mediated Wnt signaling for dorsal *Foxj1* patterning and thus SM specification and downstream LR determination. This notion was supported by induction of *Foxj1* expression upon ventral activation of Wnt signaling (Fig. 22). In concordance with this, a second GRP next to the endogenous one was induced in double axes embryos (Matthias Tisler and Thomas Thumberger, personal

communication). These observations and the results of the *Xfz8*-KD in *Xenopus* indicate, that Wnt signaling in general is essential for SM specification and, consequently, LR development which most likely is conserved in large parts among the vertebrates.

I.4 The interplay of serotonin and Wnt signaling

The reduction of the canonical Wnt target gene *Xnr3* after 5-HT loss of function and the striking similarity of the LR phenotypes induced in 5-HT and *Xfz8* morphants indicated that the Wnt and 5-HT pathways are mutually dependent. Surprisingly, despite the typically described enlargement of head structures in Wnt signaling-impaired embryos, it was shown that inhibition of dorsal 5-HT signaling resulted in small or absent heads, and no effect on head development was seen after *Xfz8*-KD (Figs. 18 and 25). But expression of *Xfz8* in cells which involute during early gastrulation and end up in the head tissue, strongly suggesting a role in head development (Fig. 21 and Deardorff et al. 1998). However, in experiments published so far, the main focus was on Xfz8 function for kidney development (Satowa et al. 2004; Wallingford et al. 2001). In the majority of these experiments a dominant-negative construct was used for misexpression which inhibited gastrulation movements. This was not observed upon dorsal *Xfz8*-MO injection in this study. The unexpected mildness of the *Xfz8* phenotype described here could be due to the low MO dose which was chosen to induce laterality defects but prevented more severe effects.

To examine whether *Xfz8* and *xHtr3* act epistatic, i.e. in the same pathway, low doses of each MO were injected into the dorsal side and phenotypic changes were compared to *Xfz8*-MO and MO1-co-injected specimens at tadpole stages. These experiments showed that parallel KD of both led to a stronger inhibition of head development than observed upon single MO injections (Fig. 25 and data not shown), strongly suggesting an epistatic relation of Wnt (*Xfz8*) and 5-HT (*xHtr3*) signaling. Interestingly, a comparable phenotype was found by injection of the secreted frizzled-related protein 2 (sFRP2) (Bradley et al. 2000). The authors discussed a Wnt signaling dependent *sonic hedgehog* phenotype as the reason for the observed phenotype. It would therefore be

interesting to analyze a possible epistatic relation of sFRP2 and 5-HT signaling and the effect on sonic hedgehog activity.

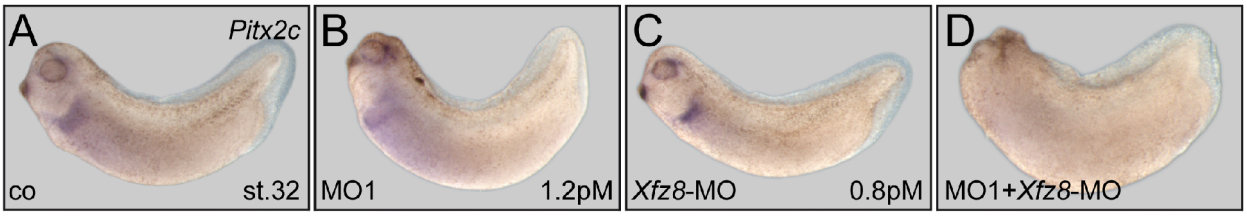

Figure 25: Epistasis of *Xfz8* and *xHtr3*
(A-D) Reduction of head structures. Low doses of the *xHtr3*-MO1 (1.2pM, **B**) and *Xfz8*-MO (0.9pM, **C**) injected dorsally only had slight influence on *Pitx2c* expression and head development. Co-injection of both led to severe reduction or absence of *Pitx2c* and head structures **(D)** compared to the uninjected control **(A)**. Embryos are shown in a lateral view, anterior to the left.
co, control; st., stage.

The dependency of Wnt on 5-HT signaling was clearly confirmed in the double axis assay. Double axes induced by *XWnt8* but not by *XDsh* or *XSia* were inhibited by parallel KD *of xHtr3* (Fig. 20). From these experiments it can clearly be concluded that xHtr3 was involved in Wnt signaling-dependent dorsal axis specification upstream of the cytoplasmic factor *XDsh*. This notion was supported by the rescue of *Foxj1* reduction in *xHtr3* morphants on the dorsal side by co-injection of *XDsh* and *β-cat* encoding mRNA. Surprisingly, however, the results of the double axis induction assay revealed differences between the MO-mediated KD and the presumed squelching of 5-HT by means of LBD application. Injection of both, the human or the frog *LBD*, abolished secondary axes induction by *XDsh*. Even for double axes induced by *XSia*, the *hLBD* decreased the number of 2° axes in a very highly significant manner (Fig. 20). These observations were supported by the finding that dorsal over-expression of *LBDs* induced NTDs whereas in MO-injected embryos open neural tubes represented isolated cases only. The described discrepancy of the KD and the *LBD* phenotype indicates that 5-HT signaling via other receptors (subunits) than of the class 3 (*xHtr3*) was needed for canonical, and probably non-canonical, Wnt signaling, as well. In addition, to date it cannot be ruled out that misexpression of the truncated receptor constructs interferes with other pathways than Wnt, e.g. the TGFβ pathway. Down-regulation of TGFβ signaling could also lead to disturbance of gastrulation movements and LR determination (Shen 2007; Onuma et al. 2002; Heasman 2006a).

I.5 *Foxj1* induction/patterning - a model

As described above, this work showed that induction of the Wnt signaling pathway on the ventral side resulted in *Foxj1* induction. *Foxj1* could either be a direct target gene of the Wnt pathway or rely on downstream signals. To investigate this correlation, an experimental approach using CHX was performed. The expression patterns of *Xbra* and *Xgsc* were shown to be expanded upon CHX incubation (results III.7 and Harvey 1991; Hopwood et al. 1989; Steinbach et al. 1998). This effect was supposed to be caused by CHX-dependent inhibition of negative regulatory events taking place in post-MBT stages (Thomas Kurth et al. 2005). Surprisingly, *Foxj1* staining was detected surrounding the embryo in an expression pattern similar to *Xbra*. This was an absolutely unexpected result as the prediction was that *Foxj1* induction would depend on maternally provided dorsal Wnt signaling components. The observed expression suggested an induction of *Foxj1* expression in the complete mesodermal tissue by maternal factors followed by its restriction to the dorsal side most likely by inhibitory factors which would be active post-MBT. In pre-MBT stages, mesodermal cell fate is induced by the vegetally localized factors VegT (T-box transcription factor) and Vg-1 (TGFβ family member) (Heasman 2006b; Lustig et al. 1996; Stennard et al. 1996). Mesoderm specification also depends on activity of the proprotein convertase xPACE4 which is needed for cleavage and consequently signaling activation of several secreted proteins, in this case presumably Vg-1 and other TGFβ familiy members (Birsoy et al. 2005).

But how is *Foxj1* regulated to end up in a defined dorsal expression? The presented experiments only allow speculative considerations about the patterning of *Foxj1*. For getting such an specific spatial expression two main criteria can be envisaged:

(1) *Foxj1* expression has to be down-regulated on the ventral side at post-MBT stages. There are several factors known to specify ventral and to repress dorsal cell fates, e.g. BMP signaling and the Notch-Delta pathway (Heisenberg et al. 2008; Khokha et al. 2005; De Robertis 2009; Ben-Zvi et al. 2008; Lane et al. 2004; Revinski et al. 2010; López et al. 2005; Maéno et al. 1994; Northrop et al. 1995). In addition, ventral patterning depends on zygotic Wnt signaling including the zygotically active ligand Wnt8 and the co-factors and transcriptional regulators Tcf1/Tcf3 (Ramel et al. 2004;

Standley et al. 2006). Ventral loss of function of BMP or Delta-Notch signaling or Wnt8 and subsequent enhancement of *Foxj1* in post-MBT stages would confirm such a repressive activity.

(2) *Foxj1* expression on the dorsal side has to be protected from ventralizing factors and maintained during development. Prevention of ventralizing signals in the organizer region is thought to be provided by BMP-inhibiting factors (De Robertis et al. 2004; Khokha et al. 2005). In the context of SM specification, the expectation would be that BMP signaling induction dorsally would lead to reduction of *Foxj1*. In this study, it was shown that overexpression of Wnt signaling components were capable of inducing *Foxj1* whereas loss of *Xfz8* expression led to *Foxj1* reduction. These observations indicated that Wnt signaling played an essential role in *Foxj1* induction and/or maintenance on the dorsal side. It will be interesting in further experiments to analyze whether ventral *Foxj1* induction upon Wnt signaling activation is a result of direct *Foxj1* regulation or via intermediate factors like *nodal-related genes*, e.g. *Xnr3*.

However, there are a few evidences which implicate that Wnt signaling is or has to be down-regulated after *Foxj1* transcription has been initiated. First, in the mouse, the canonical Wnt antagonist Chibby, which is a β-cat binding protein, was shown to be a direct target of Foxj1 in the lung (Love et al. 2010). Furthermore, in *Xenopus* the reduced *Foxj1* expression in 5-HT morphants could be restored by *XDsh* and *β-cat* co-expression but was severely reduced upon *XSia* co-injection (data not shown). These observations indicate that down-regulation of canonical Wnt signaling was possibly required for *Foxj1* maintenance upstream of *XSia* and downstream of *XDsh/β-cat*. As further evidence, the transcriptional co-repressor Tcf4/Grg-4 of Wnt signaling is expressed in the superficial layer of the animal hemisphere and of the MZ, in a punctated pattern in the skin and in the pronephri, resembling at least a part of the *Foxj1* expression (Molenaar et al. 2000). It is therefore tempting to speculate that in *Foxj1*-expressing tissue canonical Wnt signaling is inhibited. Interestingly, during gastrulation and the development of the pronephic duct, a switch between canonical an non-canonical Wnt signaling is thought to be necessary for establishment of the ciliated epithelium (Oteiza et al. 2010; Antic et al. 2010; Borovina et al. 2010; Masazumi Tada et al. 2009; Kim and Han 2005b; Kwan 2003; Karner et al. 2009; Sharma et al. 2008; Benzing et al. 2007).

Based on the above reasoning the following model is proposed for the interplay of 5-HT and Wnt signaling: 5-HT is present in all cells but enriched in the animal hemisphere, thereby providing a competence factor for Wnt signaling. *Foxj1* expression is induced by maternal factors and enhanced on the dorsal side in a 5-HT and canonical Wnt signaling dependent manner. At post-MBT stages, *Foxj1* is inhibited in the ventral and lateral mesoderm probably by Wnt8, Notch-Delta and/or BMP signaling. On the dorsal side *Foxj1* expression is maintained during gastrulation.

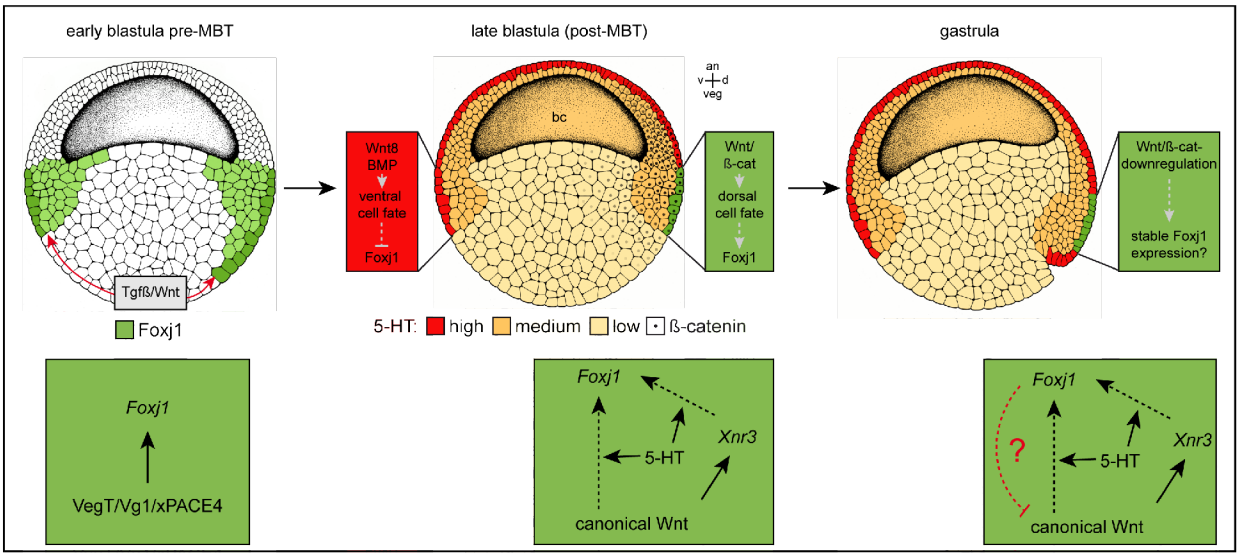

Figure 26: *Foxj1* induction - a model
Initially, *Foxj1* expression is induced by vegetally localized maternal factors like VegT/Vg1. In post-MBT stages, *Foxj1* is enhanced on the dorsal side either as a direct target of the Wnt pathway or indirectly via Wnt-dependent expression of *nodal-related genes* (e.g. *Xnr3,* specifically expressed in the SM). This is supposed to be a 5-HT-dependent process which is present in all cells but enriched in the superficial layer of the animal hemisphere. For maintenance of *Foxj1* during gastrulation it could be necessary that canonical Wnt signaling is down-regulated either by *Foxj1* target genes, like it was shown for the mouse, or by zygotic active secreted Wnt/β-cat antagonist (secreted frizzled related proteins, sFRPs).

II. Gap junctional cell-cell communication and LR asymmetry

GJC has been shown to be involved in LR axis development of several vertebrate model organisms, i.e. zebrafish, *Xenopus*, chick and rabbit (Levin et al. 1998, 1999; Hatler et al. 2009; Landesman et al. 2000; Feistel et al. 2008). However, time points and underlying mechanisms differ between species. In zebrafish, loss of function of the GJ subunit Cx43.4 affected the development of the ciliated KV and thus laterality determination (Hatler et al. 2009). In rabbit, GJC was proposed to be down-regulated in a leftward flow-dependent manner on the left side which enabled left-sided Nodal cascade induction (release of repression, Feistel et al. 2008). In chick, GJC was reported to be required for laterality development during the formation of the primitive streak. In *Xenopus*, an asymmetry of GJC along the DV axis was proposed as the basis of LR asymmetric accumulation of small molecules (Levin et al. 1998; 1999). The finding of leftward flow in frog as well necessitated re-investigation of GJC in this context. In this study, the role of GJC for symmetry breakage in *Xenopus* was analyzed in detail (see results, II.) to address the question of when and where GJC is involved in LR axis determination during embryonic development of *Xenopus.*

II.1 GJC is required in neurula stage embryos for symmetry breakage

Cx gene products are classified according to their molecular weight which makes it difficult to deduct the function or conservation from the molecule name. For example, *Cx43* was described to be mutated in patients having laterality defects and malformations of the heart (Britz-Cunningham et al. 1995). In contrast, in *Cx43*-KO mice no such defects were recorded (Reaume et al. 1995). Because of these difficulties, the relevance of GJC for LR development in *Xenopus* was examined by inhibiting GJC in general, i.e. blocking channel conductance using the long-chain alcohol HepOH. *Xenopus* embryos were cultured in HepOH-containing medium at different developmental time points. Using this culture paradigm, two critical time windows for a role of GJ in LR development could be determined as HepOH was most effective in blastula and neurula embryos. Treatment at these stages resulted in

absence of *Pitx2c* expression and heterotaxia of organ situs. Interestingly, in neurula embryos only injection of HepOH into the gastrocoel resulted in laterality defects, indicating that the tissue responsive to GJC inhibition and required for left-sided determination was located inside the embryo. In addition, this outcome could represent an explanation for the apparently contradictory data sets of studies published so far and the results discussed here. Levin and his colleagues found that inhibitors for GJ were most effective between early blastula (stage 5) and late gastrula (stage 12; Levin et al. 1998). In these stages SM cells are located at the dorsal side in a superficial layer exposed to the surrounding culture medium. In later stages, after gastrulation is completed (stage 12.5), SM-derived GRP cells are positioned inside the embryo and thus probably not accessible for inhibitor treatment by simple incubation. Knowing that (1) leftward flow across the GRP is necessary for symmetry breakage and (2) assuming that induction of the Nodal cascade requires the transfer of an as yet unknown signal from the lateral-most GRP cells to the left LPM helped to perform a more targeted HepOH treatment for the here presented study. Thereby, the conclusion was drawn that leftward flow, which takes place in the gastrocoel of neurula stage embryos, and GJC are connected during LR development. But still, HepOH treatment could also result in unspecific effects like general alcohol-dependent defects or even blockage of intracellular Ca^{2+} signaling (Yelin et al. 2005; Guan et al. 1997).

II.2 The role *xCx26* in LR development

Levin and his colleagues showed that ventral over-expression of *xCx43*, *xCx37* and *xCx26* and dorsal loss of function by injection of the dominant-negative construct *H7* led to laterality defects (Levin et al. 1998). In the present study, based on the proposed ability to form heterotypic channels as well as their endodermal expression in stages relevant for leftward flow, *xCx26* and *xCx32* have been examined in detail (results, II.2-5.and Ayad et al. 2006). It is assumed that the subunit composition of a GJ channel determines the selectivity for passing molecules suggesting that single subunit inhibition could result in altered cell-cell conductance (Ayad et al. 2006; Barrio et al. 1992). In addition to the overlapping expression of *xCx26* and *32*, over-expression of tagged

xCx26 and 32 protein confirmed a co-localization at the membrane in a pattern described as typical for the formation of so-called GJ plaques. These observations suggested a common function of both subunits. Furthermore, parallel loss and gain of function of both subunits were performed leading to loss of *Pitx2c* expression upon unilateral left-sided but not right-sided injections. However, careful investigation of the role of each subunit strongly indicated that *xCx26* but not *xCx32* had an effect on LR development in single KD and over-expression experiments. It seems therefore justified to conclude that only xCx26 plays a role in LR specification in the frog *Xenopus*.

Next, loss of function was used to analyze the role of *xCx26* in laterality development in more detail. In *xCx* morphants left-sided *Pitx2c* expression was rescued by co-expression of the TGFβ factor *Nodal* (Fig. 8 and (Schweickert et al. 2000; Schier 2003; Tian et al. 2006). The induction of the Nodal cascade is a consequence of leftward flow at the posterior midline and, most likely, of the bilateral Nodal expression in the lateralmost GRP cells (Kawasumi et al. 2011; Oki et al. 2007; Schweickert et al. 2007; Blum et al. 2009; Vonica et al. 2007). The rescue of *xCx*-KD by *Nodal* co-expression indicated that *xCx26*-dependent GJC was neither required for competence of the LPM to propagate Nodal signaling nor for induction of *Pitx2c* by Nodal. These observations are compatible with the 'ion-flux' model in which dorsal cell-cell communication via GJ is necessary for left-sided Nodal cascade induction (Levin et al. 1998). Furthermore, in the study presented here, it was shown that a functional target of the specific loss of one GJ subunit, the *xCx26*, was represented by the GRP. SEM analysis revealed a decrease in GRP cilia length and an increase in GRP cell size in morphant embryos. Similar effects were described in zebrafish when *xCx43.4*-MO was targeted to the developing KV (Hatler et al. 2009). Interestingly, cilia length was shown to be regulated by fibroblast growth factor (FGF) signaling in zebrafish and *Xenopus* (Neugebauer et al. 2009). In addition, FGF signaling has been implicated in regulation of cell-cell conductance via gap junctions but, to date, it is not clear whether FGF regulates the opening status of GJ in a positive or negative manner (Le et al. 2001; Zhou et al. 1999). Conversely, it was found that inhibition of FGF signal transduction using SU5402, an inhibitor of the FGF receptor 1, did not lead to shorter cilia but to loss of the *Xnr1*-expressing cells of the GRP (Isabelle Schneider, personal communication). Notably, in *xCx* morphants expression of *Xnr1* in the lateral-most GRP cells was diminished, as

well. However, SEM analysis did not reveal a loss of somitic cells in *xCx26*-MO-injected specimens. This suggests that FGF might be an upstream factor regulating development of somitic GRP cells in which GJC is relevant for *Xnr1* expression.
However, loss of GJC activity by HepOH injection at leftward flow stages indicated that GJ cell-cell connection was also required for LR development at stages, in which the bilateral marker gene expression of *Xnr1* and the morphogenesis of the GRP was already completed. Thus, a second, later function can be envisaged.

II.3 GJ activity downstream of flow - a model

Possible insights come from work in rabbit, in which GJC was implicated in left-sided Nodal cascade induction by a release-of-repression mechanism (Feistel et al. 2008). These authors proposed that GJ are required in an open status to repress Nodal cascade induction via FGF signaling. Leftward flow at the PNC initiated a release of this repression by attenuation of cell-cell conductance on the left side only. But in the present study, inhibition of GJC resulted in an absence of Nodal cascade induction in the LPM which was not easily explained in the release-of-repression hypothesis. However, despite the opposing effect on left-sided marker gene expression, a second function of GJC on leftward flow event is possible also in *Xenopus*. GJ channel and hemichannel activity has been associated with Ca^{2+} levels in the cytoplasm and in the extracellular space (Evans et al. 2006; Jiang et al. 2005; Martínez et al. 2009; Thimm et al. 2005; Laird 2006b; Efimov 2006). Hemichannels are not connected to a counterpart of a neighboring cell and thought to release small molecules into the extracellular space. One model is that they are closed under resting conditions and get opened by intracellular increase and/or extracellular decrease of the Ca^{2+} concentration (Evans et al. 2006). Cell-cell communication via GJ has an evident role in triggering Ca^{2+} exchange between cells and propagation of Ca^{2+} waves, thereby amplifying the signal of this important second messenger (Sáez et al. 1989; Boitano et al. 1992; Evans et al. 2006). Furthermore, Ca^{2+} was described to be involved in LR development in the context of leftward flow in zebrafish and mouse (Sarmah et al. 2005; McGrath et al. 2003; Shiratori et al. 2006; Slusarski et al. 2007; McGrath 2003; Kramer-Zucker et al. 2005). At the left margin of the flow-generating structures, an increase of intracellular

Ca^{2+} was shown for both model organisms, which is assumed to be a result of the bending of sensory cilia (McGrath et al. 2003; Shiba et al. 2005). The underlying mechanism of how asymmetric Ca^{2+} influx could result in induction of the left-sided Nodal cascade, is not yet clear. One possibility would be a direct impact of Ca^{2+} on Nodal protein secretion and/or processing. Nodal is a so-called morphogen which can diffuse and bind to its receptor in the extracellular space and activate downstream signaling at a distance from the protein source (Schier 2009). The secretion of the protein could occur in a Ca^{2+}-dependent manner as Ca^{2+} is one key regulator of exocytosis. This relation is best described for the synaptic release of neurotransmitters (Bean et al. 1994; Pang et al. 2010). To enable signaling activation, the Nodal proprotein has to be cleaved by subtilisin-like proprotein convertases which are shown to be functional in a Ca^{2+}-dependent manner (Molloy et al. 1992; Anderson et al. 1997). Remarkably, *xFurin*, a proprotein convertase of *Xenopus,* displays a specific expression pattern in the somites in neurula stage embryos which could indicate a function for this very convertase for Nodal signaling in the somitic margin of the GRP downstream of flow (Nelsen et al. 2005). In addition, pharmacological inhibition of subtilisin-like convertases by injection into the LPM of neurula and early tadpole *Xenopus* embryos led to laterality defects (Toyoizumi et al. 2006). An interesting experimental approach to enlighten the interplay of Ca^{2+} and *xFurin* would be to elevate the Ca^{2+} level of GRP cells by adding ionophores followed by analysis of Nodal induction in the LPM. If *Nodal* expression would be induced bilaterally and xFurin would be the target of the increased Ca^{2+} concentration, the parallel *xFurin* loss of function should restore this phenotype.

In summary, in this study *xCx26* was shown to be necessary for GRP development and bilateral *Xnr1* expression at the GRP margin. However, a second function for GJ should be taken into account based on the observation, that blockage of GJ in leftward flow stages resulted in absence of the left-sided Nodal cascade. One possibility is, that inhibition of GJC led to disturbed regulation of the second messenger Ca^{2+} on the left side.

II.4 *EGFP* fusion constructs - a tool for studying Xnr1 *in vivo*

The morphogen Xnr1 and its homologous in other model organisms represents a key player for LR development (Shen 2007; Hirokawa et al. 2006; Schier 2009). For left-sided determination it is needed in the left LPM of tadpoles and, prior to that, in the posterior midline in a bilateral pattern at the margin of the GRP/PNC/KV (Kawasumi et al. 2011; Brennan et al. 2002; Hojo et al. 2007; Hashimoto et al. 2004; Vonica et al. 2007; Saijoh 2003). To date, it is not clear how the Nodal signal from the midline gets transferred to the LPM. Interestingly, Nodal itself gets distributed extracellularly in a process dependent on glycosaminoglycans (GAGs) in mouse (Oki et al. 2007)). As discussed above, data from the present work are suggestive of a mechanism in which GJC is required for Nodal secretion and/or extracellular distribution in *Xenopus*. To analyze the putative relationship between extracellular transport of Nodal protein and GJC *in vivo,* an assay to visualize *Xnr1* was set up in this study. Williams et al. (2004) have used an eGFP tagged *Xnr2* construct to examine the distribution of Nodal protein in animal caps. A similar fusion construct of *Xnr1* has been designed for the work presented here. Unfortunately, it was not possible to trace the distribution of full-length Xnr1::eGFP despite its proven biologically active character (Fig. 11, 13). As visualization of Nodal in the mouse in an identical approach was not successful as well, there may be several parameters rendering Xnr1/Nodal "invisible": (1) downstream signaling is already activated by a very low Nodal concentration and/or (2) since the turn-over of the mature protein is supposed to be quite fast, the protein level might drop below the detection threshold. Therefore, the tagged version of the functional full-length Xnr1 did not represent a useful tool to analyze Nodal distribution *in vivo*. However, the non-functional deletion constructs seemed to be a more convenient assay to visualize Xnr1 localization without affecting cell fate. An eGFP-tagged mature protein domain lacking the signaling domain required for protein secretion, stayed in the injected cell lineage as expected. In contrast, the eGFP prodomain fusion protein harboring also the signal peptide was found to be located extracellularly, both at its site of production as well as at a distance to the injected cells. It was not clear whether the GFP staining and the subcellular positioning of the prodomain overlapped completely, because in between the prodomain and the eGFP the cleavage site for proprotein convertases was present.

In addition, in the skin of tadpole stage embryos the latter was found to be enriched in vesicles which were localized apically in ciliated cells but not secreted in the extracellular space, which was rather unexpected. These observations indicate that the prodomain and the eGFP have been separated in the tissue, most likely by convertases, which challenged the extrapolation from GFP detection to prodomain localization. Due to this, the distribution should be re-investigated in future experiments and compared to the distribution of a similar construct harboring a mutated cleavage site.

The full-length construct lacking the cleavage site was found to be secreted but was not detectable in non-injected adjacent tissue. This strongly suggested that the extracellular distribution of the Nodal prodomain relies on the presence of the cleavage site. This observation did not match the general hypothesis that the prodomain should be necessary for the protein stability and thus for long-range distribution in the extracellular space (Good et al. 2005; Jing et al. 2006; Blanchet et al. 2008; Tian et al. 2008). Interestingly, the construct lacking the Furin site was shown to have no effect on LR development when misexpressed on the right side but disturbed laterality when injected into the left side (Axel Schweickert, personal communication). This suggested that the Furin deletion construct might have a dominant-negative function. However, evidences coming from experiments with a *Xnr2* construct harboring a mutated cleavage site indicated that non-processed protein retains some of its function for Nodal signaling (Eimon et al. 2002). To investigate if misexpression of the cleavage deletion construct inhibits LR determination by inhibition of Nodal signaling, markers of the left-sided cascade might be examined. If the latter would be found to act in a dominant-negative manner, it could represent a useful tool to analyze Nodal signaling in general.

III. New roles for serotonin and gap junctions: integration into a leftward flow-dependent process

The data presented here implicate a role of 5-HT and GJC in the context of leftward flow rather than in a 'early' mechanism proposed by the 'ion-flux' hypothesis during early cleavage. The results discussed above lead to the following 6-step model for LR axis determination in *Xenopus*: (1) In early cleavage stages 5-HT can be found symmetrically distributed along the DV and LR axes. In blastula embryos it is enriched in the superficial layer in the animal hemisphere and serves as competence factor for development of the SM. (2) In blastula stages the SM marker *Foxj1* is induced in the MZ by maternal factors. (3) With the onset of zygotic gene transcription (post-MBT) *Foxj1* expression is down-regulated in the ventral and lateral mesoderm. At the dorsal organizer region *Foxj1* transcription gets intensified and maintained in a defined superficial cell layer during gastrulation, which was shown to depend on Wnt and 5-HT signaling. (4) After gastrulation, the GRP is located at the posterior part of the gastrocoel roof (Shook et al. 2004). During neurulation, monocilia become longer and get polarized to the posterior pole of each cell (Schweickert et al. 2007). The lateral-most GRP cells are part of the pre-somitic mesoderm and express several Nodal signaling factors, i.e. *Xnr1*, *Derrière* and *Coco* (Vonica et al. 2007; Blum at al. 2007b). Outgrowth of the cilia and bilateral expression of *Xnr1* rely on GJC, i.e. function of xCx26. (5) In neurula stage embryos, GRP cilia rotate in a clockwise fashion to drive an extracellular fluid flow towards the left side which initiates downstream signaling (Schweickert et al. 2007). One target of leftward flow was shown to be the Nodal inhibitor Coco which is down-regulated at the mRNA level on the left side in post-flow stages (Schweickert et al. 2010). To date the underlying mechanism is not known in detail. Here, it should be assumed that a second process acts downstream of leftward flow involving an increase of intracellular Ca^{2+} as it was shown for mouse and fish (Shiba et al. 2005; Tabin et al. 2003; Sarmah et al. 2005). Hemichannels and/or GJ might play a role in amplification and propagation of the Ca^{2+} signal thereby triggering various processes: secretion of Nodal and cleavage of the proprotein by subtilisin-like convertases in the extracellular space. Even initiation of somitic GRP cell ingression into the underlying tissue by changing cell adhesion properties could rely on the Ca^{2+}

level, e.g. on Wnt/Ca^{2+} signaling (Siezen et al. 1997; Wedlich 2002; Oteiza et al. 2010; Anderson et al. 1997; Molloy et al. 1992; Slusarski et al. 2007). (6) Finally, in early tadpole stages the left sided Nodal cascade is activated in the left LPM which governs asymmetric organ morphogenesis (Hamada et al. 2002; Schweickert et al. 2000; Shiratori et al. 2006; Bakkers et al. 2009; Raya et al. 2004; Hirokawa et al. 2006; 2009).

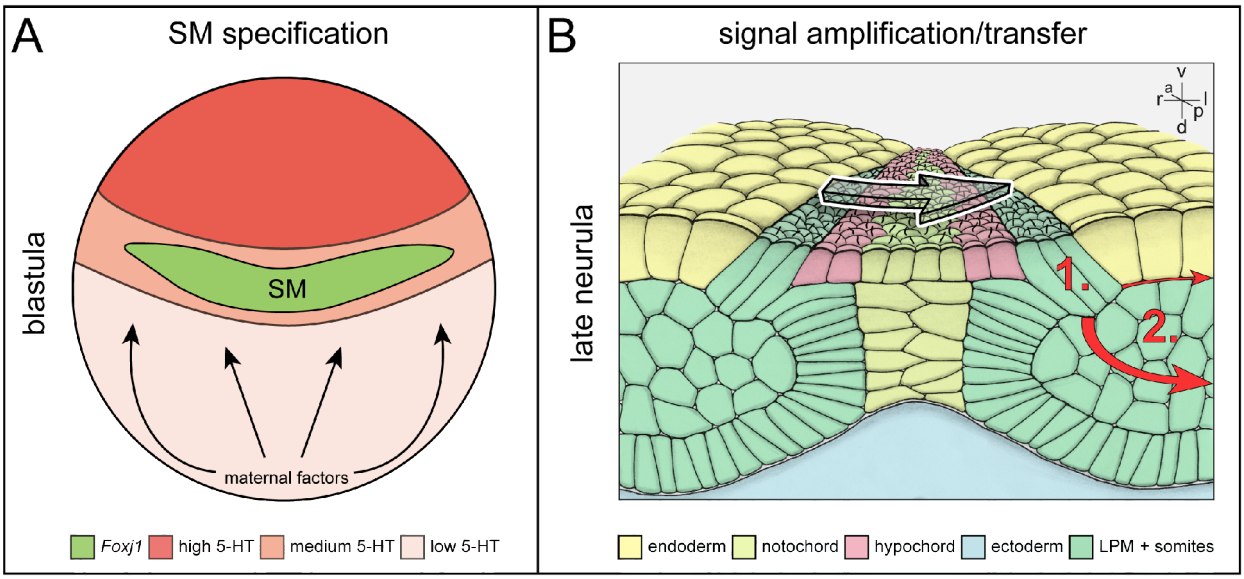

Figure 27: The model for 5-HT and GJ activity during symmetry breakage
(A) 5-HT can be found in all cells of the blastula stage but is enriched in the superficial layer of the animal hemisphere. The superficial mesoderm, marked by *Foxj1* expression, is induced by maternal factors (VegT, Vg-1) and maintained by dorsal signaling (Wnt). This process depends on 5-HT signaling to take place.
(B) In the late neurula, leftward flow, generated by motile cilia rotating in a clockwise fashion, induces downstream signals: (1) Down-regulation of *Coco* expression on the left side only. A second signal is proposed to be the increase of Ca^{2+} in the cell. (2) The activated signal is transferred to the left LPM. This involves most likely extracellular Nodal distribution what results in left-sided Nodal cascade induction. This picture is modified after Schweickert et al. 2010.
5-HT, serotonin; a, anterior; d, dorsal; l, left; p, posterior; r, right; SM, superficial mesoderm; v, ventral.

Methods and Material

I. Methods

I.1 *X. laevis:* Embryological procedures

I.1.1. *In vitro* fertilization

X. laevis can be kept in tanks filled with 18-22 °C cold water. For experiments, *X. laevis* females were stimulated for ovulation by injection of human chorion gonadotropin (b-HCG, Sigma; 400-500µl) subcutaneously. About 12 hours after injection females started to spawn and kept going for 6-10 hours. Eggs have been obtained by gently squeezing and collected in culture dishes. For sperm extraction the testicles of males were removed and stored in 1xMBSH at 4°C for 2 weeks. For fertilization a small peace of a testicle was macerated and added to freshly obtained eggs. After gently mixing movement of sperms was induced by lowering the salt concentration of the 1xMBSH using water. 40min after fertilization the jelly coat was removed by incubation with 2% Cystein/DDW (pH8) for 7min. Isolated eggs have been washed 4-5x in 0.1xMBSH and cultivated in 0.1xMBSH/1% agarose containing Petri dishes or transferred into 1xMBSH for microinjection.

I.1.2 Fixation

Embryos were cultivated to the stage of interest and then transferred into 4ml of freshly prepared 1xMEMFA (WMISH), 1ml of 4%PFA (IHC) or 2%PFA/2.5%GA (SEM) for fixation. After incubation for 1-2h at room temperature or overnight at 4°C embryos were washed in buffer and either stored in ethanol at -20°C or further prepared for IHC or post-fixed in a second step for SEM.

I.1.3 Incubation

Heptanol

For whole mount incubation experiments, the alcohol was applied directly into the culture medium. An emulsion of 1µl heptanol (HepOH) or 1µl undecanol (UNOH) in 0.1ml culture medium (1:100) was freshly prepared before each experiment by heavy vortexing and ultrasonication until the liquid appeared milky. This was followed by another dilution of 1:100 (total amount 3ml) and ultrasonication. For cultivation a 12-well plate was used, each well filled with 3ml 0.1xMBSH or 0.01% alcohol/0.1xMBSH and a maximum of 40 embryos. Additional controls were cultivated in 0.01% ethanol (ETOH). The embryos were washed carefully at the stage indicated and transferred to 0.1xMBSH/1% agarose containing Petri dishes. Preparation for SEM analysis was done at stage 17/18, *Pitx2c* was evaluated at stage 28-32 and the organ situs at stage 45.

Cycloheximide

Embryos were transferred into medium containing 10µg/ml Cycloheximide (CHX) at stage 7/8 (post-MBT). Therewith, protein synthesis is reduced to a level of 5-10% Cascio et al. 1987; Kurth et al. 2005) . As control for development, half of the embryos were cultivated in 0.1xMBSH in the absence of CHX. Treatments were performed in 12-well plates without agarose coating to prevent variations of the CHX concentration. Embryos were fixed when the control developed stage 10.

I.1.4 Microinjection

For the injection the embryos were transferred to 2% Ficoll/1xMBSH solution in a Petri dish coated with 1% agarose. Embryos were injected at the 4/8-cell stage using a Harvard Apparatus setup with a thin glass-needle (5-10µm diameter). Drop size was calibrated to about 7-8 nl per injection. In all experiments only 4/8-cell embryos with a clear dorso-ventral segregation of pigment were used for injections (Danilchik et al. 1988; Klein 1987) and only correctly targeted specimens were processed for further

analysis. The targeting was controlled by co-injection of either lineage tracer mRNAs (eGFP, mGFP, mRFP; diluted to a concentration of about 50-100ng/µl) or rhodamine-B-dextran.

Knock-down(KD)

For specific KD of single genes, morpholinos (MO) provided by GeneTools were used. MOs are synthetic, small, stable antisense oligo-nucleotides which bind complementary to the target sequence thereby preventing mRNA translation or modify pre-mRNA splicing (www.gene-tools.com). As efficiency and target gene activity varied, every MO was titrated and injected in different concentrations (0.8-1.7pM). As control experiment injections with the standard control oligo offered by Genetools were performed (co-MO). MOs used in this work were:

xCx26-MO:	5'- AGCGTTCCCCAATCCATTGTTACGG -3'
xCx26UTR-MO:	5'- ATATTGGTCTCTGTGCGCTGACTTC -3'
xCx32-MO:	5'- TGGCGTATAATCCTGCCCAATTCAT -3'
Htr3-MO1:	5'- GATGTTAAGTGTAGAGTCATTCTGG -3'
Htr3-MO2:	5'- ACAGATCAGAGTGTTTGCTTTGTCA -3'
Xfz8-MO:	5'- GCAGCGACAGATACGGACACTCCAT -3'
Co-MO:	5'- CCTCTTACCTCAGTTACAATTTATA -3'

Axis/Foxj1 induction

Secondary axes were induced by microinjection of 8pg *XSia-GR* (Kodjabachian et al. 2001), 80pg *XWnt8* or 1200pg *XDsh*-mRNA into a single ventral blastomere at the 4/8-cell stage. A subset of embryos was co-injected with 1.5-1.7pmol co-MO or *xHtr3*-MO1, *xLBD* or *hLBD*-mRNA. To activate XSia protein function, *XSia-GR* injected specimens were treated with 10µg/ml dexamethasone 30min post-injection. Embryos were cultured in 0.1xMBSH up to stage 20-30. Secondary axis induction was empirically classified into three categories: complete 2° axis; partial 2° axis lacking the head and no induction of 2° axis (results Fig. 20). The rescue of *Foxj1* dorsally was achieved by co-injection of MO1 and 1200pg *XDsh* or 640pg *β-cat*-mRNA and have been compared to injections of MO1 alone (injections scheme as described in Vick et al. 2009).

I.1.5 Scanning electron microscopy (SEM)

Embryos were freshly dissected (to uncover the GRP) in 0.1xMBSH and fixed in a mixture of 2% paraformaldehyde (PFA) and 2.5% glutaraldehyde (GA) for 1hr at room temperature or overnight at 4°C. The specimens were washed three times for 10min in 0.1M phosphate buffer (PB, pH7.5) and were then postfixed for 1-2hrs in 1% OsO_4/0.1M PB at 4°C. After extensive washing embryos were gradually dehydrated in an ethanol series and stored in 100% ETOH at -20°C until submitted to the drying procedure. Critical point drying was performed using CO_2 as drying agent. Embryos were sputter with gold and viewed under a LEO DSM 940A.
Evaluation of GRP cell size and cilia parameters was done by selecting a square of 1000 x 1000 pixels (corresponding to a width of 86µm) at the centre of the GRP in SEM pictures (magnification 500-fold). The analysis was performed using the open source program ImageJ in which measurement of the cell size (polygonal outline), cilia length (segmented line) and polarization (posterior, central, other) was carried out (Sbalzarini et al. 2005). The ciliation rate was calculated as the ratio of cilia over cells (separately in each GRP SEM photograph). Cell size, cilia length and statistical significances were calculated by the Mann-Whitney-U test (Bonferroni corrected) in statistical R (R developmental core team 2008).

I.1.6 Flow analysis

For analysis of leftward flow at the GRP, a semi-automated tool was used. Again, as for GRP morphological SEM studies, the two opensource programs, ImageJ and statistical-R were used. For visualization of extracellular particle movement driven by ciliary motility, fluorescent beads were added to the GRP and their motion was documented by taking time-lapse movies in a time window of 25s. Only the central region of the GRP was analysed what was achieved by applying a mask of a defined size. Particle movement was analysed using the ImageJ plug-in ParticleTracker, measurements and statistics were calculated. Slow and random movements which most likely displayed Brownian motion were excluded using the Rayleigh's test of uniformity on each trajectory. Particles movements which reach a mean resultant length (rho) of 0.6 were

count as being directed. The resulting data were summarized and significances have been calculated by analysing the mean resultant length towards the left side against the mean length of all trajectories excluding random movement. Significances were calculated by Mann-Whitney-U test (Bonferroni corrected) in statistical-R. This analysis was developbed by Thomas Thumberger (formerly Weber) and is described in detail in Vick et al. (2009) and Thumberger 2011.

I.2 Cloning

I.2.1 Total RNA isolation

Total RNA was isolated using a standardized protocol. 1-4 embryos were transferred into Trifast (PEQGold) and macerated. After incubation at room temperature 200µl chloroform have been added and vortexed for 15sec, incubated at room temperature for 5min and centrifuged. The aqueous phase was transferred into a new reaction tube, 500µl isopropanol were added. After vortexing 10min incubation at room temperature, the sample have been centrifuged for 15min at 4°C and 14000rpm. Supernatant was discarded, RNA pellet was washed using 75% ethanol. Discarding the supernatant and drying was followed by resuspension in 30µlH_2O. The final RNA concentration was measured and the RNA was stored at -80°C.

I.2.2 Reverse transcriptase-polymerase chain reaction (RT-PCR)

1µg total RNA was used for preparation of cDNA. RNA and 0,5µl random hexamers (Promega) were diluted in H_2O to a final amount of 14µl. After 5min at 70°C and snap cooling on ice the following components were added:

5µl M-MLV RT Buffer (5x)
1.25µl dNTPs (10mM)
3.75µl H_2Odest
1µl M-MLV Reverse transcriptase

with volume of 25µl. After 10min at RT, 60min at 50°C the reaction was stopped by 15min at 70°C. The cDNA was stored at -20°C.

I.2.3 Standard PCR

1µl of the prepared cDNA was taken for amplification of the requested genes (see below). Each reaction contained:

1µl cDNA
5µl Taq Buffer (5x)
2.5µl dNTPs (2mM)
1µl forward primer
1µl reverse primer
0.2µl Taq polymerase
14.3µl H_2O

with a final volume of 25µl. As negative control cDNA was left out, as positive/loading control the housekeeping gene *elongation factor α* (*EFα*) was chosen. The standard PCR protocol included the following steps:

(1) Denaturation step, 5min at 95°C
(2) Denaturation step, 30sec at 95°C
(3) Primer annealing, 45sec at a temperature dependent on the primer pair
(4) Elongation, 1-4min at 72°C, dependent on the sequence length
(5) Stop of reaction, 8°C for ever

The steps (2)-(4) were repeated 28-35 times. For subsequent ligation into PGEM-T-Easy an extra step was programmed (10min at 70°C), in which an adenosine was added at each 3'-terminus by the Taq-polymerase.

Connexins

XCx26 constructs were cloned according to the published sequences for *X. laevis* (#NM_001087009.1) and *X. tropicalis* (#NM_001016984.2). An *eGFP* containing sequence was obtained by the Wallingford lab (*Cs^{2+}-eGFP-tau*) and *eGFP* was subloned by Thomas Thumberger. The following primers have been used :

RT-PCR and *in situ* hybridization (813/874bp):

xCx26for	5'- cgtaacaatggattggggaa	-3'
xCx26UTRfor	5'- cacagacagagacagaagaact	-3'
xCx26rev	5'- ctccatatgaatcattgggg	-3'

Full-length coding sequence (CDS, 747bp):

xCx26Ecocodfor	5'- cgaattcatggattggggaacgc	-3'
xCx26Xhocodrev	5'- acctcgagctaatgttctttctgtt	-3'

EGFP fusion:

xCx26Xhofuserev	5'- acctcgagatgttctttctgtt	-3'

XCx32 constructs were cloned according to the published sequences for *X. laevis* (#NM_001101749) and *X. tropicalis* (#NM_001001240). The following primers have been used :

RT-PCR and *in situ* hybridization (541):

xCx32for	5'- tcacttcttccccatctcac	-3'
xCx32UTRfor	5'- agctgagatt tagtgcctag	-3'
xCx32rev	5'- ggagcagtgtaaacgaaacg	-3'

Full-length coding sequence (CDS, 795bp):

xCx32Ecocodfor	5'- ctgaattcatgaattgggcaggattata	-3'
xCx32Xhocodrev	5'- ctctcgagttaggaggtagaacagtg	-3'

RFP fusion:

xCx32Xhofuserev	5'- ctctcgagggaggtagaacagtg	-3'
RFPXhofor	5'- ctcgagatggcctcctccgaggacgtc	-3'
RFPXbarev	5'- tctagaaatgcaattgttgttgttaac	-3'

For obtaining expression by RT-PCR without detection of genomic DNA, primers were designed complementary to a sequence in front of the putative intron site (Fig. 5; xCx26/32_5'UTRfor). The intron site was known for *X. tropicalis* an assumed for *X. laevis* based on sequence alignment. For the *xCx26::GFP* and *xCx32::RFP* fusion constructs reverse primers lacking the stop-codon were used to prepare C-terminal GFP/RFP tagged-proteins (fuserev). Sequences were cloned into the PGEM-T-Easy vector. The CDS were subcloned into the Eco/Xho site of the Cs^{2+} or the Cs^{2+}-eGFP/RFP expression vector (Rupp et al.,1994) .

Xnr-constructs

The *Xnr2::GFP*-construct was provided by Williams et al. (2004). For cloning of *Xnr1* fusion constructs corresponding to #NM_001085796 the following primers have been used:

Signaling and prodomain (843bp):

Xnr1Clacodfor1	5'- atcgatatggcatttctgacagc	-3'
Xnr1Stucodrev1	5'- aggcctgctccttctgtgtctcctaat	-3'

Mature domain (378bp):

Xnr1Xhocodfor2	5'- ctcgagaacaggaatgaaaaccat	-3'
Xnr1Xbacodrev2	5'- tctagattaactgcacccacattc	-3'

Signaling and prodomain lacking the furin cleavage site (828bp):

Xnr1StucodΔFrev	5'- aggcctaataccaggcactctactagctt	-3'

EGFP coding sequence (732bp):

eGFPStucodfor	5'- aggcctatggtgagcaagggcgag	-3'
eGFPXhocodrev	5'- ctcgagcttgtacagctcgtcca	-3'

The sequences were ligated into the PGEM-T-Easy vector and subcloned into the Cs^{2+}-expression vector (Rupp et al.,1994). Four fusion constructs have been designed: the full length *Xnr1::eGFP* and the deletion constructs *Xnr1ΔP::eGFP*, *Xnr1ΔM::eGFP* and *Xnr1ΔF::eGFP* (see results II.6, Fig. 10).

Serotonin

The full length *Xenopus xHtr3* (pCMV-SPORT6) clone (#BC044101) was obtained by the RZPD (Berlin, Germany). Full length human *hHTR3*-clone (Niesler et al. 2007) and the truncated splice variant missing loop F and C were used (corresponds to accession number CAA05853.1, HTR3AT, here *hsv*; (Niesler et al. 2008; Walstab J, Hammer C, Bönisch H, Rappold G 2008; Thompson et al. 2006; Brüss et al. 2000a). RT-PCR analysis (*xHtr3*), cloning of the rescue-construct (*xHtr3*) and of truncated versions of the *X. laevis* and the human subunit (*xLBD, hLBD*) was done by Susanne Bogusch (University of Hohenheim, Stuttgart, Germany). The following primers have been used:

RT-PCR (869bp):

xHtr3for	5'- cattggaatggaccaatgaata	-3'
xHtr3rev	5'- gtcaggccggttatttgtgtt	-3'

Rescue-construct with changed morpholino binding site:

xHtr3rescuefor	5'- atatcgatatgaccttgcatctcacgagcctgctgctc	-3'
xHtr3rescuerev	5'- atctcgagttatgttgcccaaacaataataagaat	-3'

Ligand binding domains (*xLBD* and *hLBD*):

xLBDfor	5'- atgaattcatgactctacacttaacatctctgc	-3'
xLBDrev	5'- caataaaacgggcccctgttgtttagctcgag	-3'
hLBDfor	5'- atgaattcatgcttggaaagctcgctatgctgctg	-3'
hLBDrev	5'- atctcgagtcagctgaccacatagaagaggggccgc	-3'

The PCR products were subcloned into the Cs^{2+} expression vector (Rupp et al.,1994). All sequences have been verified by sequencing.

I.2.3 Ligation

PCR products have been ligated into the PGEM-T-Easy vector. Each reaction contained:

2.5µl Rapid Ligation buffer (2x)
0.5µl PGEM-T Easy Vector
0.5µl T4 DNA Ligase
0.5µl H_2O
1µl PCR product

After gently mixing the reaction incubated at 4°C over night followed by transformation of competent E. coli (XL1-blue) using the heat shock method. The bacteria solution was plated onto LB-agar plates (100µg/ml ampicillin, 0.5mM IPTG, 80µg/ml X-Gal) and incubated over night at 37°C. Blue staining indicated no insertion of a DNA fragment into the multiple cloning site of the vector whereas white colonies were further analysed.

I.2.4 Selection

Mini preparation

Plasmid DNA from E. coli cultures was isolated using a modified alkaline lysis protocol. All centrifugation steps were done at 4°C. 3ml of selective LB medium (100µg/ml Ampicillin) were inoculated with a single bacteria colony from a selective plate and grown overnight with vigorous shaking at 37°C. 2ml of the culture were poured into a microcentrifuge tube and bacteria were pelleted in a microcentrifuge at 6000g for 15min. The supernatant was discarded and the pellet resuspended by heavy vortexing in 100µl P1 buffer. When the bacteria suspension appeared uniform, 200µl of P2 buffer were added and the tube was inverted several times to thoroughly mix the reagents. Alkaline lysis was allowed to proceed for 5min and was then stopped by neutralizing with 150µl of P3, again inverting the tube several times. After 20min of incubation on ice, the lysate was cleared from the fluffy white precipitate containing genomic DNA, cell debris, proteins and potassium dodecyl sulphate by centrifugation in a microcentrifuge at full speed for 10min. 400µl of the clear supernatant were transferred to a fresh microcentrifuge tube and mixed well with 1ml of 100% Ethanol to precipitate the plasmid DNA. After precipitation for 30min at -20°C the plasmid DNA was pelleted by centrifuging at full speed for 10min. The pellet was washed in 70% ethanol, centrifuged briefly, dried and re-suspended in 50µl sterile DDW.

Restriction enzyme digests of DNA (20µl)

To check for insertion of the correct PCR product after mini-prep, inserts were released from the plasmids by digestion with a restriction enzyme cutting on both sides of the multiple cloning site. Typically to 5µl of plasmid-DNA, 2µl 10x buffer, 0.2 µl BSA and 0.5µl enzyme were added, the mixture was filled up with 12.3µl sterile DDW to a final volume of 20µl and incubated at 37°C for 2hrs. After digestion the whole volume of the reaction was analysed on an agarose gel. The products of each reaction were checked on a standard 1% agarose gel supplemented with an end concentration 0.4µg/ml ethidium bromide solution.

1.2.5 DNA amplification (midi preparation)

100ml of selective LB medium (100µg/ml ampicillin) were inoculated with 1ml of a positively tested bacteria culture and grown overnight in a 1000ml conical flask with vigorous shaking at 37°C. Bacteria were harvested by centrifugation, lysed and DNA was purified following the Promega “PureYield Plasmid Midiprep System” using the vacuum method. The concentration of nucleic acids in aqueous solutions was determined via spectrophotometry. The ratio of absorption (A) at 260nm and 280nm wavelength indicated the purity of the solution (pure nucleic acid solution: 1.8 for DNA, 2.0 for RNA). The content of either DNA or RNA was inferred from the A260 value with 1 unit corresponding to 50µg/µl DNA and 40µg/µl RNA.
For subloning into other vectors (e.g. Cs^{2+}) the insert was separated by specific digestion which was followed by purification of the fragment and new ligation.

I.2.6 MRNA synthesis

Restriction enzyme digests of DNA (50µl)
For linearization digests typically 10µg of plasmid DNA was used in a 50µl reaction. 2µl of restriction enzyme were used and the digestion was incubated overnight at 37°C. Approximately 600ng of the digestion were controlled on a 1% agarose gel.

Synthesis of capped RNA

For capped RNA synthesis the Ambion kit mMESSAGE mMACHINE (High yield capped RNA Transcription kit) was used. For the reaction 4µl nuclease free H_2O, 10µl 2xNTP/CAP (ATP, 10mM; CTP, 10mM; UTP, 10mM; GTP, 2mM, cap analog, 8mM), 2µl 10xbuffer, 2µl linearized CS^{2+}(~2µg) and 2µl enzyme mixture (containing SP6 RNA polymerase) were mixed. After incubation for 2hrs at 37°C, 1µl DNase was added with a subsequent incubation of 15min. Then mRNA was twice phenol-chloroform extracted and precipitated in isopropyl alcohol. Concentration of the mRNA was then determined by spectrophotometry and the quality by running on an agarose gel.

I.3 Whole-mount *in situ* hybridization

In vitro transcription of RNA probes

200ng linearized plasmid with the insert of interest was used as a template. 20u of either Sp6 or T7 polymerase were added to a mixture of template, 4µl transcription buffer, 0.5µl (= 20units) RNasin, 2µl DTT and 2µl 10x Dig-Mix. After adding sterile DDW to a final volume of 20µl the mixture was incubated at 37°C for 2hrs. After gel check with 2µl in 10µl DDW on a 1% agarose gel, 115µl 100% EtOH and 3.75µl 4M LiCl were added to the mixture and RNA was precipitated at -20°C for at least 30min. After centrifuging 13 000rpm at 4°C for 20min; the resulting pellet was rinsed in 70% EtOH and centrifuged again for 5min. The pellet was air-dried and resuspended in 50µl of a 1:1 mixture of sterile DDW and formamide. The RNA was stored at -80°C.

In situ hybridization

Whole mount in situ hybridization used to detect the expression pattern of specific genes in Xenopus embryos. Protocol originally adapted from the De Robertis lab (Belo et al., 1997).

Day 1: All steps (except Proteinase K) until pre-hybridization were performed on ice. On the first day of the procedure, tissue was prepared for taking up the antisense RNA probe, which hybridizes to the endogenous target RNA. Embryos were rehydrated from storage in 100% ethanol through a graded series of 75%, 50% and 25% ethanol in PBS^-. Embryos were washed three times for at least 5min in PBS^-w and then the tissue was permeabilized for ~15-20min in 10µg/µl Proteinase K in PBS^-w at RT. Digestion was stopped in 2mg/ml glycine followed by three washing steps in PBS^-w for 5min each. The tissue was then refixed for 15min at RT in 4% PFA supplemented with 0.2% glutaraldehyde. After washing three times in PBS^-w for 5min the embryos were transferred into a 1:1 mixture of hybridization solution and PBS^-w. After equilibration in 100% hybridization solution, a pre-hybridization period in 900µl hybridization solution at

65°C for 2-3hrs eliminated endogenous phosphatases. Depending on the concentration of RNA, about 1µl of antisense probe (~20ng) diluted in 100µl hybridization solution was added to the vial and the embryo was incubated with the probe overnight at 70°C.

Day 2: On the second day excess antisense probe was removed in high stringency washing steps and the tissue was prepared for incubation with the anti-digoxygenin antibody. In a first step, 1 to 3 washing steps (30min each) in 100% hybridization mix at 70°C were used to reduce background staining depending on the probe. Then the solution was again replaced with 800µl hybridization solution. In three steps (5min each) each 400µl of 2xSSC (pH4.5) were added and the embryo was washed twice in 2xSSC (pH7) at 70°C afterwards. The washing steps in SSC were followed by four washing intervals in MABw, twice at RT for 10min and another two times at 70°C for 30min. Afterwards, embryos were washed three times in PBS^{-}w at RT for 10min each and were then pre-incubated in antibody-blocking buffer at 4°C for 2hrs. In a second tube, the anti-digoxygenin antibody coupled to alkaline phosphatase was diluted 1/10,000 and pre-blocked for the same time. After the 2hrs of pre-incubation, the blocking buffer was replaced with the antibody-solution and the embryos were incubated with the antibody overnight at 4°C on a laboratory shaker.

Day 3: On the third day, unbound antibody was removed in extensive washing steps and the staining reaction was started. Embryos were rinsed and then washed six times for 45min each in PBS^{-}w containing 0.1% BSA. The washing in BSA was followed by two washing steps with PBS-w for 30min each and embryos were then transferred into AP1 buffer, which adjusts the pH of the tissue for the optimal reaction of the alkaline phosphatase. AP1 buffer was changed 1-4 times according to probe type and then replaced by a 1:1 mixture of AP1 buffer and BMPurple, the substrate for the alkaline phosphatase. The staining process was controlled and stopped by washing in PBS-w, when the expected signal had reached a dark blue to violet color. A gradual methanol series intensified the signal and the embryos were afterwards stored in 100% methanol at -20°C.

Histological analysis of embryos after in situ hybridization

After rehydration embryos were equilibrated in a small volume of embedding medium (~1ml). 2ml of embedding medium were mixed shortly but vigorously with 140µl of glutaraldehyde and poured into a square mold formed of two glass brackets. The mixture was allowed to harden and the equilibrated embryo was transferred upon the surface of the block, excess embedding medium was carefully removed. Another 2ml of embedding medium mixed with glutaraldehyde were poured into the mold so that the embryo was now sandwiched between two layers of embedding mix. The hardened block was trimmed with a razor blade and glued onto a plate. The plate was mounted into the holder of the vibratome and 30µm thick sections were prepared. The sections were arranged onto glass slides, embedded with mowiol and protected with glass cover slips.

Statistical analysis

Statistical calculations of marker gene expression patterns were performed using Fisher exact test (http://www.physics.csbsju.edu/stats/fisher.form.html) unless indicated otherwise.

Photo documentation

Documentation of living or fixed embryos was performed after stepwise rehydration in PBS^- with a Zeiss dissecting microscope STEREO Discovery.V12 or a LEICA MZFLIII with a digital camera (AxioCam HRc, Zeiss). Analyses of vibratome sections were performed with a Zeiss microscope Axioskop 2 with a digital camera (AxioCam HRc, Zeiss). For image processing (contrast, background, arrangement, layout, etcetera) Photoshop CS3 and Illustrator CS3 (both Adobe Systems) was used – in most cases with the very very kind and professional help of Thomas Weber (University of Hohenheim). All raw drawings were made by Bernd Schmid after instruction and then further processed with Photoshop and Illustrator by Philipp Vick, Thomas Thumberger and myself..

II. Buffers, Solutions and Media

II.1 *In situ* hybridization

10x Phosphate Buffered Saline (PBS, 1l)

80g NaCl
2g KCl
14.4g Na_2HPO_4
2.4g KH_2PO_4
800ml DDW
adjust pH to 7.4, add DDW to 1L, autoclave

1x PBSw (500ml)

50ml PBS^- (10x)
500µl Tween20
add DDW to 500ml

1x Alkaline Phosphatase Buffer (AP1, 1l)

100ml TRIS (pH 9.5, 1M)
20ml NaCl (5M)
50ml $MgCl_2$ (1M)
adjust pH to 9.5, add DDW to 1l

1x Maleic Acid Buffer (MAB, 1l)

11.61g Maleic Acid (100mM)
30ml NaCl (5M)
800ml DDW
adjust pH to 7.5, add DDW to 1l, autoclave

20x Sodium Citrate Buffer (SSC, 1l)

175.3g NaCl

88.2g Sodium citrate

800ml DDW

adjust pH to 7, add DDW to 1l, autoclave

Hybridization solution (1l)

10g Boehringer Block

500ml Formamide

250ml SSC (20x)

Heat to 65°C for 1 hour

120ml DDW

100ml Torula RNA (10mg/ml in DDW, dissolved at 65°C; filtered)

2ml Heparin (50mg/ml in 1xSSC pH 7)

5ml Tween20 (20%)

10ml CHAPS (10%)

10ml EDTA (0.5M)

filter (5µm)

Antibody Blocking Buffer (1l)

10g Boehringer Block

dissolve in 800ml PBS^- at 70°C, vortex frequently,

100ml Goat Serum (30min at 56°C heat inactivated)

add PBS^- to 1l, filter (0.45µm)

1ml Tween-20

II.2 Frog experiments

5x MBSH (1l)

25.7g NaCl

0.375g KCl

1g $NaHCO_3$

1g $MgSO_4*7H_2O$

0.39g $(CaNO_3)_2*4H_2O$

0.3g $CaCl_2*2H_2O$

11.9g Hepes

5 ml Penicillin/Streptomycin

add DDW to 1l, adjust pH of 7.4, filter (0.45µm)

10xMEMFA (1ml)

500ml MOPS (0.1M, pH 7.4)

200ml EGTA (2mM)

10ml $MgSO_4$ (1M)

add DDW to 1l, autoclave

1x MEMFA (100ml)

10ml MEMFA (10x)

10ml Formaldehyde (37%)

80ml H_2O

Gurdon's buffer

88mM NaCl

15mM HEPES

1mM KCl

15mM Tris-HCl, pH 7.6

Ficoll

2% Ficoll diluted in 1xMBSH

Cystein

2% Cystein diluted in DDW, adjust pH to 7.99

II.3 Bacteria culture

Super Optimal Catabolite repression medium (S.O.C., 500ml)

2.5g Yeast extract
10g Tryptone
1ml NaCl (1M)
1.25ml KCl (1M)
5ml $MgCl_2$ (1M)
5ml $MgSO_4$ (1M)
1.8g Glucose
autoclave

Lysogeny Broth (LB) medium (1l)

10g Tryptone
10g NaCl
5g Yeast extract
add DDW to 1l, adjust pH to 7 (for LB agar add 15g/l agar) autoclave

II.4 DNA preparation

P1 (Re-suspension buffer)

50mM TRIS-HCl
10mM EDTA (pH8)
add RNaseA (DNase free) to a final concentration of 100µg/ml

P2 (Lysis buffer)

0,2M NaOH
1% SDS

P3 (Neutralization buffer)

3M Potassium acetate, pH 5.5

II.5 Other applications

Embedding medium for vibratome sections

2.2g Gelatine
135g Bovine Serum Albumin
90g Sucrose
dissolve in 450ml PBS.

Mowiol (Mounting medium)

96g Mowiol 488
24g Glycerol
24ml DDW
stir for 2h, then add
48ml TRIS 0.2M pH 8.5
stir for 20min at 50°C
centrifuge for 15min at 5000rpm, keep supernatant
and store at -20°C.

50x Tris Acetate EDTA Electrophoresis Buffer (TAE, 1l)

15.1g Tris base
57.1ml Glacial acetic acid
100ml EDTA (0.5M, pH8)
add DDW to 1l, adjust pH to 8.5

Sörensen phosphate buffer

Stock solution A: 0.2M $NaH_2PO_4 * H_2O$
Stock solution B: 0.2M Na_2HPO_4
for 200ml 0.1M, pH 7.4: 19ml A + 81ml B + 100ml H_2O
for 200ml 0.1M, pH 7.0: 39ml A + 61ml B + 100ml H_2O

II.6 Sources of supply

II.6.1 Chemicals and lab-ware

Acetic acid	AppliChem, Darmstadt
Agarose	Roth, Karlsruhe
Albumin fraction V	AppliChem, Darmstadt
Ampicillin	AppliChem, Darmstadt
Anti-Digoxigenin-AP	Roche, Mannheim
BM Purple	Roche, Mannheim
Boehringer Block	Roche, Mannheim
Bovine serum albumin	AppliChem, Darmstadt
BSA	AppliChem, Darmstadt
CAS-Block	Invitrogen, Karlsruhe
CHAPS	Sigma, Schnelldorf
Chloroform	Merck, Darmstadt
Cystein	Roth, Karlsruhe
Desoxynucleosidtriphosphate (dNTPs)	Promega, Mannheim
DIG RNA Labeling Mix	Roche, Mannheim
Dimethylsulfoxid (DMSO)	Roth, Karlsruhe
Disodium hydrogen phosphate	AppliChem, Darmstadt
Dithioreitol (DTT)	Promega, Mannheim
DMSO	Roth, Karlsruhe
EDTA	Roth, Karlsruhe
Ethanol	Roth, Karlsruhe
Ethidium Bromide	Roth, Karlsruhe
Ethyl-p-Aminobenzoat (Benzocain)	Sigma, Schnelldorf
Ethylenediamine tetraacetic acid EDTA	Roth, Karlsruhe
Ethyleneglycol tetraacetic acid EGTA	Roth, Karlsruhe
Ficoll	AppliChem, Darmstadt
FluoSphere Fluorescent beads 500nm	Invitrogen, (Molecular Probes), Karlsruhe

Formaldehyd	AppliChem, Darmstadt
Forceps (#3, #5)	Fine Science Tools, Heidelberg
Formamide	Roth, Karlsruhe
Gelatine	Roth, Karlsruhe
Glass coverslips	Roth, Karlsruhe
Glass slides	Roth, Karlsruhe
Glucose	AppliChem, Darmstadt
Glutaraldehyde	AppliChem, Darmstadt
Glycerol	Roth, Karlsruhe
Glycin	AppliChem, Darmstadt
Goat serum	Sigma, Schnelldorf
HCG (human chorionic gonadotropin)	Sigma, Schnelldorf
HCl (37%)	Merck, Darmstadt
Hepes	AppliChem, Darmstadt
Heparin	Sigma, Schnelldorf
Heptanol	Roth, Karlsruhe
Injection-needle Sterican (0,4x20 mm)	B. Braun, Melsungen
Injection syringe F1, 1ml	B. Braun, Melsungen
Lambda-DNA	Promega, Mannheim
Ligase (T4-Ligase)	Promega, Mannheim
Lithium chloride	Serva, Heidelberg
Loading Buffer	AppliChem, Darmstadt
Magnesium chloride	Roth, Karlsruhe
Magnesium sulfate	AppliChem, Darmstadt
Maleic acid	Roth, Karlsruhe
Methanol	Roth, Karlsruhe
Micro centrifuge tubes	Sarstedt, Nümbrecht
Objective slides	Roth, Karlsruhe
Oligonucleotides	Operon, Cologne
Osmium tetroxide	Plano, Wetzlar
Parafilm	Roth, Karlsruhe
Paraformaldehyde	AppliChem, Darmstadt

PBS+ (10x)	Gibco (Invitrogen) Karlsruhe
Penicillin/Streptomycin	Gibco (Invitrogen) Karlsruhe
pGEM-T-Easy-Vektor	Promega, Mannheim
Phenol/chloroform (Rotiphenol)	Roth, Karlsruhe
Plastic pipettes	Sarstedt, Nümbrecht
2-Propanol	Roth, Karlsruhe
Proteinase K	Roth, Karlsruhe
Rhodamine-B-dextran	Molecular Probes (Invitrogen), Karlsruhe
RNAse A	Roth, Karlsruhe
RNAsin	Promega, Mannheim
Rose-Gal	Roth, Karlsruhe
Saccharose	Applichem, Darmstadt
Sodium acetate	Roth, Karlsruhe
Sodium chloride	Roth, Karlsruhe
Sodium citrate	Roth, Karlsruhe
Sodium dihydrogen phosphate	AppliChem, Darmstadt
Sodium hydroxide	AppliChem, Darmstadt
Sp6-RNA-Polymerase	Promega, Mannheim
Sucrose	AppliChem, Darmstadt
Syringe filters	Whatman, Dassel
T7-RNA-Polymerase	Promega, Mannheim
Taq-DNA-Polymerase (Go-Taq)	Promega, Mannheim
Torula RNA	Sigma, Schnelldorf
TRIS base	AppliChem, Darmstadt
TRIS HCl	AppliChem, Darmstadt
Triton-X100	Serva, Heidelberg
Tryptone	AppliChem, Darmstadt
Tween-20	AppliChem, Darmstadt
X-Gal	Roth, Karlsruhe

II.6.2 Kits

DNA-Purification-Kit (Easy-Pure)	Biozym, Hessisch Oldendorf
mMESSAGE mMACHINE SP6	Ambion, Darmstadt
pGEM-T Easy Vector System	Promega, Mannheim
PureYield Plasmid Midiprep System	Promega, Mannheim
PeqGOLD TriFast	Peqlab, Erlangen

II.6.3 Proteins and Antibodies

Restriction enzymes and buffers	Promega, Mannheim
Modifying enzymes and buffers	Promega, Mannheim
Mouse anti-acetylated α-tubulin	Sigma, Schnelldorf
Rabbit anti-serotonin	Chemicon
Anti-digoxigenin-AP	Roche, Mannheim
Cy3 Anti-Mouse IgG F(ab')$_2$ fragment	Sigma, Schnelldorf
Cy2 Anti-Mouse-conjugated Fab fragment IgG (H+L)	Jackson ImmunoResearch,Suffolk
Alexa Fluor 488 donkey Anti-Rabbit IgG (H+L)	Invitrogen, Karlsruhe

II.6.4 Special Hardware

Peltier Thermal Cycler PTC-200	Biozym, Hessisch Oldendorf
Vibratome	Leica, Bensheim
Stereo microscope	Zeiss, Oberkochen
Zeiss DSM 940A	Zeiss, Oberkochen
LSM 5 Pascal	Zeiss, Oberkochen
Axioplan 2	Zeiss, Oberkochen
Critical point dryer CPD 030	Balzers, Austria
Sputter coater SCD 050	Balzers, Austria
LEO DSM 940A	Zeiss, Oberkochen

II.6.5 Animals

Adult African clawed frogs (*Xenopus laevis*) were obtained from Guy Pluck, Xenopus express, Ancienne Ecole de Vernassal, Le Bourg 43270, Vernassal, Haute-Loire, France. They were kept species-appropriate at a 12h light-cycle in the animal facility of the Institute of Zoology, University of Hohenheim.

Some parts of the Materials and Methods sections have been adapted from Feistel 2007 and Vick 2009.

Acknowledgment

The following collaborators contributed equally to the serotonin project (alphabetical order): Tina Beyer (SEM preparation and analysis, microinjections, rescue experiments, WMISH, DA axis assay, CHX incubation experiment), Mike Danilchik (5-HT IHC and documentation, 5-HT injection), Thomas Thumberger (formerly Weber; leftward flow analysis and calculation, establishment of computer based analysis-tool, SEM analysis and calculation, microinjections, WMISH) and Philipp Vick (cloning, microinjections, DA assay, WMISH). Susanne Bogusch performed the RT-PCR expression analysis, cloned the *LBDs, xFL*, *hsv*, *Mosite::GFP* and helped with microinjections and WMISH. Beate Niesler gave advice for serotonin receptor handling and cloning. Peter Walentek (*Foxj1 in situ* construct), Maike Getwan (Coco, Xnr1), Isabelle Schneider (Coco, Xnr1, SEM) and Bärbel Ulmer (DA assay) helped with the experimental performance. Melanie Eberhardt and Anke Pachur performed staining analysis and experiments for the Coco/Xnr1 study and Veronika Städele helped with KD of the *xCxs*. Axel Schweickert helped with all projects by giving advice, performing experiments and discussion of results.

Furthermore, thanks to Abraham Fainsod, Janet Heasman, Chris Kintner, Jean Lauder, Michael Levin, Randy Moon and Herbert Steinbeisser for plasmids, *Xfz8*-MO and antibodies, Werner Amselgruber for providing the SEM facility and Karen Müller for help with SEM analysis. This work was funded by the Landesgraduiertenförderung Baden-Württemberg, the Deutsche Forschungs-gemeinschaft, Böhringer Ingelheim Fonds (CSHL course) and the Gesellschaft für Enwicklungsbiologie and the Society for Developmental Biology (support of meetings).

References

Adams, D. S., Robinson, K. R., Fukumoto, T., Yuan, Shipeng, Albertson, R. C., Yelick, P., Kuo, L., McSweeney, M., and Levin, Michael (2006). Early, H+-V-ATPase-dependent proton flux is necessary for consistent left-right patterning of non-mammalian vertebrates. Development (Cambridge, England) 133, 1657-71.

Afzelius, B. (1976). A human syndrome caused by immotile cilia. Science 193, 317-319.

Amerongen, R. van, and Nusse, R. (2009). Towards an integrated view of Wnt signaling in development. Development (Cambridge, England) 136, 3205-14.

Anderson, E. D., VanSlyke, J. K., Thulin, C. D., Jean, F., and Thomas, G. (1997). Activation of the furin endoprotease is a multiple-step process: requirements for acidification and internal propeptide cleavage. The EMBO journal 16, 1508-18.

Antic, D., Stubbs, J. L., Suyama, K., Kintner, C., Scott, M. P., and Axelrod, J. D. (2010). Planar cell polarity enables posterior localization of nodal cilia and left-right axis determination during mouse and Xenopus embryogenesis. PloS one 5, e8999.

Ayad, W. a, Locke, D., Koreen, I. V., and Harris, A. L. (2006). Heteromeric, but not homomeric, connexin channels are selectively permeable to inositol phosphates. The Journal of biological chemistry 281, 16727-39.

Bakkers, J., Verhoeven, M. C., and Abdelilah-Seyfried, S. (2009). Shaping the zebrafish heart: from left-right axis specification to epithelial tissue morphogenesis. Developmental biology 330, 213-20.

Barnes, N. M., and Sharp, T. (1999). A review of central 5-HT receptors and their function. Neuropharmacology 38, 1083-1152.

Barrio, L. C., Suchyna, T., Bargiello, T., Xu, L. X., Roginski, R. S., Bennett, M. V., and Nicholson, B J (1992). Gap junctions formed by connexins 26 and 32 alone and in combination are differently affected by applied voltage. Proceedings of the National Academy of Sciences of the United States of America 89, 4220.

Basu, B., and Brueckner, Martina (2008). Cilia : Multifunctional Organelles at the Center of Vertebrate Left – Right Asymmetry 1st ed. (Elesvier Inc.)

Bean, A. J., Zhang, X., and Hökfeld, T. (1994). Peptide secretion: what do we know? The FASEB journal 8, 630-638.

Belo, José António et al. (2009). Generating asymmetries in the early vertebrate embryo: the role of the Cerberus-like family. The International journal of developmental biology 53, 1399-407.

Ben-Zvi, D., Shilo, B.-Z., Fainsod, A., and Barkai, N. (2008). Scaling of the BMP activation gradient in Xenopus embryos. Nature 453, 1205-11.

Benzing, T., Simons, M., and Walz, G. (2007). Wnt signaling in polycystic kidney disease. Journal of the American Society of Nephrology : JASN 18, 1389-98.

Berbari, N. F., O'Connor, A. K., Haycraft, C. J., and Yoder, B. K. (2009). The primary cilium as a complex signaling center. Current biology : CB 19, R526-35.

Bevans, C. G., Kordel, M., Rhee, S. K., and Harris, a L. (1998). Isoform composition of connexin channels determines selectivity among second messengers and uncharged

molecules. The Journal of biological chemistry 273, 2808-16.

Beyer, T. (2006). Ultrastrukturelle und funktionelle Analyse der Gastrocoel Roof Plate des afrikanischen Krallenfrosches Xenopus laevis. Diploma thesis.

Birsoy, B., Berg, L., Williams, P Huw, Smith, James C, Wylie, C. C., Christian, Jan L, and Heasman, J. (2005). XPACE4 is a localized pro-protein convertase required for mesoderm induction and the cleavage of specific TGFbeta proteins in Xenopus development. Development (Cambridge, England) 132, 591-602.

Bisgrove, B W, Essner, J J, and Yost, H J (1999). Regulation of midline development by antagonism of lefty and nodal signaling. Development (Cambridge, England) 126, 3253-62.

Blanchet, M.-H., Le Good, J. A., Mesnard, D., Oorschot, V., Baflast, S., Minchiotti, G., Klumperman, J., and Constam, D. B. (2008). Cripto recruits Furin and PACE4 and controls Nodal trafficking during proteolytic maturation. The EMBO journal 27, 2580-91.

Blum, M. et al. (2007a). Ciliation and gene expression distinguish between node and posterior notochord in the mammalian embryo. Differentiation; research in biological diversity 75, 133-46.

Blum, M. et al. (2007b). Ciliation and gene expression distinguish between node and posterior notochord in the mammalian embryo. Differentiation; research in biological diversity 75, 133-46.

Blum, M., Weber, T., Beyer, T., and Vick, P. (2009). Evolution of leftward flow. Seminars in cell & developmental biology 20, 464-71.

Boer, T. P. de, Kok, B., Roël, G., Veen, T. a B. van, Destrée, O. H. J., Rook, M. B., Vos, M. a, Bakker, J. M. T. de, and Heyden, M. a G. van der (2006). Cloning, embryonic expression, and functional characterization of two novel connexins from Xenopus laevis. Biochemical and biophysical research communications 349, 855-62.

Boitano, S., Dirksen, E., and Sanderson, M. (1992). Intercellular propagation of calcium waves mediated by inositol trisphosphate. Science 258, 292-295.

Bolton, V. N., Oades, P. J., and Johnson, M. H. (1984). The relationship between cleavage, DNA replication, and gene expression in the mouse 2-cell embryo. Journal of embryology and experimental morphology 79, 139-63.

Borovina, A., Superina, S., Voskas, D., and Ciruna, B. (2010). Vangl2 directs the posterior tilting and asymmetric localization of motile primary cilia. Nature cell biology 12, 407-412.

Bradley, L., Sun, B., Collins-Racie, L., LaVallie, E., McCoy, J., and Sive, H. (2000). Different activities of the frizzled-related proteins frzb2 and sizzled2 during Xenopus anteroposterior patterning. Developmental biology 227, 118-32.

Brennan, J., Norris, D. P., and Robertson, E. J. (2002). Nodal activity in the node governs left-right asymmetry. Genes & Development, 2339-2344.

Britz-Cunningham, S. H., Shah, M. M., Zuppan, C. W., and Fletcher, W. H. (1995). Mutations of the Connexin43 gap-junction gene in patients with heart malformations and defects of laterality. The New England journal of medicine 332, 1323-9.

Bryja, V. et al. (2009). The Extracellular Domain of Lrp5 / 6 Inhibits Noncanonical Wnt Signaling In Vivo. Molecular Biology of the Cell 20, 924 -936.

Brüss, M., Barann, M., Hayer-Zillgen, M., Eucker, T., Göthert, M., and Bönisch, H. (2000a). Modified 5-HT 3A receptor function by co-expression of alternatively spliced human 5-HT 3A receptor isoforms. Naunyn-Schmiedeberg's Archives of Pharmacology 362, 392-401.

Brüss, M., Barann, M., Hayer-Zillgen, M., Eucker, T., Göthert, M., and Bönisch, H. (2000b). Modified 5-HT3A receptor function by co-expression of alternatively spliced human 5-HT3A receptor isoforms. Naunyn-Schmiedeberg's archives of pharmacology 362, 392-401.

Bukauskas, F. F., Bukauskiene, a, Bennett, M. V., and Verselis, V. K. (2001). Gating properties of gap junction channels assembled from connexin43 and connexin43 fused with green fluorescent protein. Biophysical journal 81, 137-52.

Buznikov, G. A., Peterson, R. E., Nikitina, L. A., Bezuglov, V. V., and Lauder, J. M. (2005). The Pre-nervous Serotonergic System of Developing Sea Urchin Embryos and Larvae: Pharmacologic and Immunocytochemical Evidence. Neurochemical research 30, 825-837.

Capdevila, J., Vogan, K J, Tabin, C J, and Izpisúa Belmonte, J C (2000). Mechanisms of left-right determination in vertebrates. Cell 101, 9-21.

Cascio, S., and Gurdon, J. B. (1987). The initiation of new gene transcription during Xenopus gastrulation requires immediately preceding protein synthesis. Development (Cambridge, England) 100, 297-305.

Cha, B. J., and Gard, D. L. (1999). XMAP230 is required for the organization of cortical microtubules and patterning of the dorsoventral axis in fertilized Xenopus eggs. Developmental biology 205, 275-86.

Cha, S.-W., Tadjuidje, E., Tao, Q., Wylie, Christopher, and Heasman, J. (2008). Wnt5a and Wnt11 interact in a maternal Dkk1-regulated fashion to activate both canonical and non-canonical signaling in Xenopus axis formation. Development (Cambridge, England) 135, 3719-29.

Chanson, M., Bruzzone, R., Bosco, D., and Meda, P. (1989). Effects of n-alcohols on junctional coupling and amylase secretion of pancreatic acinar cells. Journal of cellular physiology 139, 147-56.

Chazaud, C., Chambon, P., and Dollé, P. (1999). Retinoic acid is required in the mouse embryo for left-right asymmetry determination and heart morphogenesis. Development (Cambridge, England) 126, 2589-96.

Chen, C., and Shen, M. M. (2004). Two Modes by which Lefty Proteins Inhibit Nodal Signaling. Current 14, 618-624.

Chen, Yu, and Schier, A. F. (2002). Lefty Proteins Are Long-Range Inhibitors of Squint-Mediated Nodal Signaling. Current 12, 2124-2128.

Choi, D.-S., Kellermann, O., Richard, S., Colas, J.-F., Bolaños-jimenez, F., Tournois, C., Launay, J.-M., and Maroteaux, L. (2006). Mouse 5-HT2B Receptor-mediated Serotonin Trophic Functions. Annals of the New York Acadamy of Sciences 1, 1749-6632.

Choi, S.-C., and Han, J.-K. (2002). Xenopus Cdc42 regulates convergent extension movements during gastrulation through Wnt/Ca2+ signaling pathway. Developmental biology 244, 342-57.

Colas, J.-F., and Schoenwolf, G. (2001). Towards a Cellular and Molecular Understanding of. Developmental Dynamics 145, 117-145.

Constance Lane, M., Davidson, L., and Sheets, M. D. (2004). BMP antagonism by Spemann's organizer regulates rostral-caudal fate of mesoderm. Developmental biology 275, 356-74.

Cooke, J. (2004). Developmental mechanism and evolutionary origin of vertebrate left/right asymmetries. Biological reviews 79, 377-407.

Cruciat, C.-M., Ohkawara, B., Acebron, S. P., Karaulanov, E., Reinhard, C., Ingelfinger, D., Boutros, M., and Niehrs, C. (2010). Requirement of prorenin receptor and vacuolar H+-

ATPase-mediated acidification for Wnt signaling. Science (New York, N.Y.) 327, 459-63.

Cui, Y., Brown, J. D., Moon, R T, and Christian, J L (1995). Xwnt-8b: a maternally expressed Xenopus Wnt gene with a potential role in establishing the dorsoventral axis. Development (Cambridge, England) 121, 2177-86.

Curran, J. E., and Woodruff, R. I. (2007). Passage of 17 kDa calmodulin through gap junctions of three vertebrate species. Tissue & cell 39, 303-9.

Côté, F., Fligny, C., Bayard, E., Launay, J.-M., Gershon, M. D., Mallet, J., and Vodjdani, G. (2007). Maternal serotonin is crucial for murine embryonic development. Proceedings of the National Academy of Sciences of the United States of America 104, 329-34.

Dale, L., and Slack, J. M. (1987). Regional specification within the mesoderm of early embryos of Xenopus laevis. Development (Cambridge, England) 100, 279-95.

Danilchik, M. V., and Black, S. D. (1988). The first cleavage plane and the embryonic axis are determined by separate mechanisms in Xenopus laevis : I. Independence in undisturbed embryos. Developmental biology 128, 58-64.

Davis, E. E., Brueckner, Martina, and Katsanis, N. (2006). The emerging complexity of the vertebrate cilium: new functional roles for an ancient organelle. Developmental cell 11, 9-19.

De Boer, T. P. et al. (2005). Cloning and functional characterization of a novel connexin expressed in somites of Xenopus laevis. Developmental dynamics : an official publication of the American Association of Anatomists 233, 864-71.

De Robertis, E M (2009). Spemann's organizer and the self-regulation of embryonic fields. Mechanisms of development 126, 925-41.

De Robertis, Edward M, and Kuroda, H. (2004). Dorsal-ventral patterning and neural induction in Xenopus embryos. Annual review of cell and developmental biology 20, 285-308.

Deardorff, M. a, Tan, C., Conrad, L. J., and Klein, P. S. (1998). Frizzled-8 is expressed in the Spemann organizer and plays a role in early morphogenesis. Development (Cambridge, England) 125, 2687-700.

Doran, S. a (2004). Effect of serotonin on ciliary beating and intracellular calcium concentration in identified populations of embryonic ciliary cells. Journal of Experimental Biology 207, 1415-1429.

Efimov, I. R. (2006). Connections, connections, connexins: towards systems biology paradigm of cardiac arrhythmia. Journal of molecular and cellular cardiology 41, 949-51.

Eimon, P. M., and Harland, Richard M (2002). Effects of heterodimerization and proteolytic processing on Derrière and Nodal activity: implications for mesoderm induction in Xenopus. Development (Cambridge, England) 129, 3089-103.

Essner, Jeffrey, Amack, J., Nyholm, M., Harris, E. , and Yost, Joseph (2005). Kupffer's vesicle is a ciliated organ of asymmetry in the zebrafish embryo that initiates left-right development of the brain, heart and gut. Development (Cambridge, England) 132, 1247-60.

Essner, Jeffrey, Vogan, Kyle J, Wagner, M. K., Tabin, Clifford J, Yost, H Joseph, and Brueckner, Martina (2002a). Conserved function for embryonic nodal cilia. Nature 418, 37-8.

Essner, Jeffrey, Vogan, Kyle J, Wagner, M. K., Tabin, Clifford J, Yost, H Joseph, and Brueckner, Martina (2002b). Conserved function for embryonic nodal cilia. Nature 418, 37-8.

Evans, W. H., De Vuyst, E., and Leybaert, L. (2006). The gap junction cellular internet: connexin hemichannels enter the signalling limelight. The Biochemical journal 397, 1-14.

Feistel, K. (2006). Determination of Laterality in the Rabbit Embryo : Studies on Ciliation and Asymmetric Signal Transfer. Naturwissenschaften.

Feistel, K., and Blum, M. (2008). Gap junctions relay FGF8-mediated right-sided repression of Nodal in rabbit. Developmental dynamics : an official publication of the American Association of Anatomists 237, 3516-27.

Field, S. et al. (2011). Pkd1l1 establishes left-right asymmetry and physically interacts with Pkd2. Development 138, 1131-1142.

Fisher, M. E., Isaacs, H. V., and Pownall, M. E. (2002). Corrigendum eFGF is required for activation of XmyoD expression in the myogenic cell lineage of eFGF is required for activation of XmyoD expression in the myogenic cell lineage of Xenopus laevis. Development, 1307-1315.

Fukumoto, T., Kema, I., and Levin, M. (2005). Serotonin signaling is a very early step in patterning of the left-right axis in chick and frog embryos. Current biology: CB 15, 794-803.

Fukumoto, T., and Levin, Michael (2005). Serotonin Transporter Function Is an Early Step in Left-Right Patterning in Chick and Frog Embryos. 02115, 349-363.

Gardner, A. J., and Evans, J. P. (2006). Mammalian membrane block to polyspermy: new insights into how mammalian eggs prevent fertilisation by multiple sperm. Reproduction, fertility, and development 18, 53-61.

Gaspar, P., and Cases, Olivier Maroteaux, L. (2003). The developmental role of serotonin: news from mouse molecular genetics. Nature neuroscience 4, 1002-1012.

Gerhart, J., Danilchik, M., Doniach, T., Roberts, S., Rowning, B., and Stewart, R. (1989). Cortical rotation of the Xenopus egg: consequences for the anteroposterior pattern of embryonic dorsal development. Development (Cambridge, England) 107 Suppl, 37-51.

Gilbert, S. F. (2000). Developmental Biology.

Gimlich, R. L., and Gerhart, J. C. (1984). Early cellular interactions promote embryonic axis formation in Xenopus laevis. Developmental Biology 104, 117-130.

Glinka, A., Delius, H., Blumenstock, C., and Niehrs, C. (1996). Combinatorial signalling by Xwnt-ll and Xnr3 in the organizer epithelium. Mechanisms of Development 60, 221-231.

Good, J. A. L., Joubin, K., Giraldez, A. J., Ben-haim, N., Chen, Yu, Schier, A. F., Constam, D. B., Boveresses, C., and Epalinges, C.- (2005). Nodal Stability Determines Signaling Range. Current 15, 31-36.

Guan, X., Cravatt, B. F., Ehring, G. R., Hall, J. E., Boger, D. L., Lerner, R. a, and Gilula, N. B. (1997). The sleep-inducing lipid oleamide deconvolutes gap junction communication and calcium wave transmission in glial cells. The Journal of cell biology 139, 1785-92.

Gurdon, B. J. B. (1960). The Effects of Ultraviolet Irradiation on Uncleaved Eggs of Xenopus laevis. Comparative and General Pharmacology 101, 299-311.

Guthrie, S., Turin, L., and Warner, A (1988). Patterns of junctional communication during development of the early amphibian embryo. Development (Cambridge, England) 103, 769-83.

Hamada, Hiroshi, Meno, C., Watanabe, D., and Saijoh, Yukio (2002). Establishment of vertebrate left-right asymmetry. Nature reviews. Genetics 3, 103-13.

Hanafusa, H., Masuyama, N., Kusakabe, M., Shibuya, H., and Nishida, E. (2000). The TGF-β family member derrière is involved in regulation of the establishment of left–right asymmetry. EMBO Reports 1, 32-39.

Harvey, R. P. (1991). Widespread expression of MyoD genes in Xenopus embryos is amplified in presumptive muscle as a delayed response to mesoderm induction. Proceedings of the National Academy of Sciences of the United States of America 88, 9198-202.

Hashimoto, H., Rebagliati, M., Ahmad, N., Muraoka, O., Kurokawa, T., Hibi, M., and Suzuki, T. (2004). The Cerberus/Dan-family protein Charon is a negative regulator of Nodal signaling during left-right patterning in zebrafish. Development (Cambridge, England) 131, 1741-53.

Hashimotoa, M., and Hamada, Hiroshi (2010). Translation of anterior–posterior polarity into left–right polarity in the mouse embryo. Current opinion in genetics & development 20, 433-437.

Hatler, J. M., Essner, Jeffrey J, and Johnson, R. G. (2009). A gap junction connexin is required in the vertebrate left-right organizer. Developmental biology 336, 183-91.

Heasman, J. (2006a). Maternal determinants of embryonic cell fate. Seminars in cell & developmental biology 17, 93-8.

Heasman, J. (2006b). Maternal determinants of embryonic cell fate. Seminars in cell & developmental biology 17, 93-8.

Heisenberg, C.-P., and Solnica-Krezel, L. (2008). Back and forth between cell fate specification and movement during vertebrate gastrulation. Current opinion in genetics & development 18, 311-6.

Heuberger, J., and Birchmeier, W. (2010). Interplay of cadherin-mediated cell adhesion and canonical Wnt signaling. Cold Spring Harbor perspectives in biology 2, a002915.

Hirokawa, Nobutaka, Tanaka, Yosuke, and Okada, Yasushi (2009). Left-right determination: involvement of molecular motor KIF3, cilia, and nodal flow. Cold Spring Harbor perspectives in biology 1, a000802.

Hirokawa, Nobutaka, Tanaka, Yosuke, Okada, Yasushi, and Takeda, Sen (2006). Nodal flow and the generation of left-right asymmetry. Cell 125, 33-45.

Hojo, M. et al. (2007). Right-elevated expression of charon is regulated by fluid flow in medaka Kupffer ' s vesicle. Society, 395- 405.

Hoppler, S., Brown, J. D., and Moon, R T (1996). Expression of a dominant-negative Wnt blocks induction of MyoD in Xenopus embryos. Genes & Development 10, 2805-2817.

Hopwood, N. D., Pluck, A., and Gurdon, J. B. (1989). MyoD expression in the forming somites response to mesoderm induction in Xenopus embryos. EMBO Journal 8, 3409 - 3417.

Ishitani, T., Kishida, S., Hyodo-miura, J., Ueno, Naoto, Yasuda, J., Waterman, M., Shibuya, H., Moon, Randall T, and Ninomiya-tsuji, J. (2003). The TAK1-NLK Mitogen-Activated Protein Kinase Cascade Functions in the Wnt-5a / Ca 2ƨ Pathway To Antagonize Wnt / □ -Catenin Signaling. Society 23, 131-139.

Itoh, K., Jacob, J., and Sokol, S. (1998). A role for Xenopus Frizzled 8 in dorsal development. Mechanisms of development 74, 145-57.

Jiang, J. X., and Gu, S. (2005). Gap junction- and hemichannel-independent actions of connexins. Biochimica et biophysica acta 1711, 208-14.

Jing, X., Zhou, S., Wang, W., and Chen, Yu (2006). Mechanisms underlying long- and short-range nodal signaling in Zebrafish. Mechanisms of development 123, 388-94.

Juszczak, G. R., and Swiergiel, A. H. (2009). Properties of gap junction blockers and their behavioural, cognitive and electrophysiological effects: animal and human studies. Progress in neuro-psychopharmacology & biological psychiatry 33, 181-98.

Kamura, K., Kobayashi, D, Uehara, Y., Koshida, S., Iijima, N., Kudo, A., Yokoyama, T, and Takeda, H (2011). Pkd1l1 complexes with Pkd2 on motile cilia and functions to establish the left-right axis. Development 138, 1121-1129.

Karcher, C., Fischer, A., Schweickert, A., Bitzer, E., Horie, S., Witzgall, R., and Blum, M. (2005). Lack of a laterality phenotype in Pkd1 knock-out embryos correlates with absence of polycystin-1 in nodal cilia. Differentiation 73, 425-432.

Karner, C. M., Chirumamilla, R., Aoki, S., Igarashi, P., Wallingford, John B, and Carroll, T. J. (2009). Wnt9b signaling regulates planar cell polarity and kidney tubule morphogenesis. Nature genetics 41, 793-9.

Kawasumi, A., Nakamura, T., Iwai, N., Yashiro, K., Saijoh, Yukio, Belo, Jose Antonio, Shiratori, H., and Hamada, Hiroshi (2011). Left-right asymmetry in the level of active Nodal protein produced in the node is translated into left-right asymmetry in the lateral plate of mouse embryos. Developmental biology.

Khokha, M. K., Yeh, J., Grammer, T. C., and Harland, Richard M (2005). Depletion of three BMP antagonists from Spemann's organizer leads to a catastrophic loss of dorsal structures. Developmental cell 8, 401-11.

Kim, G.-H., and Han, J.-K. (2005a). JNK and ROKalpha function in the noncanonical Wnt/RhoA signaling pathway to regulate Xenopus convergent extension movements. Developmental dynamics : an official publication of the American Association of Anatomists 232, 958-68.

Kim, G.-H., and Han, J.-K. (2005b). JNK and ROKalpha function in the noncanonical Wnt/RhoA signaling pathway to regulate Xenopus convergent extension movements. Developmental dynamics : an official publication of the American Association of Anatomists 232, 958-68.

Klein, S. L. (1987). The first cleavage furrow demarcates the dorsal-ventral axis in Xenopus embryos. Developmental biology 120, 299-304.

Kodjabachian, L., and Lemaire, P. (2001). Siamois functions in the early blastula to induce Spemann's organiser. Mechanisms of Development 108, 71-79.

Kramer-Zucker, A. G., Olale, F., Haycraft, C. J., Yoder, B. K., Schier, A. F., and Drummond, I. a (2005). Cilia-driven fluid flow in the zebrafish pronephros, brain and Kupffer's vesicle is required for normal organogenesis. Development (Cambridge, England) 132, 1907-21.

Kurth, T, and Hausen, P. (2000). Bottle cell formation in relation to mesodermal patterning in the Xenopus embryo. Mechanisms of development 97, 117-31.

Kurth, Thomas, Meissner, S., Schäckel, S., and Steinbeisser, Herbert (2005). Establishment of mesodermal gene expression patterns in early Xenopus embryos: the role of repression. Developmental dynamics : an official publication of the American Association of Anatomists 233, 418-29.

Kwan, K. M. (2003). Xbra functions as a switch between cell migration and convergent extension in the Xenopus gastrula. Development 130, 1961-1972.

Laird, D. W. (2006a). Life cycle of connexins in health and disease. The Biochemical journal 394, 527-43.

Laird, D. W. (2006b). Life cycle of connexins in health and disease. The Biochemical journal 394, 527-43.

Landesman, Y., Goodenough, D. a, and Paul, D. L. (2000). Gap junctional communication in the early Xenopus embryo. The Journal of cell biology 150, 929-36.

Landesman, Y., and Sokol, S. Y. (1997). Xwnt-2b is a novel axis-inducing Xenopus Wnt, which

is expressed in embryonic brain. Mechanisms of development 63, 199-209.

Lauder, J., Wallace, J., and Krebs, H. (1981). Roles for serotonin in neuroembryogenesis. Advances in experimental medicine and biology 133, 477-506.

Lauf, U., Lopez, P., and Falk, M. M. (2001). Expression of fluorescently tagged connexins: a novel approach to rescue function of oligomeric DsRed-tagged proteins. FEBS letters 498, 11-5.

Le, A.-C. N., and Musil, L. S. (2001). A novel role for FGF and extracellular signal-regulated kinase in gap junction-mediated intercellular communication in the lens. The Journal of Cell Biology 154, 197-216.

Levin, M, and Mercola, M (1999). Gap junction-mediated transfer of left-right patterning signals in the early chick blastoderm is upstream of Shh asymmetry in the node. Development (Cambridge, England) 126, 4703-14.

Levin, M, and Mercola, M (1998). Gap junctions are involved in the early generation of left-right asymmetry. Developmental biology 203, 90-105.

Levin, M. (2004). the Embryonic Origins of Left-Right Asymmetry. Critical Reviews in Oral Biology 15, 197-206.

Levin, Michael (2006). Is the early left-right axis like a plant, a kidney, or a neuron? The integration of physiological signals in embryonic asymmetry. Birth defects research. Part C, Embryo today : reviews 78, 191-223.

Levin, Michael, Johnson, R. L., Stern, C. D., Kuehn, M., and Tabin, C. (1995). Determining Left-Right Asymmetry in Chick Embryogenesis. Cell 82, 803-814.

Levin, Michael, Thorlin, T., Robinson, K. R., Nogi, T., and Mercola, Mark (2002). Asymmetries in H+/K+-ATPase and cell membrane potentials comprise a very early step in left-right patterning. Cell 111, 77-89.

Lin, X., and Xu, X. (2009). Distinct functions of Wnt/beta-catenin signaling in KV development and cardiac asymmetry. Development 136, 207-217.

Lustig, K. D., Kroll, K. L., Sun, E. E., and Kirschner, M. W. (1996). Expression cloning of a Xenopus T-related gene (Xombi) involved in mesodermal patterning and blastopore lip formation. Development (Cambridge, England) 122, 4001-12.

López, S. L., Rosato-Siri, M. V., Franco, P. G., Paganelli, A. R., and Carrasco, A. E. (2005). The Notch-target gene hairy2a impedes the involution of notochordal cells by promoting floor plate fates in Xenopus embryos. Development (Cambridge, England) 132, 1035-46.

Maisonneuve, C., Guilleret, I., Vick, P., Weber, T., Andre, P., Beyer, T., Blum, M., and Constam, D. B. (2009). Bicaudal C, a novel regulator of Dvl signaling abutting RNA-processing bodies, controls cilia orientation and leftward flow. Development (Cambridge, England) 136, 3019-30.

Marszalek, J. R., Ruiz-Lozano, P., Roberts, E., Chien, K. R., and Goldstein, L. S. (1999). Situs inversus and embryonic ciliary morphogenesis defects in mouse mutants lacking the KIF3A subunit of kinesin-II. Proceedings of the National Academy of Sciences of the United States of America 96, 5043-8.

Martínez, A. D., Acuña, R., Figueroa, V., Maripillan, J., and Nicholson, B. (2009). Gap-junction channels dysfunction in deafness and hearing loss. Antioxidants & redox signaling 11, 309-22.

Maéno, M., Ong, R. C., Suzuki, a, Ueno, N, and Kung, H. F. (1994). A truncated bone morphogenetic protein 4 receptor alters the fate of ventral mesoderm to dorsal mesoderm:

roles of animal pole tissue in the development of ventral mesoderm. Proceedings of the National Academy of Sciences of the United States of America 91, 10260-4.

McGrath, J (2003). Cilia are at the heart of vertebrate left–right asymmetry. Current Opinion in Genetics & Development 13, 385-392.

McGrath, James, Somlo, S., Makova, S., Tian, X., and Brueckner, Martina (2003). Two populations of node monocilia initiate left-right asymmetry in the mouse. Cell 114, 61-73.

Moiseiwitsch, J. (2000). The role of serotonin and neurotransmitters during craniofacial development. Critical Reviews in Oral Biology ral biology and medicine 11, 230-239.

Molenaar, M., Brian, E., Roose, J., Clevers, H., and Destrée, O (2000). Differential expression of the Groucho-related genes 4 and 5 during early development of Xenopus laevis. Mechanisms of development 91, 311-5.

Molloy, S. S., Bresnahan, P. a, Leppla, S. H., Klimpel, K. R., and Thomas, G. (1992). Human furin is a calcium-dependent serine endoprotease that recognizes the sequence Arg-X-X-Arg and efficiently cleaves anthrax toxin protective antigen. The Journal of biological chemistry 267, 16396-402.

Moon, Randall T., and Kimelman, David (1998). From cortical rotation to organizer gene expression: toward a molecular explanation of axis specification in Xenopus. BioEssays 20, 536-546.

Mosimann, C., Hausmann, G., and Basler, K. (2009). Beta-catenin hits chromatin: regulation of Wnt target gene activation. Nature reviews. Molecular cell biology 10, 276-86.

Murai, K., Vernon, A. E., Philpott, A., and Jones, P. (2007). Hes6 is required for MyoD induction during gastrulation. Developmental biology 312, 61-76.

Nakaya, M.-aki, Biris, K., Tsukiyama, T., Jaime, S., Rawls, J. A., and Yamaguchi, T. P. (2005). Wnt3a Links Left-Right Determination with Segmentation and Anterior-Posterior Axis Elongation. Development 132, 5425-5436.

Nebigil, C. G., Hickel, P., Messaddeq, N., Vonesch, J.-luc, Douchet, M. P., Monassier, L., György, K., Matz, R., and Andriantsitohaina, R. (2001). Ablation of Serotonin 5-HT2B Receptors in Mice Leads to Abnormal Cardiac Structure and Function. Circulation 103, 2973-2979.

Nelsen, S., Berg, L., Wong, C., and Christian, Jan L (2005). Proprotein convertase genes in Xenopus development. Developmental dynamics : an official publication of the American Association of Anatomists 233, 1038-44.

Neugebauer, J. M., Amack, J. D., Peterson, A. G., Bisgrove, Brent W, and Yost, H Joseph (2009). FGF signalling during embryo development regulates cilia length in diverse epithelia. Nature 458, 651-4.

Niehrs, C., and Boutros, M. (2010). Trafficking, acidification, and growth factor signaling. Science signaling 3, pe26.

Niehrs, C., and Shen, J. (2010). Regulation of Lrp6 phosphorylation. Cellular and molecular life sciences : CMLS 67, 2551-2562.

Niesler, B. (2011). 5-HT 3 Receptors : Potential of individual isoforms for personalised therapy. Department of Human Molecular Genetics.

Niesler, B., Kapeller, J., Hammer, C., and Rappold, G. (2008). Serotonin type 3 receptor genes: HTR3A, B, C, D, E. Pharmacogenomics 9, 501-504.

Niesler, B. et al. (2007). Characterization of the Novel Human Serotonin Receptor Subunits 5-

HT3C, 5-HT3D, and 5-HT3E. Molecular Pharmacology, 8-17.

Nieuwkoop, P. D. (1969). The Formation of the Mesoderm in Urodelean Amphibians. Development Genes and Evolution 163, 298-315.

Nonaka, S, Tanaka, Y, Okada, Y, Takeda, S, Harada, a, Kanai, Y., Kido, M., and Hirokawa, N (1998). Randomization of left-right asymmetry due to loss of nodal cilia generating leftward flow of extraembryonic fluid in mice lacking KIF3B motor protein. Cell 95, 829-37.

Nonaka, Shigenori, Shiratori, H., Saijoh, Yukio, and Hamada, Hiroshi (2002). Determination of left – right patterning of the mouse embryo by artificial nodal flow. Nature 418, 96-99.

Nonaka, Shigenori, Yoshiba, S., Watanabe, D., Ikeuchi, S., Goto, T., Marshall, W. F., and Hamada, Hiroshi (2005). De novo formation of left-right asymmetry by posterior tilt of nodal cilia. PLoS biology 3, e268.

Northrop, J., Woods, a, Seger, R., Suzuki, a, Ueno, N, Krebs, E., and Kimelman, D (1995). BMP-4 regulates the dorsal-ventral differences in FGF/MAPKK-mediated mesoderm induction in Xenopus. Developmental biology 172, 242-52.

Okada, Y, Nonaka, S, Tanaka, Y, Saijoh, Y, Hamada, H, and Hirokawa, N (1999). Abnormal nodal flow precedes situs inversus in iv and inv mice. Molecular cell 4, 459-68.

Okada, Yasushi, Takeda, Sen, Tanaka, Yosuke, Belmonte, J.-C. I., and Hirokawa, Nobutaka (2005). Mechanism of nodal flow: a conserved symmetry breaking event in left-right axis determination. Cell 121, 633-44.

Oki, S., Hashimoto, R., Okui, Y., Shen, M. M., Mekada, E., Otani, H., Saijoh, Yukio, and Hamada, Hiroshi (2007). Sulfated glycosaminoglycans are necessary for Nodal signal transmission from the node to the left lateral plate in the mouse embryo. Development (Cambridge, England) 134, 3893-904.

Onuma, Y., Takahashi, S., Yokota, C., and Asashima, M. (2002). Multiple nodal-related genes act coordinately in Xenopus embryogenesis. Developmental biology 241, 94-105.

Oteiza, P. et al. (2010). Planar cell polarity signalling regulates cell adhesion properties in progenitors of the zebrafish laterality organ. Development (Cambridge, England) 3468, 3459-3468.

Pachur, A. (2007). Klonierung und Charakterisierung der Gene Xnr 1, BicC und Ablim -1/ -2 in Neurulaembryonen des Krallenfrosches Xenopus laevis.

Pang, Z. P., and Südhof, T. C. (2010). Cell Biology of Ca 2 + -Triggered Exocytosis. Cell 22, 496-505.

Park, T. J., Gray, R. S., Sato, A., Habas, R., and Wallingford, John B (2005). Subcellular localization and signaling properties of dishevelled in developing vertebrate embryos. Current biology : CB 15, 1039-44.

Pazour, G. J. (2004). Intraflagellar transport and cilia-dependent renal disease: the ciliary hypothesis of polycystic kidney disease. Journal of the American Society of Nephrology : JASN 15, 2528-36.

Pohl, B., and Knöchel, W. (2004). Isolation and developmental expression of Xenopus FoxJ1 and FoxK1. Development genes and evolution 214, 200-205.

Praetorius, H. a, and Spring, K. R. (2001). Bending the MDCK Cell Primary Cilium Increases Intracellular Calcium. Journal of Membrane Biology 184, 71-79.

Rackauskas, M., Neverauskas, V., and Skeberdis, V. A. (2010). Diversity and properties of connexin gap junction channels. Medicina (Kaunas, Lithuania) 46, 1-12.

Ramel, M.-C., and Lekven, A. C. (2004). Repression of the vertebrate organizer by Wnt8 is mediated by Vent and Vox. Development (Cambridge, England) 131, 3991-4000.

Rankin, C. T., Bunton, T., Lawler, A. M., and Lee, S.-J. (2000). Regulation of left-right patterning in mice by growth/differentiation factor-1. Nature genetics 24, 262-265.

Rao, T. P., and Kühl, M. (2010). An updated overview on Wnt signaling pathways: a prelude for more. Circulation research 106, 1798-806.

Raya, A., and Izpisua Belmonte, J. C. (2004). Unveiling the establishment of left-right asymmetry in the chick embryo. Mechanisms of development 121, 1043-54.

Raya, A., and Izpisúa Belmonte, Juan Carlos (2004). Sequential transfer of left-right information during vertebrate embryo development. Current opinion in genetics & development 14, 575-81.

Reaume, A., Sousa, P. de, Kulkarni, S., Langille, B., Zhu, D., Davies, T., Juneja, S., Kidder, G., and Rossant, J. (1995). Cardiac malformation in neonatal mice lacking connexin43. Science 267, 1831-1834.

Revinski, D. R., Paganelli, A. R., Carrasco, A. E., and López, S. L. (2010). Delta-Notch signaling is involved in the segregation of the three germ layers in Xenopus laevis. Developmental biology 339, 477-92.

Rupp, R.A., Snider, L., and Weintraub, H. (1994). Xenopus embryos regulate the nuclear localization of XMyoD. Genes Dev 8, 1311-1323.

Saijoh, Y (2003). Left–right patterning of the mouse lateral plate requires nodal produced in the node. Developmental Biology 256, 161-173.

Saijoh, Yukio, Oki, S., Tanaka, C., Nakamura, T., Adachi, H., Yan, Y.-ting, Shen, M. M., and Hamada, Hiroshi (2005). Two Nodal-Responsive Enhancers Control Left – Right Asymmetric Expression of Nodal. North, 1031-1036.

Sakuma, R. et al. (2002). Inhibition of Nodal signalling by Lefty mediated through interaction with common receptors and efficient diffusion. Genes to cells : devoted to molecular & cellular mechanisms 7, 401-12.

Saneyoshi, T., Kume, S., Amasaki, Y., and Mikoshiba, K. (2002). The Wnt/calcium pathway activates NF-AT and promotes ventral cell fate in Xenopus embryos. Nature 417, 295-9.

Sarmah, B., Latimer, A. J., Appel, B., and Wente, S. R. (2005). Inositol polyphosphates regulate zebrafish left-right asymmetry. Developmental cell 9, 133-45.

Satir, P (1980). Structural basis of ciliary movement. Environmental health perspectives 35, 77-82.

Satir, Peter, Pedersen, L. B., and Christensen, S. T. (2010). The primary cilium at a glance. Journal of cell science 123, 499-503.

Satow, R., Chanb, T.-chuan, and Asashima, M. (2004). The role of Xenopus frizzled-8 in pronephric development. Biochemical and biophysical research communications 2, 487-494.

Sbalzarini, I. F., and Koumoutsakosa, P. (2005). Feature point tracking and trajectory analysis for video imaging in cell biology. Journal of Structural Biology 151, 182-195.

Scharf, S. (1980). Determination of the dorsal-ventral axis in eggs of Xenopus laevis: Complete rescue of uv-impaired eggs by oblique orientation before first cleavage*1. Developmental Biology 79, 181-198.

Schier, A. F. (2009). Nodal morphogens. Cold Spring Harbor perspectives in biology 1,

a003459.

Schier, A. F. (2003). Nodal signaling in vertebrate development. Review Literature And Arts Of The Americas, 589-621.

Schneider, Igor, Houston, D. W., Rebagliati, M. R., and Slusarski, Diane C (2008). Calcium fluxes in dorsal forerunner cells antagonize beta-catenin and alter left-right patterning. Development (Cambridge, England) 135, 75-84.

Schweickert, A., Campione, M., Steinbeisser, Herbert, and Blum, M. (2000). Pitx2 isoforms : involvement of Pitx2c but not Pitx2a or Pitx2b in vertebrate left - right asymmetry. Mechanisms of Development 90.

Schweickert, A., Vick, P., Getwan, M., Weber, T., Schneider, Isabelle, Eberhardt, M., Beyer, T., Pachur, A., and Blum, M. (2010). The Nodal Inhibitor Coco Is a Critical Target of Leftward Flow in Xenopus. Current biology : CB 20, 738-743.

Schweickert, A., Weber, T., Beyer, T., Vick, P., Bogusch, S., Feistel, K., and Blum, M. (2007). Cilia-driven leftward flow determines laterality in Xenopus. Current biology : CB 17, 60-6.

Sharma, N., Berbari, N. F., and Yoder, B. K. (2008). Ciliary Dysfunction in Developmental Abnormalities and Diseases 1st ed. (Elesvier Inc.)

Sheldahl, L. C., Slusarski, Diane C, Pandur, P., Miller, J. R., Kühl, M., and Moon, Randall T (2003a). Dishevelled activates Ca2+ flux, PKC, and CamKII in vertebrate embryos. The Journal of cell biology 161, 769-77.

Sheldahl, L. C., Slusarski, Diane C, Pandur, P., Miller, J. R., Kühl, M., and Moon, Randall T (2003b). Dishevelled activates Ca2+ flux, PKC, and CamKII in vertebrate embryos. The Journal of cell biology 161, 769-77.

Shen, M. M. (2007). Nodal signaling: developmental roles and regulation. Development (Cambridge, England) 134, 1023-34.

Shiba, D., Takamatsu, T., and Yokoyama, Takahiko (2005). Primary cilia of inv/inv mouse renal epithelial cells sense physiological fluid flow: bending of primary cilia and Ca2+ influx. Cell structure and function 30, 93-100.

Shiratori, H., and Hamada, Hiroshi (2006). The left-right axis in the mouse: from origin to morphology. Development (Cambridge, England) 133, 2095-104.

Shook, D. R., Majer, C., and Keller, R. (2004). Pattern and morphogenesis of presumptive superficial mesoderm in two closely related species, Xenopus laevis and Xenopus tropicalis. Developmental biology 270, 163-85.

Siezen, R. J., and Leunissen, J. a (1997). Subtilases: the superfamily of subtilisin-like serine proteases. Protein science : a publication of the Protein Society 6, 501-23.

Simard, A., Giorgio, L. D., Amen, M., Westwood, A., Amendt, B. A., and Ryan, A. K. (2009). The Pitx2c N-Terminal Domain Is a Critical Morphogenesis. Health (San Francisco), 2459 -2470.

Simons, M. et al. (2005). Inversin, the gene product mutated in nephronophthisis type II, functions as a molecular switch between Wnt signaling pathways. Nature genetics 37, 537-43.

Simons, M., and Mlodzik, M. (2008a). Planar cell polarity signaling: from fly development to human disease. Annual review of genetics 42, 517-40.

Simons, M., and Mlodzik, M. (2008b). Planar cell polarity signaling: from fly development to human disease. Annual review of genetics 42, 517-40.

Sive, H. L., Grainger, R. M., and Harland, Richard M. (2000). Early Development of Xenopus laevis: A Laboratory Manual (CSH laboratories).

Slusarski, D C, Yang-Snyder, J., Busa, W. B., and Moon, R T (1997). Modulation of embryonic intracellular Ca2+ signaling by Wnt-5A. Developmental biology 182, 114-20.

Slusarski, Diane C, and Pelegri, F. (2007). Calcium signaling in vertebrate embryonic patterning and morphogenesis. Developmental biology 307, 1-13.

Smith, J C, Hagemann, a, Saka, Y., and Williams, P H (2008). Understanding how morphogens work. Philosophical transactions of the Royal Society of London. Series B, Biological sciences 363, 1387-92.

Smith, W. C., Mckendry, R., Ribisi, S., and Harland, Richard M (1995). A nodal- Related Gene Defines a Physical and Functional within the Spemann Organizer. Cell 82, 37-46.

Sokol, S. Y. (1996). Analysis of Dishevelled signalling pathways during Xenopus development. Current biology : CB 6, 1456-67.

Song, H., Hu, J., Chen, W., Elliott, G., Andre, P., Gao, B., and Yang, Y. (2011). Planar cell polarity breaks the bilateral symmetry by controlling ciliary positioning. Developmental Genetics 466, 378-382.

Sosinsky, G. E., and Nicholson, Bruce J (2005). Structural organization of gap junction channels. Biochimica et biophysica acta 1711, 99-125.

Spemann, H., and Mangold, H. (1924). Über Induktion von Embryonalanlagen durch Implantation artfremder Organisatoren. Arch. mikr. Anat. und Entw. mech. 100, 599-638.

Standley, H. J., Destrée, Olivier, Kofron, M., Wylie, Chris, and Heasman, J. (2006). Maternal XTcf1 and XTcf4 have distinct roles in regulating Wnt target genes. Developmental biology 289, 318-28. Available at: http://www.ncbi.nlm.nih.gov/pubmed/16325796 [Accessed May 14, 2011].

Steinbach, O. C., Ulshöfer, a, Authaler, a, and Rupp, R. a (1998). Temporal restriction of MyoD induction and autocatalysis during Xenopus mesoderm formation. Developmental biology 202, 280-92.

Stennard, F., Carnac, G., and Gurdon, J. B. (1996). The Xenopus T-box gene, Antipodean, encodes a vegetally localised maternal mRNA and can trigger mesoderm formation. Development (Cambridge, England) 122, 4179-88.

Storm van's Gravesande, K., and Omran, H. (2005). Primary ciliary dyskinesia: Clinical presentation, diagnosis and genetics. Informa healthcare 37, 439-449.

Street, H., and Ms, O. (1998). Cell cycle transition Xenopus laevis. Cell Cycle, 537-548.

Stubbs, J. L., Oishi, I., Belmonte, J. C. I., and Kintner, C. (2008). The forkhead protein Foxj1 specifies node-like cilia in Xenopus and zebrafish embryo. Nature genetics 40, 1454-1460.

Sulik, K., Dehart, D. B., Iangaki, T., Carson, J. L., Vrablic, T., Gesteland, K., and Schoenwolf, G. C. (1994). Morphogenesis of the murine node and notochordal plate. Developmental dynamics : an official publication of the American Association of Anatomists 201, 260-78.

Supp, D. M., Witte, D. P., Potter, S. S., and Brueckner, M (1997). Mutation of an axonemal dynein affects left-right asymmetry in inversus viscerum mice. Nature 389, 963-6.

Sáez, J. C., Connor, J. a, Spray, D. C., and Bennett, M. V. (1989). Hepatocyte gap junctions are permeable to the second messenger, inositol 1,4,5-trisphosphate, and to calcium ions. Proceedings of the National Academy of Sciences of the United States of America 86, 2708-12.

Tabin, C. (2005). Do we know anything about how left–right asymmetry is first established in the vertebrate embryo? Journal of molecular histology 36, 317-323.

Tabin, Clifford J, and Vogan, Kyle J (2003). A two-cilia model for vertebrate left-right axis specification. Genes & Development, 1-6.

Tada, M, and Smith, J C (2000). Xwnt11 is a target of Xenopus Brachyury: regulation of gastrulation movements via Dishevelled, but not through the canonical Wnt pathway. Development (Cambridge, England) 127, 2227-38.

Tada, Masazumi, and Kai, M. (2009). Noncanonical Wnt/PCP signaling during vertebrate gastrulation. Zebrafish 6, 29-40.

Takeda, S, Yonekawa, Y., Tanaka, Y, Okada, Y, Nonaka, S, and Hirokawa, N (1999). Left-right asymmetry and kinesin superfamily protein KIF3A: new insights in determination of laterality and mesoderm induction by kif3A-/- mice analysis. The Journal of cell biology 145, 825-36.

Tanaka, C., Sakuma, R., Nakamura, T., Hamada, Hiroshi, and Saijoh, Yukio (2007). Long-range action of Nodal requires interaction with GDF1. Genes & development 21, 3272-82.

Tanaka, Yosuke, Okada, Yasushi, and Hirokawa, Nobutaka (2005). FGF-induced vesicular release of Sonic hedgehog and retinoic acid in leftward nodal flow is critical for left-right determination. Nature 435, 172-7.

Team, R. D. C. (2008). R: A language and environment for statistical computing. R Foundation for Statistical Computing, Vienna, Austria.

Thimm, J., Mechler, A., Lin, H., Rhee, S., and Lal, R. (2005). Calcium-dependent open/closed conformations and interfacial energy maps of reconstituted hemichannels. The Journal of biological chemistry 280, 10646-54.

Thompson, A. J., and Lummis, S. C. R. (2006). 5-HT3 Receptors. Current PharmPharm 12, 3615-3630.

Thumberger, Thomas (2011). Towards a unifying model of symmetry breakage in vertebrates. PhD thesis, University of Hohenheim.

Tian, J., Andrée, B., Jones, C. M., and Sampath, K. (2008). The pro-domain of the zebrafish Nodal-related protein Cyclops regulates its signaling activities. Development (Cambridge, England) 135, 2649-58.

Tian, T., and Meng, a M. (2006). Nodal signals pattern vertebrate embryos. Cellular and molecular life sciences : CMLS 63, 672-85.

Toyoizumi, R., Takeuchi, S., and Mogi, K. (2006). Subtilisin-like proprotein convertase activity is necessary for left-right axis determination in Xenopus neurula embryos. Development genes and evolution 216, 607-22.

Vick, P. (2009). Functional dissection of leftward flow. PhD thesis, University of Hohenheim.

Vick, P., Schweickert, A., Weber, T., Eberhardt, M., Mencl, S., Shcherbakov, D., Beyer, T., and Blum, M. (2009). Flow on the right side of the gastrocoel roof plate is dispensable for symmetry breakage in the frog Xenopus laevis. Developmental biology 331, 281-91.

Vonica, A., and Brivanlou, A. H. (2007). The left-right axis is regulated by the interplay of Coco, Xnr1 and derrière in Xenopus embryos. Developmental biology 303, 281-94.

Wallingford, J B, Rowning, B. a, Vogeli, K. M., Rothbächer, U., Fraser, S. E., and Harland, R M (2000). Dishevelled controls cell polarity during Xenopus gastrulation. Nature 405, 81-5.

Wallingford, J B, Vogeli, K. M., and Harland, R M (2001). Regulation of convergent extension in Xenopus by Wnt5a and Frizzled-8 is independent of the canonical Wnt pathway. The International journal of developmental biology 45, 225-7.

Wallingford, John B, and Mitchell, B. (2011). Strange as it may seem: the many links between Wnt signaling, planar cell polarity, and cilia. Genes & development 25, 201-13.

Walstab J, Hammer C, Bönisch H, Rappold G, N. B. (2008). Naturally occurring variants in the HTR3B gene significantly alter properties of human heteromeric 5-hydroxytryptamine-3A/B receptors. Pharmacogenetics and genomics 18, 793-802.

Wang, G., Cadwallader, A., Jang, D., Tsang, M., Yost, H., and Amack, J. (2011). The Rho kinase Rock2b establishes anteroposterior asymmetry of the ciliated Kupffer's vesicle in zebrafish. Development 138, 45-54.

Weaver, C., and Kimelman, David (2004). Move it or lose it: axis specification in Xenopus. Development (Cambridge, England) 131, 3491-9.

Wedlich, D. (2002). The polarising role of cell adhesion molecules in early development. Current Opinion in Cell Biology 14, 563-568.

Williams, P Huw, and Hagemann, A. (2004). Visualizing Long-Range Movement of the Morphogen Xnr2 in the Xenopus Embryo. Current 14, 1916-1923.

Winklbauer, R., Medina, a, Swain, R. K., and Steinbeisser, H (2001). Frizzled-7 signalling controls tissue separation during Xenopus gastrulation. Nature 413, 856-60.

Wolda, S. L., Moody, C. J., and Moon, R. T. (1993). Overlapping Expression of Xwnt-3A and Xwnt-1 in Neural Tissue of Xenopus laevis Embryos. Developmental Biology 155, 146-57.

Wolpert, L. (1969). Positional information and the spatial pattern of cellular differentiation. journal of theoretical biology 25, 1-47.

Yadav, V. K. et al. (2008). Lrp5 controls bone formation by inhibiting serotonin synthesis in the duodenum. Cell 135, 825-37.

Yelin, R., Schyr, R. B.-H., Kot, H., Zins, S., Frumkin, A., Pillemer, G., and Fainsod, A. (2005). Ethanol exposure affects gene expression in the embryonic organizer and reduces retinoic acid levels. Developmental biology 279, 193-204.

Yost, H J (1990). Inhibition of proteoglycan synthesis eliminates left-right asymmetry in Xenopus laevis cardiac looping. Development (Cambridge, England) 110, 865-74.

Zhang, M., Bolfing, M. F., Knowles, H. J., Karnes, H., and Hackett, B. P. (2004). Foxj1 regulates asymmetric gene expression during left-right axis patterning in mice. Biochemical and biophysical research communications 324, 1413-20.

Zhou, L., Kasperek, E. M., and Nicholson, B J (1999). Dissection of the molecular basis of pp60(v-src) induced gating of connexin 43 gap junction channels. The Journal of cell biology 144, 1033-45.

Zile, M. H., Kostetskii, I., Yuan, S, Kostetskaia, E., St Amand, T. R., Chen, Y, and Jiang, W. (2000). Retinoid signaling is required to complete the vertebrate cardiac left/right asymmetry pathway. Developmental biology 223, 323-38.

Curriculum vitae

I. Personal details

Name	Tina Beyer
Title	Biologist/Diploma
Nationality	german
Date; place of birth	29.06.1981, Dresden
Marital status	unmarried

II. Personal background

since February 1, 2007	**PhD student**
	Stuttgart, University of Hohenheim
2001 - 2006	**Student of biology**
	Stuttgart, University of Hohenheim
	September 1, 2006: Diploma, grade 1.0
	main subject: zoology
	subsidiary subjects: microbiology, physiology
1992 - 2001	secondary school
	Max-Born-Gymnasium Backnang
	June 19, 2001: university entrance qualification 2.4
1988 - 1991	primary school
	Dresden - Weixdorf, 1991 Burgstetten - Erbstetten

III. PhD thesis

Title	**'The role of serotonin and gap junctions in left-right development of *Xenopus laevis'***
	Advisor: Prof. Dr. Martin Blum, Stuttgart, University of Hohenheim
Support	LGF, 2-year scholarship (Landesgraduiertenförderung)

IV. Further skills

Technical skills	▪ DNA-/RNA-Preparation
	▪ Molecular Cloning
	▪ In-situ hybridization (Xenopus, mouse, rabbit)
	▪ Immunohistochemistry (Xenopus)
	▪ Microinjections (Xenopus)
	▪ Microsurgery / transplantation (Xenopus)
	▪ Incubation assays (Xenopus)
	▪ Laser Scan-Microscopy
	▪ Scanning Electron-Microscopy
IT skills	▪ MS Office / OpenOffice
	▪ Adobe Illustrator / Photoshop
	▪ Statistica
	▪ ImageJ
	▪ AxioVision
Language	▪ English (good in speech and writing)
Other matters	▪ Member of the GFE and SDB (German and American Society for Developmental Biology)
	▪ Registered in ResearchGate, scientific network

V. Publications

1. Schweickert et al., **'The Nodal Inhibitor Coco Is a Critical Target of Leftward Flow in Xenopus'**, *Current Biology* (2010)
2. Blum et al., **'Xenopus, an ideal model system to study vertebrate left-right asymmetry'**, *Developmental Dynamics: An Official Publication of the American Association of Anatomists* (2009)
3. Maisonneuve et al., **'Bicaudal C, a novel regulator of Dvl signaling abutting RNA-processing bodies, controls cilia orientation and leftward flow'**, *Development* (2009)
4. Blum et al., **'Evolution of leftward flow'**, *Seminars in Cell & Developmental Biology* (2009)

5. Vick et al., **'Flow on the right side of the gastrocoel roof plate is dispensable for symmetry breakage in the frog Xenopus laevis'**, *Developmental Biology* (2009)
6. Schweickert et al., **'Cilia-driven leftward flow determines laterality in Xenopus'**, *Current Biology* (2007)
7. Martin Blum et al., **'Ciliation and gene expression distinguish between node and posterior notochord in the mammalian embryo'**, *Differentiation; Research in Biological Diversity* (2007)

VI. Conference/Course participations

October 7-8, 2010 'From Signal to Structure in Embryogenesis and Organogenesis', University of Freiburg, Freiburg, Germany

August 5-9, 2010 69th Annual SDB Meeting, Convention Center, Albuquerque/NM, USA (participation sponsored by GFE and SDB)

October 26 – 29, 2009 German-Italian *Xenopus* Meeting, German-Italian Centre, Loveno di Menaggio, Italy

March 25 – 28, 2010 18th Meeting of the German Society for Developmental Biology, Hannover, Germany

September 8-12, 2008 12. International *Xenopus* Meeting, Leiwen/Trier, Germany (participation sponsored by LGFG)

April 5 - 15, 2008 Cell and Developmental Biology of *Xenopus* Cold Spring Harbor Laboratory, NY, USA (participation sponsored by Böhringer Ingelheim Fonds)

October 22-25, 2007 German-Italian *Xenopus* Meeting, German-Italian Centre, Loveno di Menaggio, Italy

May 14-16,2007 'Ettan™ DIGE Basic Course: From sample labelling to scanning', University of Hohenheim, Stuttgart, Germany

July 16-19, 2006 3rd workshop on 'Early Developmental Processes in Vertebrates', TU Dresden, Germany